Master thesis

Sensitivity of discharge characteristics to the spatial resolution of regional climate models

Ingrid van den Brink
September 2017

Deltares
Enabling Delta Life
UNIVERSITY OF TWENTE.

Sensitivity of discharge characteristics to the spatial resolution of regional climate models

Master thesis Water Engineering & Management
University of Twente
Faculty of Engineering Technology
Civil Engineering & Management

Author:
Ingrid van den Brink
i.m.vandenbrink@alumnus.utwente.nl

Graduation committee:
University of Twente, Department of Water Engineering and Management
Prof. Dr.J.C.J. Kwadijk
Dr. ir. M.J.Booij

Deltares, Hydrology department:
Dr. ir. F. Sperna Weiland

Enschede, September 2017

Summary

Regional Climate Models (RCMs) coupled with General Circulation Models (GCMs) are among the most important tools to generate future climate projections. The output of these models is used for various effect studies, such as the effect of climate change on discharge characteristics. To simulate the discharge, hydrological models are used. These models need reliable precipitation, temperature and data to calculate the potential evapotranspiration as input. These datasets are simulated by the RCMs and are often adjusted using bias correction and/or statistical downscaling before forcing the hydrological models. An important improvement which has been carried out last decades is the increase in RCM spatial resolution. A higher resolution improves the lands surface representation and the possibility to simulate important small-scale precipitation. However, there are some constraints on increasing the RCM spatial resolution. First, this process is time consuming and second, a higher resolution demands significant computational resources. Therefore, it is important to study the balance between the effect of increasing the resolution on the model output and the investments needed to increase the resolution. The effect of increasing RCM spatial resolution on the simulated precipitation and temperature has often been studied. However, the effect of increasing RCM spatial resolution on simulated discharges has been rarely explored. Previous studies expected beforehand that an increase in RCM spatial resolution leads to better simulated discharges. However, these studies concluded that the effect of RCM spatial resolution on discharge characteristics depend on the size of the catchment, the topography of the catchment and the hydrological model choice. This has led to the following research objective:

To assess the sensitivity of discharge characteristics to RCM spatial resolution (12.5, 25 and 50 km) simulated by different versions of HBV having different parameterizations for catchments with different characteristics (sizes and topography) in the Rhine basin.

To assess the sensitivity of discharge characteristics to RCM spatial resolution, the total model performance is obtained. This total model performance is reflected by the ratio of the mean and standard deviation of the simulated discharge for the three RCM resolutions and the mean and standard deviation of the observed discharge. The influence of the RCM resolution on the total model performance is analysed for four sub-catchments in the Rhine catchments having different characteristics (sizes and topography), the Main (large and lowland), the West Alpine (large and mountainous), Kinzig (small and lowland) and Reuss Seedorf (small and mountainous). Further, to obtain the sensitivity of discharge characteristics to RCM spatial resolution when simulated by different hydrological models, different versions of HBV are used. These versions are the calibrated, semi-calibrated an un-calibrated HBV model having the same model structure, but different parameter sets. Therefore, not the choice of hydrological model, but the choice of hydrological model – parameter estimation is analysed.

However, not only the total model performance is analyzed. The RCM spatial resolution is one of the many components which need to be chosen within the modeling chain. Other choices are for example the choice of bias correction technique and the choice of hydrological model. Each choice leads to a different model output and therefore a different total model performance. To make sure that the results showing the sensitivity of discharge characteristics to RCM spatial resolution are really caused by the change in spatial resolution and not influenced by other aspects, no bias correction or statistical downscaling are applied on the output of the RCMs. Further, the two most important contributions to the total model performance are the hydrological model performance and the RCM performance. To be able to understand the results of the total model performance, the contribution of the hydrological model performance and RCM performance are analysed as well. The hydrological model performance is obtained by comparing the simulated discharges forced with observed meteorological data to observed discharge data. The RCM performance is analysed by comparing the simulated discharge forced with RCM data to the simulated discharges forced with observed meteorological data. The RCM performance is further analysed by comparing the output of

the RCM, namely the simulated precipitation, temperature and potential evapotranspiration (calculated using the Makkink method) with the observed meteorological data.

To be able to analyse the total model performance, the hydrological model performance and the RCM performance, some other choices needed to be made as well. First, the RCM RACMO has been selected having three different spatial resolutions (12.5, 25 and 50 km). This RCM is forced with re-analysis data which show a clear representation of historical climate conditions. Therefore, comparison with observations is possible. Second, the hydrological model HBV-96 has been selected since this model is often used for hydrological modelling. Third, the selected study area is the Rhine catchment since among others a lot of observed datasets are available for this catchment. At last, although this study does not focus on climate change impacts, both low and high flow conditions are considered in the validation since RCMs are often applied for climate change impact studies.

The results show that the topography does not influence the sensitivity of discharge characteristics to RCM spatial resolution. The discharge characteristics are not sensitive to RCM spatial resolution in terms of hydrological model – parameter estimation. Only the size of the sub-catchments influences the sensitivity of discharge characteristics to RCM spatial resolution. In general, an increase in RCM spatial resolution leads to a small increase in total model performance for the two larger sub-catchments West Alpine and Main. This conclusion is supported by previous research as well. Further, this increase in total model performance is larger for high discharges than for annual discharges. Only for low discharges this increase is not observed. Beforehand it was expected that the increase in total model performance of smaller sub-catchments when increasing the RCM spatial resolution would be larger. The reason for this is that an increase in RCM spatial resolution leads to a better representation of small scale precipitation patterns. For catchments having a size of around 20000 km^2 and for the runoff evolution of a daily timescale, the fine-scale distribution of precipitation within the catchment is less important. However, for smaller sub-catchments it would be expected that the fine scale precipitation is more important. This study did analyse smaller sub-catchments, Reuss Seedorf (836 km^2) and Kinzig (928 km^2) where this appeared to be not the case. The reason for this could be that no bias correction has been applied in this research. Previous research concluded that another advantage of an increase in RCM spatial resolution is that this leads to biases which are less spatially variable and more systematic and therefore easier to correct.

In conclusion, this study shows that for larger sub-catchments an increase in RCM spatial resolution results in a small increase in total model performance. Further, the hydrological model choice and topography are not relevant for the sensitivity of discharge characteristics to the increase of RCM spatial resolution. It is recommended to focus further research on the dependency of the bias correction method and increase in RCM spatial resolution. Furthermore, in order to generalize the findings, it would be good to analyse performances at least for pairs of catchments with similar characteristics to evaluate whether the results are random or do apply to similar catchments. At last, if the total model performance shows an increase or decrease when increasing the RCM spatial resolution, this is not necessarily caused by only the changes in spatial RCM resolutions. These results can as well be influenced by for example a very low performance of the hydrological model or a bias correction method.

Preface

I am very interested in hydrological modelling and the different components of the model process influencing the model performance. Jaap Kwadijk taught me that hydrological models are used as tool to support decisions making, but are not a perfect fit of the reality. I am interested in increasing the performance of simulated discharges. Therefore, my research is about the sensitivity of discharge characteristics to RCM spatial resolution. This report represents the thesis of the master Water Engineering and Management – track River and Coastal Engineering.

I would like to thank my supervisors Jaap Kwadijk and Martijn Booij of the University of Twente. They always had time in their schedule to discuss issues with me, to answer questions or to discuss the most readable structure of the report. Further, I would like to thank my supervisor Frederiek Sperna Weiland from Deltares. She helped me to implement the hydrological model, to understand FEWS and she helped me with a lot of other technical questions. Further, I would like to thank Erik van Meijgaard and Jules Beersma working for the KNMI for providing the data of the used Regional Climate Model RACMO and for helping me to understand this model. The different colleagues of Deltares I would like to thank as well. Everyone was always willing to help me. At last I would like to thank my family and friends who supported me during the thesis project.

Ingrid van den Brink

Enschede, 19 September 2017

Contents

List of figures

List of tables

1 Introduction

Extreme weather events can lead to floods and droughts which can cause a lot of social and economic damage. Because of the consequences of floods and droughts, it is important to study the effect of climate change on discharge characteristics (van der Linden & Mitchell, 2009). To study this effect, a set of scenarios, called the Representative Concentration Pathways, are developed which describe four different 21st century pathways of GHG (greenhouse gas) emissions and atmospheric concentrations, air pollutant emissions and land use (IPCC, 2014). These scenarios are used as input for General Circulation Models (GCMs) which simulate among others climate change projections. However, when the spatial resolution of a GCM is too coarse to force a hydrologic model for a smaller catchment, dynamical downscaling can be applied: the output of the GCM is used as boundary condition to force Regional Climate Models (RCMs) with a certain spatial resolution. These RCMs simulate many climate aspects including temperature and precipitation. The output of the RCMs is adjusted using a bias correction and/or statistical downscaling before it is used as input for hydrological models. These hydrological models are used to simulate the discharge in a river (te Linde, et al., 2010). This modeling process is called the 'climate impact modeling chain' (Clark, et al., 2016).

1.1 State of the art

One of the important aspects in the 'climate impact modeling chain' is the spatial resolution of Regional Climate Models (RCMs). Last decade the spatial RCM resolution is increased because a higher resolution improves the land surface representation and the possibility to simulate important small-scale precipitation (Olsson, Berg, & Kawamura, 2014). However, there are some constraints on increasing the RCM spatial resolution. In general, the process to develop a higher RCM spatial resolution is time consuming (Meijgaard, 2017). Further, the simulations at a higher resolution demand significant computational resources (Prein, et al., 2013). The RCM spatial resolution is one of the many components which need to be chosen within the 'climate impact modeling chain'. Other choices are for example the choice of bias correction technique and the choice of hydrological model. Each choice leads to a different simulated output and therefore a different model performance. Therefore, it is first important to study the effect of these different choices on the model output to quantify the spread of plausible discharges. Second, it is relevant to have insight in the balance between the effect of improving certain components on the range of discharges and the time and cost that need to be invested to improve these components, such as the bias correction method or the hydrological model choice. Most of the effects of certain choices have been studied already. However, the sensitivity of discharge characteristics to RCM spatial resolution has been rarely explored (Mendoza, et al., 2016). It is important to study the sensitivity of discharge characteristics to RCM spatial resolution. If a lower RCM spatial resolution leads to the same simulated discharge characteristics as a higher RCM spatial resolution, it could be recommended to focus further research on improving other components instead of increasing the RCM spatial resolution. In this study the topic of interest is the sensitivity of discharge characteristics to RCM spatial resolution.

1.1.1 Previous research about RCM spatial resolution

The choice of RCM spatial resolution determines how precipitation and other hydrologic variables are represented in highly heterogeneous regions (Mendoza, et al., 2016). The effect of RCM spatial resolution on discharges has been rarely studied. However, the effect of RCM spatial resolution on precipitation has been studied by (Graham, Andréasson, & Carlsson, 2007), (Kleinn, et al., 2005), (Dankers, et al., 2007), (Prein, et al., 2013) and (Olsson, Berg, & Kawamura, 2014). In general, these studies conclude that a higher RCM spatial resolution results in a better performance of simulated precipitation. Moreover, Olsson et al. (2014) concluded that the higher spatial resolution (6 km) is nearly unbiased for precipitation when compared to the 50 km resolution (Olsson, Berg, & Kawamura, 2014). Further, (Graham, Andréasson, & Carlsson, 2007) concluded that a higher RCM spatial resolution resulted in biases that were more systematic and less spatially variable in RCM simulated precipitation and temperature when compared to the lower resolution. In terms of temperature, Graham et al. (2005) concluded that a higher RCM spatial resolution resulted in a better simulated temperature in mountainous regions.

There are three studies that have focused not only on the effect of RCM spatial resolution on precipitation and temperature, but as well on discharge. Kleinn et al. (2005) studied the Rhine catchment and concluded that the high-resolution RCM CHRM (14 km) did not significantly improve the discharge performance of the hydrologic simulations compared to the low-resolution RCM (56 km), not even in the catchments in the Alpine having large differences in altitude. This is related to the way the precipitation is aggregated in the hydrological model. The mean precipitation is more important than the fine-scale distribution within the catchment. The coarser RCM resolution (56 km) is sufficient for driving the hydrological model when the whole Rhine basin is considered and when a catchment wide bias correction is applied to the precipitation fields. However, when considering smaller catchment sizes, these catchments could significantly profit from higher RCM spatial resolution (Kleinn, et al., 2005). Dankers et al. (2007) concluded that in local and sub-basin scale, the 12-km data yield better results in hydrological model performance than the 50-km resolution. However, at larger spatial scales the differences between high- and low-resolution RCM climate data and the observations are averaged out, resulting in a similar performance of the hydrological model. Further, the 12-km data led to a better representation of extreme discharge levels compared to the 50-km resolution (Dankers, et al., 2007). When looking at the differences in discharge simulated by different hydrologic models, Mendoza et al. (2016) concluded that the degree of improvement or degradation in hydrological model performance when increasing the RCM spatial resolution depends on the combination of the hydrologic model and the basin. Only the runoff ratio (basin-averaged mean annual discharge divided by the basin-averaged mean annual precipitation) shows an improvement when increasing RCM resolution. Further Mendoza et al. (2016) concluded that the sensitivity of discharge characteristics to horizontal RCM resolution is 'large', regardless of which hydrological model is chosen (Mendoza, et al., 2016). 'Large' is unquantified. In summary, the three studies by Kleinn et al. (2005), Dankers et al. (2007) and Mendoza et al. (2016) show that the choice of spatial RCM resolution influences the performance of simulated discharge. However, this influence depends on the hydrological model choice and the size and characteristics of the catchment.

1.1.2 Components within 'climate impact modeling chain'

As explained in section 1.1, apart from the choice of the RCM having a certain spatial resolution, there are many other components within the climate impact modeling chain which need to be chosen (Clark, et al., 2016). To be able to distinguish the influence of different choices of components on the model output, an overview of these different choices of components is given. Further, an overview is given of the different choices made by Kleinn et al. (2005), Dankers et al. (2007) and Mendoza et al. (2016).

1: RCM

As previously explained, when a GCM is too coarse to force a hydrological model, a downscaling technique is applied. In this approach the output of the GCM is used as boundary condition to force Regional Climate Models (RCM) with a higher spatial resolution. The RCMs can as well be forced by re-analysis data instead of GCMs. Re-analysis data are simulated historic climate conditions produced by a numerical weather prediction model that assimilates observations from the past. When a RCM is forced with re-analysis data as boundary condition instead of GCM data, the output is a clear representation of historical climate conditions (Dee, et al., 2016).

2: Preparation of data to force a hydrological model

As previously explained, the fourth step is to run the RCM and to prepare the RCM output before forcing a hydrological model. The RCM output suffers from climatic biases within the data related to incomplete knowledge of certain processes in the atmosphere and ocean (Görgen, et al., 2010). Therefore, the RCM output is prepared by applying a bias correction which leads to a better representation of the current climate conditions. This correction reduces the uncertainty within the RCM data (Kleinn, et al., 2005).

Further, there are necessary limitations of the spatial and temporal resolution of the RCMs when forcing the hydrological model (Görgen, et al., 2010). The RCM output is grid based while a hydrological model can be grid based, often with another horizontal resolution than the RCMs, or divided in sub-catchments. For each sub-catchment or grid cell the hydrological model needs one spatial mean value of the required forcing data (precipitation, temperature e.d.). There are different methods to derive this spatial mean value. Often a statistical downscaling technique is chosen. This technique makes use of statistical relationships to link the RCM output to for example observations to provide higher resolution outputs (Görgen, et al., 2010). The terms statistical downscaling and bias correction are both used interchangeably. In this research the terms are used as described in above section.

Last, some hydrological models not only need precipitation and temperature data, but potential evapotranspiration (PET) data as well as forcing input. Both temperature and precipitation data can be obtained from the RCMs output or meteorological stations. However, PET needs to be calculated using for instance Penman-Monteith (Monteith, 1965), Thorntwaite's equation (Thornthwaite, 1948) or Penman-Wendling (Berglöv, et al., 2009).

3: Hydrological models

The last step is to simulate discharge using hydrological models. There are many different types of hydrological models which can be chosen. For example, the hydrological models vary based on the level of complexity in terms of space, time and processes. The difference in space depends on the spatial discretization of the catchment. A model can be lumped, semi-distributed or distributed. In terms of time, the time-step can vary (for example hourly or daily). In terms of process description, there are physical-based models, conceptual models and empirical models (Görgen, et al., 2010). Further, the models are different based on the modeling objectives (simulation or forecast) (Görgen, et al., 2010). In general, hydrological models should be sufficiently detailed to capture the most important processes to simulate runoff, but not too detailed because computation time would then be wasted or data availability is too limited (Booij, 2005). The process description of the hydrologic model is called the hydrologic model structure (Clark, et al., 2016).

According to Booij (2005) the most appropriate model to study climate change impacts on river flooding at catchment scale is a conceptual model (Booij, 2005). Conceptual models make use of equations which are based on physics involved in the hydrological system, but are not too complex and are therefore a perfect combination of the need for simplicity and the need for a physical basis (Diermanse, 2001). However, the disadvantage of conceptual models is that first the parameter values are derived by calibration and cannot be derived from direct measurements. This is because conceptual models are usually lumped on a relative large catchment scale (Diermanse, 2001). Second, it is assumed that a model, when calibrated for a certain period, can be applied for future climate conditions. However, this assumption might not be valid since models have a high dependency on the climate of a calibration period (Wagener, et al., 2003). Third, a conceptual model can lead to over-parameterization. This means that because of a large number of parameters, different parameter combinations can give equally good output performances (Booij, 2005). At last, the parameter values might compensate for errors in the input datasets.

Overview choices made by other researches

As described in the previous sections, there are different choices which need to be made. Table 1 shows that different choices (1 to 3 are made by Dankers et al. (2007), Kleinn et al. (2005) and Mendoza et al. (2016) within their studies about the effect of RCM spatial resolution on discharge characteristics. Each choice will influence the effect of RCM spatial resolution on discharge characteristics. Because of this influence or dependency, it is difficult to relate the results only to changes in RCM spatial resolution.

Morover, in the researches of Dankers et al. (2007), Kleinn et al. (2005) and Mendoza et al. (2016), some other choices need to be made as well. These aspects are choices depending on the research objective and (practical) conditions and are not influencing the model output. First, the study area which is selected varies in size, location and other characteristics. Second, the type of discharge can be focused on annual, high or low flow conditions. Third, the aspects where the analysis of the model performance is based on can vary. For example, the mean of the 10% highest simulated discharges can be compared to the mean of the 10% highest observed discharge (Gupta, et al., 2009) and (Görgen, et al., 2010). These choices are represented in Table 1 as well (4 to 6). Based on this Table 1 it can be seen that the results of the three studies cannot be compared because other choices are made for the study area and method to analyze the model performance.

Table 1: Choices made by Dankers et al. (2007), Kleinn et al. (2005) and Mendoza et al. (2016) for their studies about effects of RCM spatial resolution on discharge characteristics

		Dankers, et al., 2007	**Kleinn, et al., 2005**	**Mendoza, et al., 2016**
1.1	RCM	HIRHAM	CHRM	WRF
1.2	RCM Resolutions	12-km and 50-km	14-km and 56-km	4-km, 12-km and 36-km
1.3	RCM Forcing	Re-analysis data	Re-analysis data	Re-analysis data
2.1	Bias correction/ Downscaling method	Inverse distance interpolation scheme	Basin mean bias-correction & bilinear interpolation	Nearest neighbor interpolation
2.2	PET calculation	Penman-Monteith	-	-
3.1	Hydrological model structure	LISFLOOD	WaSiM-ETH 1 km	PRMS, VIC, Noah-LSM, Noah-MP
3.2	Calibrated model?	Yes	Yes	calibrating hydrological models to highest RCM spatial resolution
4.1	Study catchment	Upper Danube	Rhine	Colorado
4.2	Catchment sizes	3803 km^2 4047 km^2 5915 km^2 25624 km^2 25664 km^2 131244 m^2	13000 km^2 18000 km^2 25000 km^2 27000 km^2 145000 km^2	748 km^2 1468 km^2 1819 km^2
5	Type of discharge	Mean annual, low, high	Mean annual and daily	Mean annual, low, high
6	Aspects where the analysis of the model performance is based on	- Daily runoff averaged over a period of 30 years - Return level plots based on a generalised extreme value (GEV) distribution fit to annual maxima	- Annual cycle of mean monthly discharge averaged over a period from 1987-1994 - Daily mean runoff averaged over a period from 1987-1994 - Distribution function of daily runoff - Standard devation of l runoff (month – to – month)	- Runoff ratio (basin-averaged mean annual runoff / basin-averaged mean annual precipitation) (water balance) - Center time of runoff (timing) - Flow duration curve mid-segment slope - Flow duration curve low-segment volume (baseflow volume)

1.2 Research objective

As explained, it is important to study the sensitivity of discharge characteristics to spatial RCM resolution. Kleinn et al. (2005), Dankers et al. (2007) and Mendoza et al. (2016) conclude that the sensitivity of discharge characteristics to RCM spatial resolution depends on the catchment size/topography and hydrological model. As shown in Table 1**,** the three studies cannot be compared and the results cannot be related to only the change in RCM spatial resolution since some choices might have influenced the results**.** To be able to clarify the influence of the catchment size/topography and hydrological model, these aspects need to vary while other components, such as the bias correction, need to be fixed. This leads to the following research objective:

To assess the sensitivity of discharge characteristics to RCM spatial resolution (12.5, 25 and 50 km) simulated by different versions of HBV having different parameterizations for catchments with different characteristics (sizes and topography) in the Rhine basin.

In the following section the choices of components as described in section 1.1.2 are explained considering this research. The numbers in brackets refer to the numbers in Table 1.

1: RCM

For this research the RCM 'RACMO' has been selected (1.1). This RCM can suffer from imperfections. Therefore, the performance of the RCM will be analyzed (shown in section 2: Preparation of data to force a hydrological model). Further, the RCM is forced by re-analysis data instead of GCM outputs (1.2). When forcing the RCM using re-analysis data, the errors within the GCM are not influencing the simulated discharge. Moreover, since the re-analysis data shows a clear representation of historical climate conditions, the simulated discharge forced by the RCM can be compared to observed discharges from the same historical climate conditions. It is important to realize that it is not possible to compare daily data since it is very difficult to assimilate the precipitation as fallen in reality because precipitation strongly varies in space and time (Meijgaard, 2017) (Kysely et al., 2016). However, since re-analysis data gives a clear representation of historical data, analyses are possible when averaging the discharge over a couple of days. Further, the RCM RACMO forced by re-analysis data is available for three spatial resolutions (1.3), namely 12.5, 25 and 50 km for the period 1979-2013 (ESGF, 2016). More information about RCM RACMO is given in 2.2.

2: Preparation of data to force a hydrological model

The hydrological model is forced by the RCM RACMO output (precipitation (P) and temperature (T)). To get insight in the 'RCM performance' (1.1), the simulated discharge obtained from re-analysis RCM data is compared to the simulated discharge obtained from observed precipitation and temperature. Additionally, these two forcing meteorological datasets are compared as well. In general, hydrological models need to be forced with potential evapotranspiration (PET) (2.2). The method to calculate PET will be the same for each of the selected models to reduce the influence of the different methods on the model output. The chosen method is Makkink (explained in section 3.2). Further, no statistical downscaling and bias corrections are applied for the input data. This means that no correction is applied for the imperfections of the RCM output leading to a less good representation of the climate conditions. However, the advantage is these correction methods cannot influence the sensitivity of discharge characteristics to RCM spatial resolution.

3: Hydrological models

To study the influence of the hydrological model choice and to be able to simulate the discharges, the hydrological model HBV-96 (SMHI, 2006) is selected which is a catchment-specific calibrated conceptual model. First, this model is selected because it is available at Deltares. Second, HBV-96 is often used in studies for the Rhine catchment, such as in the Rheinblick 2050 project. At last, conceptual models are often selected for climate impact studies (1.1.2).

The hydrological model performance consists of at least two main components, the model structure (3.1) and the parameter (3.2) performance. This research focusses on the parameter performance since only one hydrological model is considered and hence hydrological model structure performance cannot be assessed. To get insight in the influence of the parameter performance on the model output, the effect of calibration can be analyzed by applying three versions of HBV-96, called the non-calibrated, semi-calibrated and calibrated HBV-96 model. It is important to keep in mind that the model structure performance (3.1) and the parameter performance (3.2) might be influencing each other. More information about the hydrological model is given in section 2.3.

4: Study area
The Rhine catchment as study area has been chosen for different reasons (4.1). First, a lot of observed discharge, precipitation and temperature data measured at different locations are available (section 2.4). Second, many research groups have studied the Rhine catchment. The most recent study is Rheinblick 2050 which main research question is: What are the impacts of future climate change on discharge of the Rhine River and its major tributaries? (Görgen, et al., 2010). Third, HBV-96 is immediately applicable for the Rhine catchment. At last, the Rhine catchment is divided in sub-catchments having different sizes and characteristics (4.2). More information about the Rhine catchment is given in 2.1.

5: Specific discharge characteristics
This study focusses on the sensitivity of low flow conditions, high flow conditions and annual flow conditions to RCM spatial resolution. Although this study does not focus on climate change impacts, both low and high flow conditions are chosen since RCMs are often applied for climate change impact studies. Therefore, it is important to know the effect of RCM spatial resolution on low and high discharges as well (5).

1.3 Research questions

The sensitivity of discharge characteristics to RCM spatial resolution depends on the size of the catchment, the topography (mountainous or lowland) and the hydrological model choice. Therefore, to achieve the objective, the objective is split into three research questions all focusing on one of the specific aspects.

1. What is the sensitivity of discharge characteristics to RCM spatial resolution when looking at different catchment sizes?
2. What is the sensitivity of discharge characteristics to RCM spatial resolution when looking at different catchment topographies (mountainous or lowlands)?
3. What is the sensitivity of discharge characteristics to RCM spatial resolution when looking at the three versions of the hydrological model HBV-96?

1.4 Outline report

In chapter 2, more background is given about the different selected components in this research. These components are the Rhine catchment, the selected RCM RACMO, the hydrological model HBV and the selected observed datasets which are used to analyse the simulated discharges. In chapter 3, the method to answer the three research questions is given. In chapter 4, the different results are shown. In chapter 5 a discussion is given where the results of this research are compared to previous research. At last, in chapter 6 the conclusion and recommendations are described.

2 Case study

In this section more background information is given about the different choices made in this research. First more information about the Rhine catchment and sub-catchments is given. Second, more information about the RCM RACMO is given. Third, in section 2.3 a description of the hydrological model HBV-96 is given. At last, the observed data are described.

2.1 Rhine catchment

The Rhine is the primary connection of one of the most important economic regions of Europe. The Rhine discharges to the Rotterdam Harbor. The human population of the basin equals around 58 million people. The Rhine River has a total length of about 1250 km with a drainage area of 185 260 km^2. The average discharge is about 2300 m^3/s and there are nine countries which are partly or entirely situated in the Rhine catchment (Uehlinger, et al., 2009). About 55% of the Rhine catchment is in German territory, about 25% in Switzerland, France and the Netherlands together and the rest of the catchment is part of Belgium, Luxembourg, Austria, Lichtenstein and Italy (Görgen, et al., 2010). The altitudinal range of the catchment from sea-level to the Alpine part is more than 4000 m. The Rhine catchment is divided in 6 regions based on altitude, namely Alpine Rhine, the High Rhine, the Upper Rhine, the Middle Rhine, the Lower Rhine and the Delta Rhine as shown in Figure 1 (Görgen, et al., 2010). The main tributaries are the Aare (17679 km^2), the Neckar (12616 km^2), Main (24833 km^2) and Moselle (27262 km^2) (Demirel, Booij, & Hoekstra, 2014).

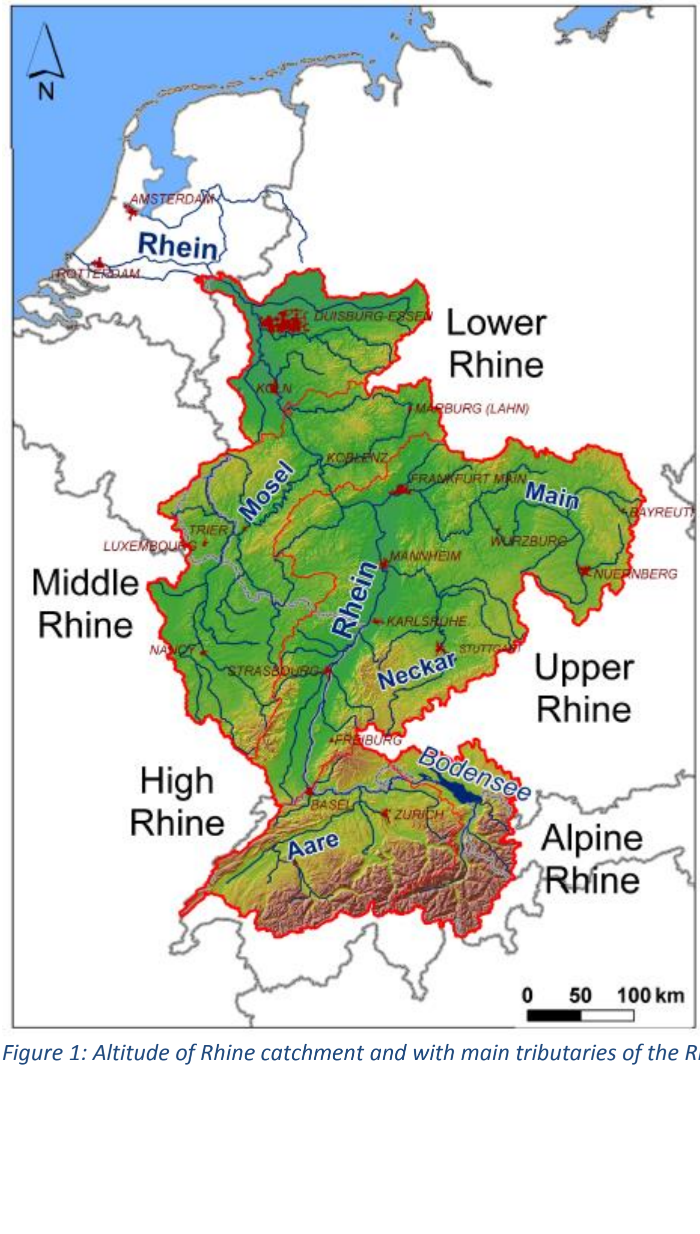

Figure 1: Altitude of Rhine catchment and with main tributaries of the Rhine (Görgen, et al., 2010)

2.2 RCM RACMO

The Regional Atmospheric Climate Model (RACMO2.0) has been developed by the Royal Netherlands Meteorological Institute (KNMI). In total there are three RACMO versions: RACMO2.0, RACMO2.1 and RACMO2.2. In this section the development of RACMO2.0 to RACMO2.2 is described.

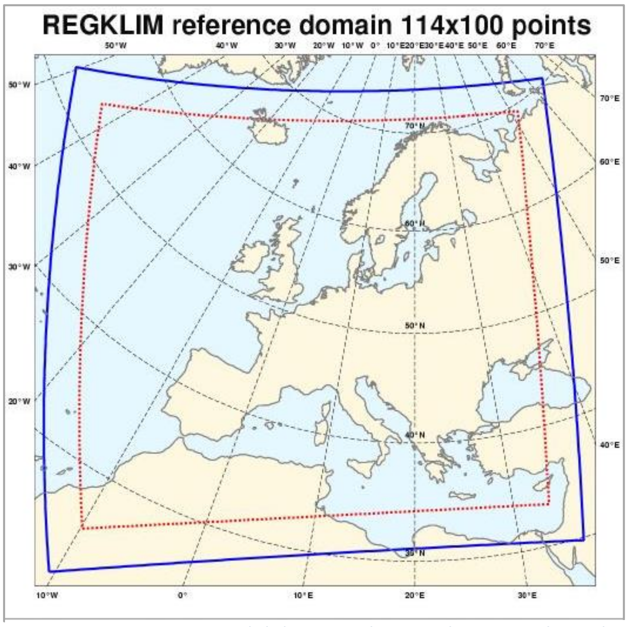

Figure 2: RACMO2.0 model domain, the area between the red and blue line is the boundary relaxation zone (Lenderink, et al., 2003)

In 2001 RACMO2.0 (Figure 2) has been developed having a horizontal resolution of approximately 49 km. This RACMO2.0 is based on the physical parameterization ECMWF, cycle cy23r4 (European Centre for Medium-Range Weather Forecast) and is forced by the GCM ECHAM5 model. The report by Lenderink et al. (2003) provides more information. To investigate the quality of RACMO2.0, the model was driven by boundary conditions given by the ECMWF ERA15 reanalysis data. Precipitation is one of the variables with the largest uncertainty in climate models, due to the large number of parameterized processes involved in the simulation. Total precipitation consists of convective (sub grid) and stratiform (large-scale) precipitation (Kysely, et al., 2016). RACMO2.0 underestimates summer precipitation which appears to be related to the underestimation of convective rain events. Over sea much more convective precipitation is produced when compared to land. Further, the extreme values of daily precipitation amounts are overestimated. Moreover, the vertical structure of the clouds seems unrealistic. The low-level cloud fraction is low and the middle level cloud cover seems overestimated (Lenderink, et al., 2003).

To improve the shortcomings of RACMO2, in 2005 RACMO2.1 has been developed. The horizontal resolution of RACMO2.1 is 25 km. The most important changes were the implementation of a new parameterization of the deep convection, a new prognostic cloud scheme and a change in the land surface scheme to allow more for soil drying (van Meijgaard, et al., 2008). Shortcomings of RACMO2.1 are the warm and dry bias in Eastern Europe. In general, RACMO2.1 is found to be a very good model, scoring best in an inter-comparison between 15 European climate models (Christensen, et al., 2010).

In 2008 RACMO2.1 has been updated to RACMO2.2. Two changes were implemented. First, the existing boundary-layer scheme has been extended with a prognostic variable for turbulent kinetic energy. Further, the soil hydrology has been more refined by introducing spatial heterogeneity into a number of soil parameters. The horizontal spatial resolution of RACMO2.2 is 12.5 km (van Meijgaard, et al., 2012).

The three RACMO versions can all be run for the three different RCM spatial resolutions, namely 12.5 km, 25 km and 50 km. In this research, the newest RACMO2.2 has been used to simulate the datasets for the three different horizontal resolutions. This means that changes between the output can only be explained in the context of RACMO2.2 (Meijgaard, 2017).

2.3 Hydrological model HBV-96

The HBV model has been developed by Bergström at the Swedish Meteorological and Hydrological Institute (SMHI) in 1972. The HBV model is a conceptual, rainfall-runoff model and can be used as a semi-distributed or lumped model (Bergström, 1976). Since the 70s many versions of the HBV model have been developed and the model has been used in more than 60 countries. However, there were some shortcomings and therefore in 1993 the Swedish Association of River Regulation Enterprises (VASO) and SMHI initiated a major revision of the structure of the HBV model leading to HBV-96 as shown in Figure 3 (Lindström, et al., 1997). The description in this section is based on the version HBV-96. However, only the parts are described which are relevant for the HBV Rhine application based on the SHMI report (Berglöv, et al., 2009).

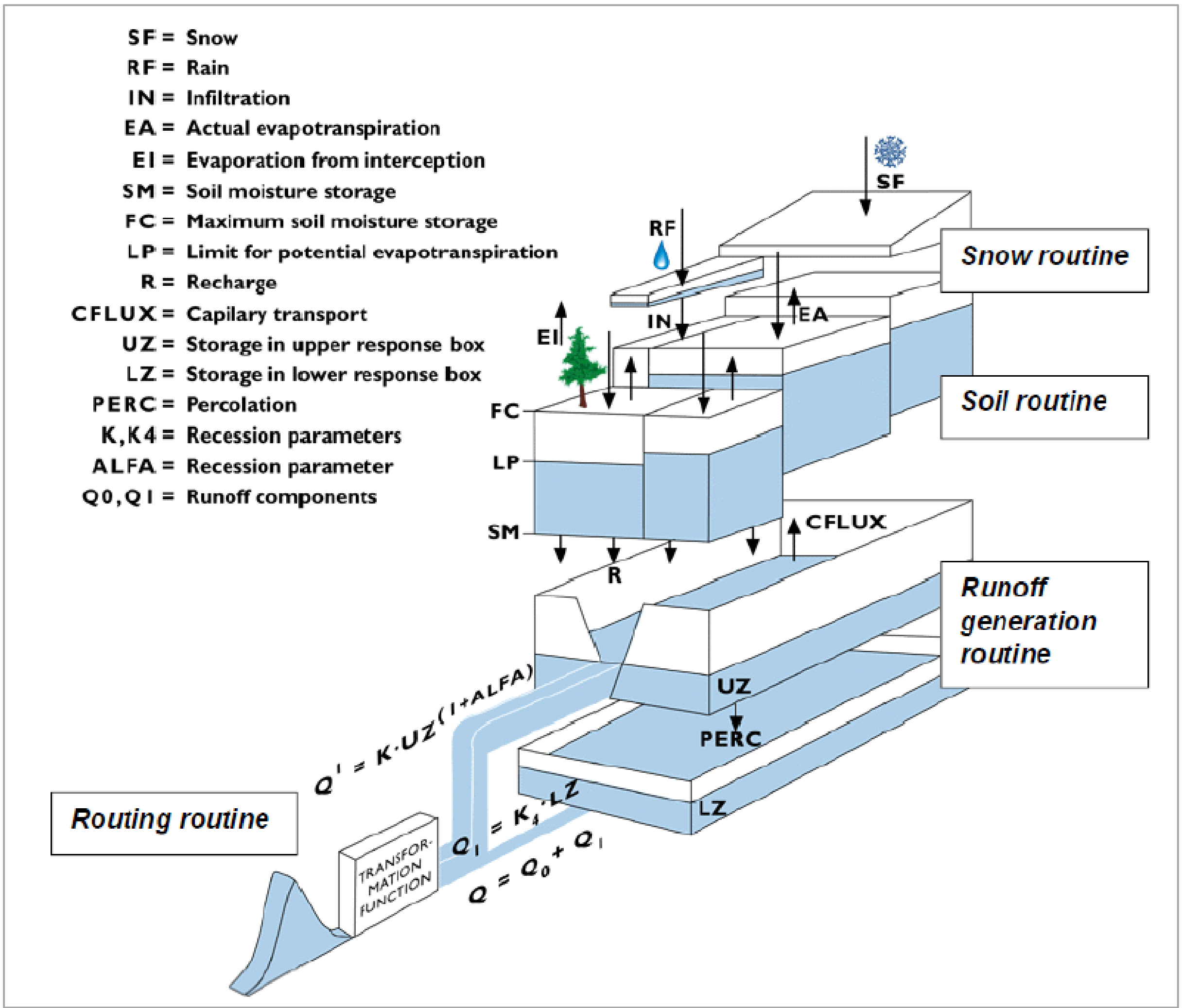

Figure 3: Schematic representation of the HBV-96 model for one sub-catchment (Hegnauer, et al., 2014) after (Lindström, et al., 1997)

General: input and discretization

The model used in this study uses daily precipitation, temperature and potential evapotranspiration data as input. The Rhine catchment is divided in sub-catchments. These sub-catchments are further divided into zones based on elevation. The elevation zones can be further divided into different vegetation zones (forested and non-forested areas). These sub-divisions are only possible in the precipitation and snow routine and the soil routine (Berglöv, et al.,2009).

1: precipitation and snow routine

The precipitation, which is the input of the model, is separated in snow and rainfall using a threshold temperature TT [^{o}C]. The calculations for precipitation and snow are made for each elevation/vegetation zone within the sub catchment. The snow accumulates resulting in a snowpack. The snowpack is assumed to retain melt water as long as the amount does not exceed a certain fraction of the snow. The snow starts to melt according to the melting factor CFMAX [mm/^{o}C * day] depending on the same threshold temperature TT [^{o}C]. The rainfall and snow melt infiltrate into the ground (soil module) (Berglöv, et al., 2009). Further, the potential evapotranspiration is calculated. First the long-term mean monthly potential evapotranspiration is calculated based on the Penman-Wendling approach. Second, the mean monthly potential evaporation is adjusted to daily values using the daily temperature (Berglöv, et al., 2009). In this research another method for calculating the PET is used (3.2).

3: soil routine

The soil routine controlls which part of the rainfall and melt water is stored in the soil, evaporates or forms excess water. The soil routine consists of the soil moisture zone (SMZ) and includes three parameters, namely the β (-), LP (-) and the FC (mm). The actual evaporation equals the potential evaporation if the actual soil moisture divided by the maximum soil moisture storage FC (mm) is above the LP (-). The LP (-) is the limit of water storage for potential evaporation and a fraction of FC (mm). A linear reduction is used when the actual soil moisture divided by the maximum soil storage FC (mm) is below the LP (-). This shows that the actual evaporation is mainly dependent on the soil moisture conditions (SMHI, 2006). Further, the β (-) determines which part of the rainfall directly contributes to the response function and which part increases the soil moisture storage. The FC (mm) determines the maximum soil moisture storage (Berglöv, et al., 2009).

4: response routine

The excess water from the soil moisture zone enters the response routine. There are two zones within the response routine, the upper zone (UZ) and the lower groundwater zone (LZ). The excess water from the soil moisture zone will be added to the storage in the upper zone (UZ). From the upper zone, water percolates to the lower reservoir according to the parameter PERC (mm/day) as long as there is water in the upper reservoir. From the upper non-linear response zone (UZ) water leaves the model as fast runoff. From the lower linear groundwater zone (LZ), water leaves the model as slow runoff. Using a transformation function, the timing and distribution of the resulting runoff is further modified Berglöv, et al., 2009)..

5: routing

In this routine the runoff of different sub-basins is linked using a simplified Muskingum approach. The river channel in each sub-catchment is divided into a number of segments, given by the parameter LAG (day). Each segment will correspond to a delay of one time step. The parameter DAMP describes the damping of the hydrograph along the river. If the DAMP is zero, the shape of the hydrograph will remain the same, so the outflow from a segment equals the inflow to the same segment during the preceding time step (Berglöv, et al., 2009).

The calibrated HBV-96 model

The parameter values for this research for the HBV-96 model structure are based on a study by Winsemius et al. (2013). This study derived the parameter uncertainty for HBV-96 using the Generalized Likelihood Uncertainty Estimation (GLUE) method. The GLUE method is used to asses and to reflect the parameter uncertainty, contained in the selection of the model parameters. For each sub-catchment first 5 or 6 calibration parameters were selected. For each sub-catchment Monte Carlo simulations are performed. The philosophy of GLUE is that instead of finding one optimal parameter set, multiple behavioral sets are selected. Based on different measures such as the Nash-Sutcliff and Relative Volume Error, the parameter sets that meet the constraints of the measures are selected as ‘behavioral sets’. Figure 4 giving an overview of the NS value of each sub-catchment (Hegnauer, et al., 2013). The datasets which have been used for the calibration are HYRAS 2.0 for precipitation and E-OBS v4 for temperature and a discharge dataset from the German Federal States, combined with the HYMOG dataset (section 2.4 (Winsemius, et al., 2013)).

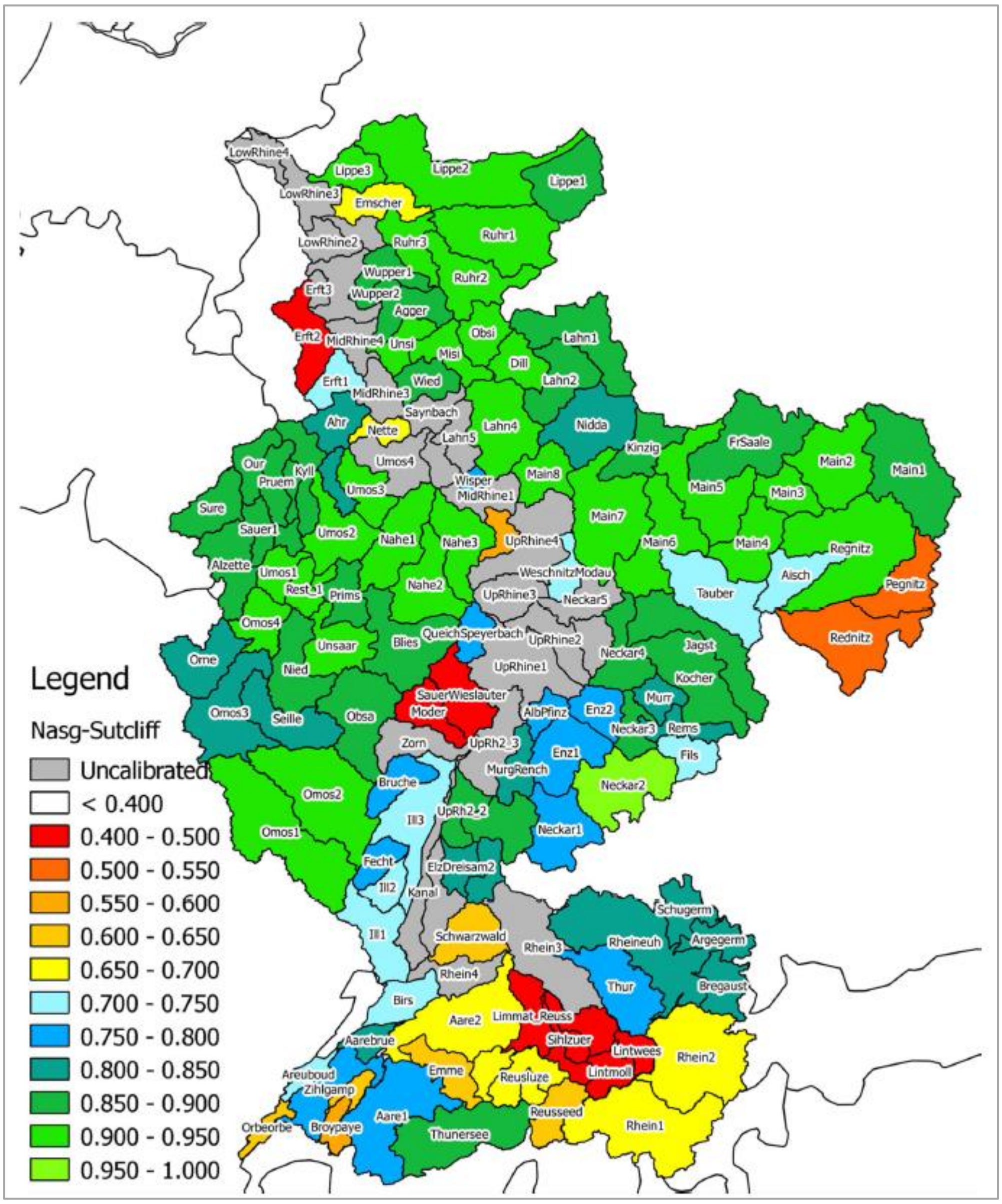

Figure 4: Overall performance of the HBV-96 model. The NS values are the optimum values for all parameter sets. This is not the NS value that corresponds to the final parameter sets per se, but it gives a good impression of the overall performance. Areas in grey were not calibrated. Calibration period 01-01-1985 to 31-12-2006 (Hegnauer, et al., 2013)

2.4 Datasets

As described in section 2.3, the hydrological models are forced by both observed data (precipitation (P), temperature (T) and potential evapotranspiration (PET)) and RCM RACMO data at three different resolutions. This leads to four different simulated discharge series. These simulated discharge series are then compared to observed discharge (Q) data. First the observed datasets are described and second the RCM RACMO data are explained. An overview of the datasets is given in Table 2.

Table 2: Overview of datasets used in this research

Type of dataset	Source of dataset	Start of time period	End of time period	Temporal resolution	Spatial resolution
Observed Q	BAFU (Switzerland)	1974 (different per station)	01-01-2011	Hourly	Station based
Observed Q	BFG (Germany)	1989 (different per station)	01-01-2008	Hourly	Station based
Observed P	HYRAS	01-01-1977	31-12-2006	Daily	~ 25 km 0.25 degree
Observed shortwave downward radiation	HYRAS	01-01-1974	31-12-2006	Daily	~ 25 km 0.25 degree
Observed T	EOBS	01-01-1955	31-08-2016	Daily	~ 25 km 0.25 degree
RCM P, T & shortwave downward radiation	RACMO	01-01-1979	31-12-2015	Daily	50 km, 25 km and 12.5 km

2.4.1 Observed data

Precipitation data

As observed precipitation data HYRAS 2.0 gridded dataset has been selected. This dataset contains a large set of observations for the period 1951-2006 from different countries. The dataset has been constructed by the Deutsche Wetterdienst (Rauthe, et al., 2013). The dataset has a resolution of 0.25 degree and a daily temporal resolution. It is based on 6200 precipitation station located in Germany and the neighboring countries. To calculate the gridded data set from station data, the REGNIE method has been used. This method is a combination of multiple linear regression considering orographic conditions (longitude, latitude, height above sea level, exposition and mountain slope) and inverse distance weighting (Rauthe, et al., 2013).

Potential evapotranspiration (PET)

PET cannot be observed but need to be calculated based on observed data. In this research the Makkink method has been used, which means that observed temperature data and shortwave radiation data are needed. The choice for this method is explained in section 3.2. The 'observed' PET is available for the period between 1974 and 2006 because of the availability of the dataset at Deltares.

Temperature data

For observed temperature data, the KNMI's 0.25 degree gridded E-OBS version 4.0 has been used. This dataset contains observations for the period 1955-2016. This dataset is grid based. The dataset has been transformed from station based to grid based by first interpolating the monthly mean temperature using three-dimensional thin-plate splines, then interpolating the daily anomalies using kriging with an external drift and then combining the monthly and daily estimates. The anomalies are obtained by calculating the difference between the daily observation and the monthly mean (Haylock, et al., 2008). The external drift is used to incorporate elevation dependencies (Goovaerts, 2000).

Discharge data

For the discharge stations the datasets collected by the BfG from the German Federal States for the period 01-11-1989 to 01-11-2007 are used (hourly) (BfG, 2017) . This dataset contains 102 discharge stations located in Germany. Further, 32 discharge locations are obtained from BAFU (Bundesambt Für Umwelt) containing hourly data from 01-01-1974 to 01-01-2011 (BAFU, 2012).

2.4.2 RACMO RCM data

The RACMO RCM has been forced by reanalysis data resulting in datasets for three resolutions, namely 12.5 km, 25 km and 50 km. The datasets have been downloaded from the CORDEX project (ESGF, 2016). As explained, the hydrological models HBV-96 and PCR-GLOBWB need precipitation, temperature and potential evapotranspiration (PET) as input data. The potential evapotranspiration need to be calculated separately using the Makkink method (section 3.2). Table 3: Overview datasets simulated by the RCM RACMOTable 3 gives an overview of the datasets of precipitation and temperature and the dataset needed to calculate the PET.

Table 3: Overview datasets simulated by the RCM RACMO and used in this research

Dataset	Unit	Time period
Precipitation	(kg m^{-2} s^{-1})	01-01-1979 – 31-12-2015
Temperature	(K)	01-01-1979 – 31-12-2015
Surface downward shortwave radiation	(W m^{-2})	01-01-1979 – 31-12-2015

3 Method

In this chapter the method to achieve the objective of this research is described. The objective of this research is divided into three research questions. The first four sections (3.1 to 3.4) of this method are needed as preparation for this thesis. In section 3.1 the selection of the sub-catchments is described. Further, before running the hydrological models, the datasets need to be prepared. This is described in section 3.2. In section 3.3 the sensitivity analysis and calibration of HBV is described and in section 3.4 the selection of the three different HBV-96 models is given. In section 3.5 the method to analyze the sensitivity of discharge characteristics to RCM spatial resolution is given, leading to the results of the three research questions.

3.1 Selection sub-catchments

As described in section 0, the sensitivity of discharge characteristics to RCM resolution depends on the catchment size/characteristics and the hydrological model. To assess the sensitivity of discharge characteristics to RCM resolution, different catchments are selected. According to the Rheinblick report, the Rhine catchment is divided in seven sub-catchments (Görgen, et al., 2010). However, it is important that the selected catchments for the analysis are not influenced by catchments upstream. This leads to five different catchments which can be selected (Table 4). The selection is based on five criteria and the results of these criteria are shown in Table 4 as well. It can be concluded that for the Alpines the West Alpine fulfills most criteria and for the lowlands the Main fulfills most criteria.

Table 4: The five catchments which are not influenced by catchments upstream and the 5 criteria per catchment

Catchments in the Rhine	1: Variety in topography	2: Relative slope (-)	3: Number of qualified discharge stations	4: Discharge stations located at outlet catchment	5: Size of catchment (Demirel, Booij, & Hoekstra, 2014)
Main	Lowlands	*0.00543*	9	*Yes*	*24833 km²*
Moselle	Lowlands	0.00767	*16*	No	27262 km²
Neckar	Lowlands	0.00783	11	No	12616 km²
East Alpine	Alpines	0.02468	5	*Yes*	16051 km²
West Alpine	Alpines	*0.02804*	*24*	*yes*	*17679 km²*

1: Variety in topography

Kleinn et al. (2005) concluded that 'even in high-altitude Alpine catchments' the stream discharge performance did not significantly improve when increasing the RCM resolution. To verify this conclusion, from the five catchments which are not influenced by upstream catchments, catchments are selected based on the topography. One catchment is selected in the mountainous Alpines (East or West Alpine) and one catchment is selected in the lowlands part of the Rhine catchment (Main, Moselle or Neckar).

2: Relative slope

Second, the two catchments are selected based on the largest (mountainous Alpines) or lowest (lowlands) difference in altitude ($\Delta a\ (m)$) of the river relative to the area in km^2 of the sub-catchment ($A\ (m^2)$. This relative slope (s_{rel}) is calculated as follows:

$$s_{rel} = \frac{\Delta a}{\sqrt{A}} \qquad \text{(Equation 1)}$$

As shown in Table 4, the Main is located in the lowlands and has the smallest relative slope. The West Alpine is located in the Alpines and has the largest relative slope. Based on this criterium the Main and West Alpine are most suitable to select.

3: Quality of the discharge stations

Third, since the simulated discharges are compared to the observed discharges, the selection of the two catchments is based on the availability of observed discharge stations within the catchments. In total there are 134 discharge stations available in the Rhine catchment containing data from 01-01-1974 to 01-01-2011. However, it depends on the discharge station if data is available for the total period. A discharge station has been approved as being 'good' if there is less than 20% missing data and if the minimum observed discharge is above zero. Based on these criteria the Moselle and West Alpine are most suitable to choose.

4: Discharge stations located at outlet catchment

Fourth, to be able to compare the simulated discharge by HBV-96 against the observed discharge, it is important that the discharge station is located at the outlet of the HBV-96 sub catchment which is the case for the Main, West Alpine and East Alpine.

5: Size of the catchment

Fifth, the studies by Dankers et al. (2007), Mendoza et al. (2016) and Kleinn et al. (2005) explain that the sensitivity of discharge characteristics to RCM spatial resolution depends on the catchment size. Therefore, it is important to select two catchment sizes, namely a 'large' catchment and a 'small' catchment. The definition of 'large' and 'small' is based on the sizes of the catchments as studied by Dankers et al. (2007), Mendoza et al. (2016) and Kleinn et al. (2005) to make sure that the definition of 'large' and 'small' is around the same to make comparison possible. The large catchments of these studies vary between 13000 km$^{\mathbf{2}}$ and 27000 km^2 with an average of 22381 km^2. Based on these sizes the Main and the West Alpine are most suitable to select.

Apart from the 'large' catchments, two smaller catchments are selected as well. The smaller catchments which are studied by Dankers et al. (2007), Mendoza et al. (2016) and Kleinn et al. (2005) vary between the 700 km$^{\mathbf{2}}$ and 6000 km^2 with an average of 2971 km^2. The selected 'smaller' catchments are located within the Main and the West Alpine to make sure that the modeled characteristics of the catchments are around the same and can therefore be compared. It is important that these smaller catchments are located upstream as well to decrease the influence of upstream catchments. Further, the quality of the discharge stations and the size of the catchments (criteria 3 and 4) are used for selection. The smaller sub-catchments need to have a size between 700 km^2 and 6000 km^2. Based on these criteria for the West Alpine the smaller sub-catchment Reuss-seedorf (836 km^2) has been selected and for the Main the sub-catchment Kinzig (928 km^2) has been selected. Figure 5 shows the selected larger and smaller catchments.

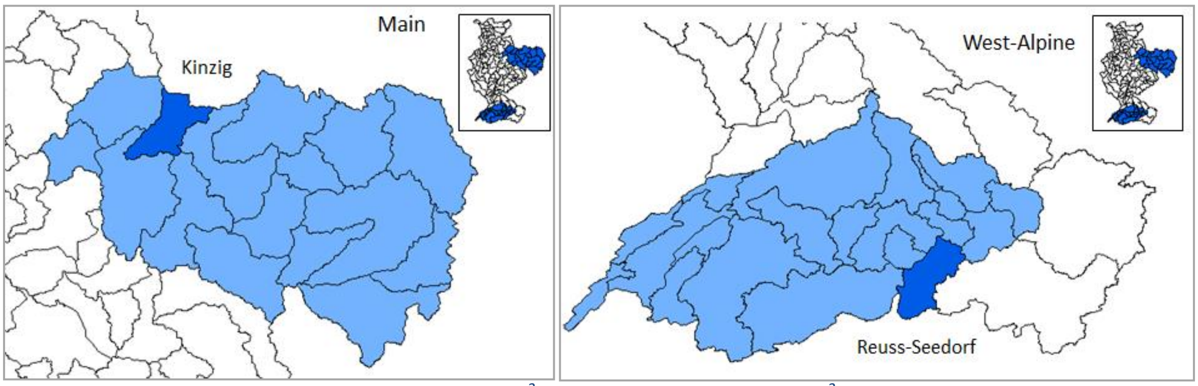

Figure 5: Selected large catchments Main (24833 km^2) and West Alpine (17679 km^2) and smaller catchments Kinzig (928 km^2) and Reuss-Seedorf (836 km^2)

3.2 Preparation of datasets

The hydrological models are forced by observed data (HYRAS) and RCM RACMO datasets (50 km, 25 km and 12.5 km). The input data needed for the hydrological model HBV-96 is precipitation (mm/day), temperature (^{o}C) and potential evapotranspiration (mm/day). The observed precipitation and temperature are already converted to the needed units. However, the RCM RACMO datasets consist of precipitation (kg m^{-2} s^{-1}) and temperature (K). Therefore, these datasets need to be converted to precipitation (mm/day) and temperature (°C). Further, the potential evapotranspiration (PET) needs to be calculated since PET cannot be observed and is not simulated by the climate model. To calculate the potential evapotranspiration, the Makkink method has been selected. This method has been chosen because the observed (HYRAS) potential evapotranspiration has been calculated based on the Makkink method. Further, the method required limited input variables (only temperature and shortwave downward radiation). Other observed datasets to calculate PET using another method were not available. PET has been calculated using equation 2 (Rijtema, 1959). A detailed calculation of PET in (mm/day) can be found in appendix (A).

$$PET = \frac{s}{s+\gamma} * \frac{6,5*10^6 R_s}{\rho_w*\lambda} \qquad \text{(Equation 2)}$$

- R_s shortwave downward radiation (W m^{-2})
- s slope of function of vapour pressure versus air temperature (hPa °C^{-1})
- ρ_w density of water (kg m^{-3})
- λ heat of vaporization (J kg^{-1})
- γ psychometric constant (hPa °C^{-1})

Spatial aggregation datasets

After the conversion of the datasets to the necessary units and the calculation of PET, the datasets need to be spatially aggregated. The RACMO datasets (spatial resolution of ~ 50 km, ~ 25 km and ~ 12.5 km) and the observed datasets HYRAS and EOBS (spatial resolution of ~ 25 km) are grid based. However, the hydrological model HBV-96 simulates daily discharge for 148 sub-catchments of the Rhine instead of grids (te Linde et al., 2008). For each sub-catchment HBV-96 needs one spatial mean value of the required forcing data (precipitation, temperature and potential evapotranspiration). Since the grids of the RACMO datasets and observed datasets do not perfectly fit the sub catchments of the hydrological model, spatial aggregation is needed as shown in Figure 6 (Görgen, et al., 2010). There are several methods and in this research the area weighted average method is chosen. This means that values for one sub-catchment are calculated by weighted averaging all grid cells (RCM/observed data) within a given sub-catchment. Appendix B shows figures of the different RACMO layers on top of the hydrological model.

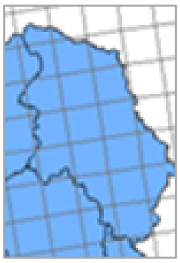

Figure 6: Example of the intersection of a grid layer and a sub-catchment

Further, in this research the HBV-96 model is used which is as well used in the GLUE analysis. The observed P and T datasets (HYRAS and EOBS) have been used for the GLUE analysis as well. HBV-96 applies an elevation correction to correct for the difference in DEM (digital elevation map) of the HYRAS dataset and the average central elevation height of the stations in each sub catchment. For the RACMO datasets the average sub-catchment elevations have been calculated by spatially aggregating the RACMO DEM. Using this height, the similar height correction method is applied as for HYRAS while running HBV-96. The average height for each catchment can vary up to 400 m in the Alpines between the three RACMO datasets mutually having a different spatial resolution and the HYRAS dataset. When applying a lapse rate of 0.6 ^{o}C / 100 m, this difference in height can lead to a temperature difference of 2.4 ^{o}C between the four datasets for one sub-catchment.

3.3 Sensitivity analysis and calibration

As described in section 3.2, Makkink is selected as method to calculate the potential evapotranspiration. However, since HBV-96 has been calibrated by using the Penman-Wendling approach and by adjusting the mean monthly PET (Görgen, et al., 2010), the HBV-96 model has to be recalibrated. As described in section 3.1, only the Main and West Alpine are used for analysis. Therefore, only these two catchments are calibrated for the new calculated PET. To perform a robust calibration, first a sensitivity analysis is performed.

3.3.1 Sensitivity analysis

The sensitivity analysis gives insight in the parameters which have the highest influence on model performance and therefore are most suitable to calibrate. To perform a sensitivity analysis, first the parameters to include are selected. Second, the sub-catchments for the sensitivity analysis are selected. Third, the 'starting' values and the ranges of the parameters for the sensitivity analysis are determined. Fourth, the objective function to analyze the sensitivity of the parameters is selected.

Selection of parameters

In previous studies, several parameters have been calibrated in the HBV model for the Rhine basin (Table 5). Based on these studies, several parameters are selected to include in a sensitivity analysis. The calibrated parameters used in the GLUE study are selected and the parameters which are calibrated in more than three studies for the Rhine. The selected parameters are fc, khq, perc, beta, alfa, lp, tt, cfmax and k4.

Table 5: Calibration parameters of HBV-96 previous research for the Rhine

	Definition	**Unit**	**1**	**2**	**3**	**4**	**5.1**	**5.2**	**6**
Fc	Maximum value of the soil moisture storage (mm)	(mm)	X	X	X	X		X	
KHQ	Recession rate	(1/day)	X	X	X	X	X	X	X
Perc	Percolation of water to the lower reservoir	(mm/day)		X	X	X	X	X	X
Beta	Control for the increase in soil moisture for every mm of precipitation	(-)		X	X	X		X	X
Alpha	Parameter for the non-linear behaviour in the response function	(-)		X		X			
Lp	Soil moisture value above which evapotranspiration reaches its potential value	(-)		X		X		X	
tt	Threshold temperature to define at which temperature snow melt occurs	(°C)			X	X		X	X
cfmax	The melting factor	(mm/day/°C)			X	X	X	X	X
K4	Linear outflow coefficient	(-)				X	X	X	X
maxbas	Time base of the triangular distribution in the transformation function	(days)				X			X
Pcalt	Lapse rate parameter for precipitation	(-)				X			
RFCF	Rainfall correction factor	(-)				X			X
Dttm	Value tob e added tot t to give the threshold temperature for snow melt	(°C)				X			
Ttint	Total length of temperature interval in which part of P that is considered to be snow decreases linearly from 1 at the lower end to 0 at upper end	(°C)				X			
Cflux	Maximum capillary flow from upper response box to soil moisture zone	(mm/day)				X			

1 (te Linde et al., 2008)	4 (SMHI, 2006)
2 (Winsemius, et al., 2013)	5 (Kersbergen, 2016) 5.1 calibration, 5.2 sensitivity analysis
3 (Hegnauer, et al., 2013)	6 (Berglöv, et al., 2009)

Selection of sub-catchments

After the parameters are selected, it is important to select the sub-catchments for sensitivity analysis. As explained previously, only the Main and the West Alpine are calibrated. Therefore, the sensitivity analysis is performed only for these two catchments. Figure 7 and Figure 8 show that these two catchments consist of several sub-catchments. The sensitivity analysis and the calibration for these sub-catchments are performed by using observed discharge time-series. However, as shown in Figure 7 and Figure 8 there are less discharge stations than sub-catchments. Therefore, the sub-catchments upstream of one discharge station are grouped. This results in the same number of groups as discharge stations. The sensitivity analysis and the calibration are performed for each group using the discharge station located at the outlet of the group. The grouped sub-catchments and observed discharge stations are shown in Figure 7 and Figure 8.

Starting values of parameters

The sensitivity analysis is performed by changing the parameter values from the current starting value (100%) to lower values (to 50%) and higher values (150%) by steps of 10%. However, the starting parameter values need to be defined. These starting (100%) parameter values are based on the parameter values as obtained by the GLUE calibration. However, the GLUE calibration led to different parameter sets for each sub-catchment even if this sub-catchment is part of the same group with one outlet discharge station. In this research the sub-catchments belonging to one group, are calibrated together. Therefore, the parameters as calibrated by GLUE are recalculated leading to one parameter set for one group. This new parameter set is then used for sensitivity analysis and as starting parameter set for the calibration. The new parameters are calculated by first giving a weight to each sub-catchment based on the area and second by calculating the average parameter value based on this weight.

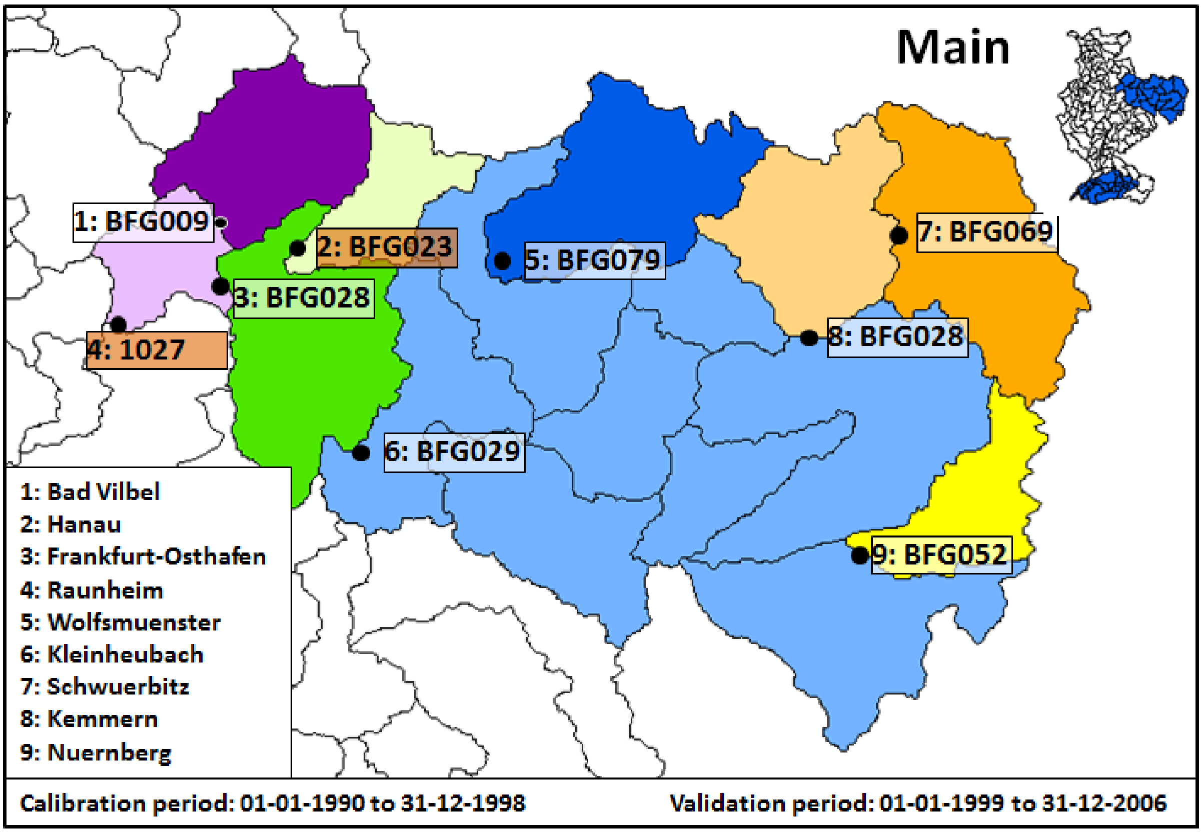

Figure 7: The Main with grouped sub-catchments. Each colour represents a group of sub-catchments. The white marked discharge stations are used for calibration. The orange marked discharge stations are used for both calibration and analysis of results

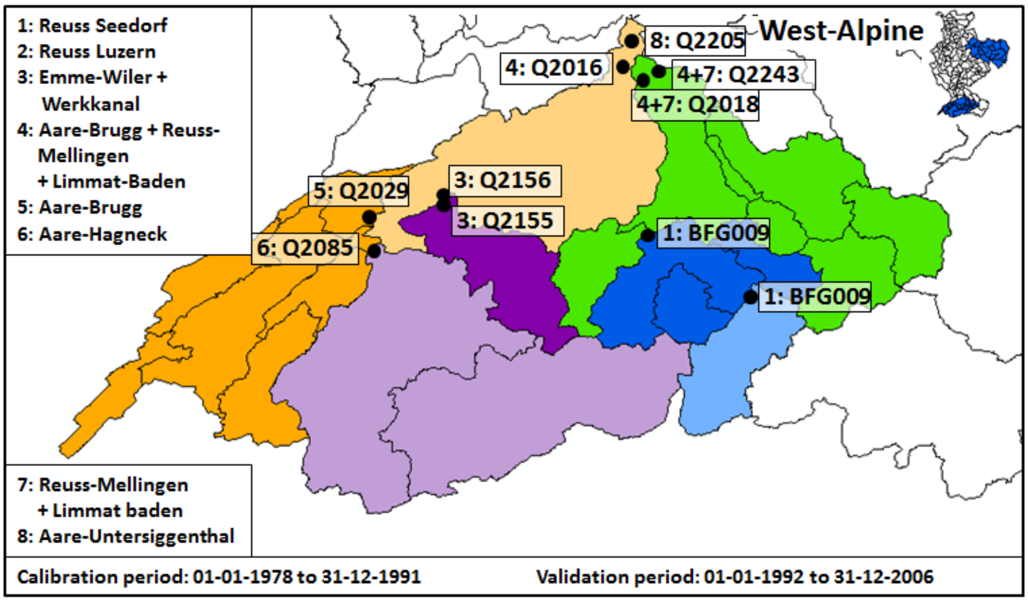

Figure 8: West Alpine with grouped sub-catchments. Each colour represents a group of sub-catchments. The orange marked discharge station number 8 is only used for analysis, number 1 for both analysis and calibration

Objective function

The sensitivity analysis is performed by changing the parameter values and then analysing the effect of changing the values on the model performance. For this analysis, the objective function KGE (Kling Gupta Efficiency) is selected. In section 3.3.2 the choice for the KGE is explained. The optimal value of KGE is 1 when representing the best model performance. Figure 9 shows an example of the sensitivity analysis. Based on this analysis most sensitive parameters are selected for calibration. Less calibration parameters reduce the computational time, increase the convergence time and decrease the chance of over-parameterization. Over-parameterization might lead to multiple acceptable parameter sets instead of a single optimal parameter set. Per group the parameters are selected which result in a KGE changing more than 10%. When this results in a selection of four or five parameters, these parameters are selected for calibration. However, when there are less or more parameters sensitive than four or five parameters, the objective function NSE (Nash Sutcliffe) is used as well (section 3.3.2). Additionally, the parameters are selected which lead to a change in NSE of more than 15%. When there are still too many or not enough sensitive parameters, the four most sensitive parameters are selected.

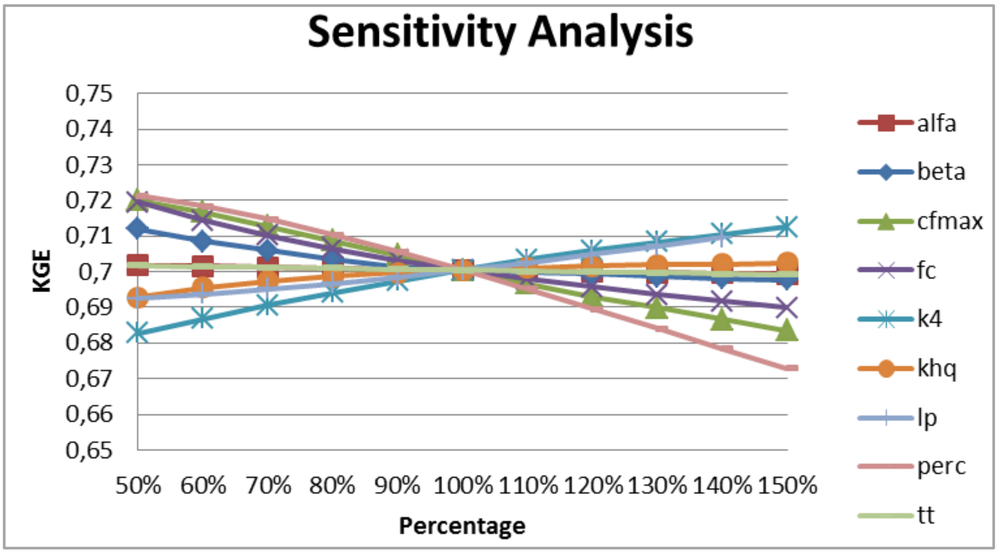

Figure 9: Example of the sensitivity analysis for one sub-catchment

3.3.2 Calibration and Validation

Based on the sensitivity analysis, the calibration parameters are selected for the different grouped sub-catchments as shown in Figure 7 and Figure 8. These parameters are calibrated following four different aspects; optimization algorithm, objective function, termination criteria and calibration period (Gupta & Sorooshian, 1995). In this the aspect parameter ranges is added. These aspects are described in this section.

Optimization algorithm

First, for calibration the Shuffled Complex Evolution method developed at the University of Arizona (SCE-UA) is chosen because it is a robust and effective calibration method. One of the most important concepts the SCE-UA is based on is that this method allows more 'regions of attraction'. This prevents the model for finding a local optimum parameter set instead of a global optimum parameter set. Another concept is that the calibration method is a combination of deterministic and stochastic approaches (Duan, Sorooshian, & Gupta, 1994). The advantage of the deterministic part is that the algorithm uses the results of the previous run to improve the next parameter set instead of running 10000 randomly generated parameter sets without memorizing previous gained knowledge (totally stochastic). Jeon et al. (2014) compared the SCE-UA method and the Genetic Algorithm (GA) method. They recommended using the SCE-UA calibration method when the model simulation does not take a long time and the user does have sufficient time for an optimization program to search for the best values of calibration parameters (Jeon, Park, & Engel, 2014). The calibration procedure is done by using Spotpy in Python (Houska, et al., 2015).

Objective Function

Second, after the optimization method is chosen, the objective function is selected. This objective function is used to calculate the model performance for each generated parameter set during calibration. The Nash-Sutcliffe Efficiency (NSE) is most widely used for calibration and evaluation of hydrological models with observed data. The MSE (Mean Squared Error) and NSE are closely related and can be calculated as follows (Gupta, et al., 2009), where $Q_{obs,i}$ is the observed discharge, $\overline{Q_{obs,\iota}}$ represents the mean of the observed discharge and $Q_{sim,i}$ the simulated discharge.

$$NSE = 1 - \frac{\sum_{i=1}^{n}(Q_{obs,i} - Q_{sim,i})^2}{\sum_{i}^{n}(Q_{obs,i} - \overline{Q_{obs,\iota}})^2} = 1 - \left(\frac{MSE}{\sigma_{obs}^2}\right)$$

Although the NSE is commonly used for calibration, there is one concern. The NSE has an oversensitivity to peak discharges and can therefore better be used to evaluate only high-discharge simulation efficiency (Muleta, 2012). It is now generally accepted that the calibration of hydrological models should be approached as multi-criteria framework.

This can be done by combining multiple objective functions to one objective function. This method is often used to be able to use a single-criterion automated search algorithm, such as the SCE-UA. However, when combining multiple criteria in evaluation, it has to be considered that these criteria are mathematically related. For example, the NSE can be decomposed into separated components. This gives a better understanding into how different criteria are interrelated and what the contribution is of different components causing a particular model performance to be 'good'. Gupta et al. (2009) decomposed the NSE to analyse the relative importance of different components in the context of hydrological modelling. As a result of this decomposition, the KGE objective function has been developed. One advantage can be that the different components are having the same weight. The KGE can be calculated as follows (Gupta, et al., 2009):

$$KGE = 1 - ED$$

$$ED = \sqrt{(r-1)^2 + (\alpha - 1)^2 + (\beta - 1)^2}$$

$$\alpha = \frac{\sigma_{sim}}{\sigma_{obs}} \qquad \beta = \frac{\mu_{sim}}{\mu_{obs}}$$

Where r is the linear correlation coefficient, α the of ratio between the relative variability in the simulated and observed values and β is the ratio between the mean simulated and mean observed discharges, i.e. it represents the bias.

Parameter ranges

Third, for each calibration parameter a lower boundary and upper boundary is defined. The calibration parameters differ per grouped sub-catchments and depend on the results of the sensitivity analysis. The boundaries are based on the boundaries as given within the GLUE report and the SMHI report. These values can vary between Germany and Switzerland (Winsemius, et al., 2013) (Hegnauer, et al., 2013) & (SMHI, 2006). In general, the given values as defined by the GLUE report are used as shown in Table 6.

Table 6: Parameter ranges for Switzerland and Germany for the nine selected calibration parameters

	alfa	beta	cfmax	fc	k4	khq	lp	perc	tt
	(-)	(-)	(mm/day/°C)	(mm)	(-)	(1/day)	(-)	(mm/day)	(°C)
Switzerland	0.2 -1.2	0 - 4	1 - 6	10 - 350	0.001 – 0.1	0.01 - 1	0.3 - 1	0.5 – 5.5	-3 - 1
Germany	0.2 -1.2	0 - 4	1 - 6	100 - 500	0.001 – 0.1	0.01 - 1	0.3 - 1	0.5 – 5.5	-2 - 2

Number of iterations

Fourth, it is decided how many calibration runs are needed for the calibration. When using the SCE-UA method, the number of runs depends on the number of runs needed to reach convergence. In this research the maximum number of runs is 10000 per sub-catchments. According to van den Tillaart et al. (2013), the amount of iterations is 4000 per sub-catchment for eight calibrating parameters for HBV (Tillaart, Booij, & Krol, 2013).

Calibration and validation period

Fifth, the calibration and validation periods need to be defined. In this research the split-sample test is used which means that the available observed time series is split into two segments, one is used for calibration and one for validation (Klemes, 1986). This method is chosen since the observed data for Switzerland consist of a period of 34 years and for Germany 19 years. To have enough dry and wet years in the calibration, the calibration period should be at least 10 to 15 years according to SMHI. The dataset for Swiss is split into two segments of 17 years. The dataset for Germany is split into a calibration period of 10 years and a validation period of 9 years. The calibration and validation period is seen in Figure 7 and Figure 8.

3.4 Three versions of the HBV-96 model

As explained in section 0 the hydrological model choice influences the model output and therefore the total model performance. The hydrological model performance is mainly influenced by the model structure performance and the parameter performance. To get insight in the parameter performance of HBV-96, the effect of calibration is analysed by comparing three versions of HBV-96. Further, when comparing the simulated discharges of the different versions of HBV-96 with the simulated discharges of different RCM spatial resolutions, the importance of RCM spatial resolution can be compared to the importance of calibration. The three versions are called the calibrated, semi-calibrated and non-calibrated HBV-96 version. The difference between the three models is the defined parameter set.

First, the parameter set for the non-calibrated HBV-model was based on the default parameter values for Swedish conditions obtained from the SMHI manual of HBV-96 (SMHI, 2006). The non-calibrated HBV model uses the same parameter values for each sub-catchment leading to one parameter set for the whole Rhine catchment. Second, between 1997 and 2004 the German Federal Institute of Hydrology (BfG) set up and calibrated the HBV model for the river Rhine in cooperation with Rijkswaterstaat. However, this model did not perform well when incorporated in the forecasting system of FEWS. The main reason was that the precipitation, temperature and evaporation data available for real-time applications differed from the ones used for calibration. Therefore, the SMHI recalibrated this model. The parameter set which is used as starting point for the recalibration, is selected as parameter set for the semi-calibrated model (Berglöv, German, Gustavsson, Harbman, & Johansson, 2009). The semi-calibrated model uses as well one parameter set for the whole Rhine catchment. Third, the parameters for the calibrated HBV-96 model are based on the calibration method as described in 3.3. This means that each of the clustered sub-catchments have the same parameter values but can be different for each cluster of sub-catchments. Appendix C shows the values of the different parameter sets for the calibrated HBV model, the semi-calibrated HBV model and the un-calibrated HBV model.

3.5 Analysis of total model performance

This section provides a method to answer the three sub-questions. In section 3.5.1, a general framework is given about the analysis of the sensitivity of discharge characteristics to RCM spatial resolution when looking at topography, size of the catchment and hydrological model parameter estimation. In section 3.5.2 the method to quantify the analysis in the first section is given. This quantification is based on the total model performance. In section 3.5.3, different components which influence the total model performance and therefore the sensitivity of discharge characteristics to RCM spatial resolution, are described.

3.5.1 General framework

As described in section 0, the sensitivity of discharge characteristics to spatial RCM resolution depends on the topography (1), the size (2) of the catchment and the hydrological model (3). The topography (1) and size of the catchments (2) are found in the four selected sub-catchments as shown in Table 7. The hydrological model – parameter estimation (3) is based on the three HBV-96 versions (calibrated, semi-calibrated and un-calibrated version). Further, as explained in section 0, the analysis is performed for low flow (A), high flow (B) and annual discharge (C).

Table 7: Overview sub-catchments with characteristics

Sub-catchment	Topography (1)	Size (2)
Main	Lowland (hilly)	Large
Kinzig	Lowland (hilly)	Small
West Alpine	Mountainous	Large
Reuss-seedorf	Mountainous	Small

The sensitivity of discharge characteristics to RCM spatial resolution is analyzed by comparing the change in total model performance when increasing the RCM spatial resolution. This model performance is based on the comparison between Q_{obs} and $Q_{sim-RCM}$ (Table 8). The method to quantify the model performance is given in section 3.5.2.

Table 8: Definition of two discharge series in this research

	Definition
Q_{obs}	Observed discharge time series
$Q_{sim-RCM}$	Simulated discharge time series obtained by HBV-96 forced with RCM RACMO data in three RCM spatial resolutions (50 km, 25 km and 12.5 km)

In summary, for each of the version of the hydrological model – parameter estimation (3), the Q_{obs} and $Q_{sim-RCM}$ are compared for the combinations A, B, C and for the different aspects topography (1) and size of the catchment (2). In the end the third aspect hydrological model – parameter estimation (3) is analysed by comparing the three versions of HBV-96. Figure 10 gives an overview of the different combinations.

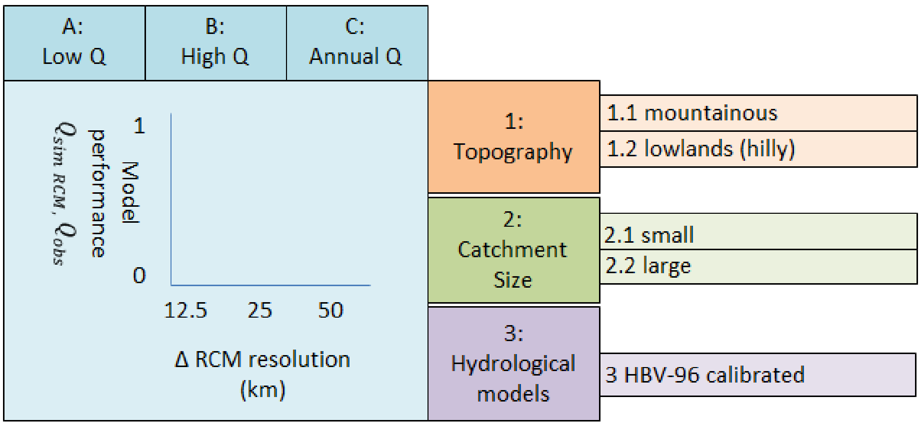

Figure 10: General framework for analysing the sensitivity of RCM spatial resolution on discharge characteristics

3.5.2 Quantification of the total model performance by statistical analysis

To quantify the sensitivity of discharge characteristics to RCM spatial resolution, the total model performance is calculated for each RCM spatial resolution based on a statistical analysis for annual discharge, high flows and low flows. No time series analysis is performed since it is not possible to compare daily re-analysis data with the daily observed data as explained in section 0.

Annual discharge

For the annual analysis both the mean (μ) and the standard deviation (σ) are calculated for the observed daily discharge and the simulated daily discharge. The ratio between the μ_{obs} and the μ_{sim} gives insight in the bias. The ratio between the σ_{sim} and the σ_{obs} gives insight in the relative variability in the simulated and observed values (Gupta et al., 2009). If the ratio is equal to one, the mean or standard deviation of the two series are equal to each other. If the ratio is above 1, it means that the mean or standard deviation of the observed discharge is overestimated. If the ratio is below 1, it means that the mean or standard deviation of the observed discharge is underestimated.

$$ratio\ \mu = \frac{\mu_{sim}}{\mu_{obs}}$$

$$ratio\ \sigma = \frac{\sigma_{sim}}{\sigma_{obs}}$$

High flows

To analyse the high flows, the flow duration curve (FDC) is used. In the FDC the empirical cumulative frequency of discharges is plotted against the percentage of time that the discharge is equalled or exceeded (Tallaksen & Lanen, 2004). The exceedance percentile for high flows is 10% (Q10) (Görgen, et al., 2010). The 10% highest simulated discharges (FDC_Q10) are compared to the 10% highest observed discharges (FDC_Q10). If the curve of the simulated discharges is above the curve of the observed discharges, the high flow is overestimated. Further, the ratio of the mean and the standard deviation are calculated for the high flows. The high flows are defined as high flows when $Q > Q10$.

Low flows

For low flows the exceedance percentile is 90% (Q90) (Görgen, et al., 2010). When comparing 10% lowest simulated discharges FDC_Q90 to the 10% lowest observed discharges (FDC_Q90), information is obtained about the over- or underestimation of the low flows. Further, the ratio of the mean and the standard deviation are calculated for the low flows. The low flows are defined as low flows when $Q < Q90$.

3.5.3 Contribution of different components to total model performance

As explained in section 3.5.1 and 3.5.2, the sensitivity of RCM spatial resolution to discharge characteristics when looking at the topography (1) and size of the catchment (2) is determined by analysing the change in total model performance when increasing the spatial resolution. The hydrological model – parameter estimation (3) is analysed by comparing the change in model performance for the three different HBV-96 models.

As explained in section 1.1.2 different choices are made within the modelling chain. These different choices influence the model output and therefore the total model performance. To understand which component contributes to the total model performance, the total model performance is divided into the hydrological model performance (1.1) and the RCM RACMO performance (1.2) as shown in Figure 11. When multiplying the two ratios indicating these two performances, the ratio of the total model performance (1) is shown. The hydrological model performance (1.1) is influenced mainly by model structure performance (1.1.1) and the parameter performance (1.1.2). In this section the difference between the performances is explained and the method to quantify these performances. The purpose of this analysis is to better understand the total model performance and therefore the sensitivity of discharge characteristics to RCM spatial resolution.

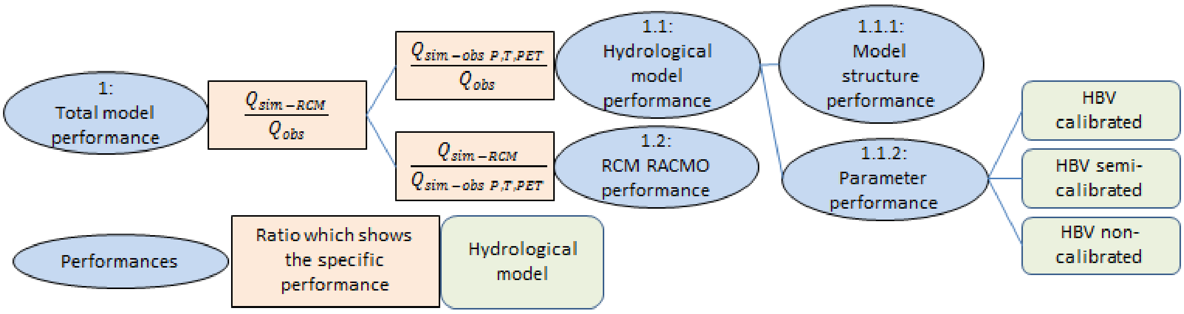

Figure 11: Overview of contribution of hydrological model and RCM RACMO performance to total model performance

Table 9: Definition of the three discharge series as used in this research

	Definition
Q_{obs}	Observed discharge time series
$Q_{sim-obs\ P,T,PET}$	Simulated discharge time series obtained by HBV-96 forced with observed meteo data (P, T , PET)
$Q_{sim-RCM}$	Simulated discharge time series obtained by HBV-96 forced with RCM RACMO data for three RCM spatial resolutions (50 km, 25 km and 12.5 km)

1.1 Dependency of total model performance on hydrological model performance

As shown in Figure 11, the hydrological model performance is presented by the ratio $Q_{sim-obs\ P,T,PET}/Q_{obs}$. The definition of these discharge series is given in Table 9. Since the simulated discharge is forced with observed meteorological data, it is assumed that the errors involved in the input data are negligible when assuming that the observed meteorological data represents the reality. It is important to keep in mind that the ratio $Q_{sim-obs\ P,T,PET}/Q_{obs}$ both represents the model structure performance (1.1.1) and the parameter performance (1.1.2).

1.1.1: Dependency of hydrological model performance on model structure performance

As explained in section 1.1.2, the hydrological model structure suffers from imperfections because of for example incomplete knowledge of certain hydrological processes. The ability of the hydrological model structure to represent the reality as good as possible is called the model structure performance (1.1.1) and influences the hydrological model performance (1.1) which is determined when comparing Q_{obs} and $Q_{sim-\ obs\ P,T,PET}$. It is not possible to analyse the model structure performance separately since no other hydrological model structures are used in this research.

1.1.2: Dependency of hydrological model performance on parameter performance

The parameter performance depends on among others the calibration of hydrological models and quality of the input data. The parameter performance (1.1.2) influences the hydrological performance (1.1) as well. It is possible to analyse the parameter performance separately when comparing the ratio of $Q_{sim-\ obs\ P,T,PET}/\ Q_{obs}$ of the calibrated HBV-96 model with the semi-calibrated and un-calibrated HBV model.

1.2: Dependency of total model performance on RCM RACMO performance

The RCM output suffers from an imperfection related to incomplete knowledge of certain processes in the atmosphere and ocean resulting in climatic biases (Görgen, et al., 2010). In this research the RCM RACMO data are on purpose not corrected for biases to make sure that the bias correction does not influence the sensitivity of discharge characteristics to RCM spatial resolution. However, the RCM RACMO performance could be different per resolution and contributes to the total model performance. Therefore, the RCM RACMO performance is analyzed by comparing the $Q_{sim-RCM}$ and the $Q_{sim-obs\ P,T,PET}$ as shown in Figure 11. Further, the RCM RACMO datasets precipitation (P), temperature (T) and potential evapotranspiration (PET) are analysed separately by comparing it to observed data. For the P and PET, the mean of the two datasets for 10% lowest, 10% highest and annual P and PET is compared. For the T, the absolute difference between observed and RACMO data is analysed.

4 Results

In section 4.1 the results of the hydrological model performance are presented. In section 0 the RCM RACMO performance is analyzed. Both hydrological model performance (section 4.1) and RCM RACMO performance (section 0) contribute to the total model performance. In section 4.3, the results of the total model performance are shown. When the total model performance is analyzed, the results of the three research questions are given by analyzing the change in total model performance when increasing the spatial resolution. The first research question is to analyze the sensitivity of discharge characteristics to RCM spatial resolution for the size of the catchment. Second, the sensitivity is analyzed for the aspect topography and third for the aspect parameter estimation. An overview of above described structure is given in Figure 12.

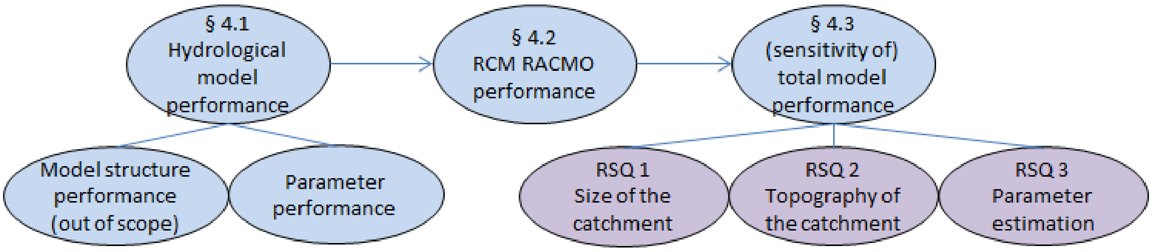

Figure 12: Overview structure of the chapter 'Results' where RSQ is defined as 'research question'. The text below the paragraph number does not necessarily correspond to the title of the paragraph.

4.1 Contribution of the hydrological model performance

In this section the results of the hydrological model performance for the calibrated HBV-96 model are presented. This hydrological model performance is shown in two ways. In section 4.1.1 the results of the calibration and validation of HBV-96 are given expressing the hydrological model performance in the objective function Kling Gupta Efficiency. In section 4.1.2 the hydrological model performance of the calibrated HBV-96 model is described by the ratio $Q_{sim-obs\ P,T,PET}/Q_{obs}$ as explained in section 3.5.3.

4.1.1 Calibration and validation HBV-96 for the Main and West Alpine

The results of the calibration and validation are presented in Figure 13 and Figure 14. As explained in section 3.3.2, only the Main and West Alpine are calibrated. Further, the objective function used for calibration is the Kling Gupta Efficiency. In Figure 13 and Figure 14, the first number represents the KGE for the calibration period and the second number the KGE for the validation period. The optimal value for KGE is 1. A value above 0.8 shows a good model performance (Rwasoka, et al., 2013).

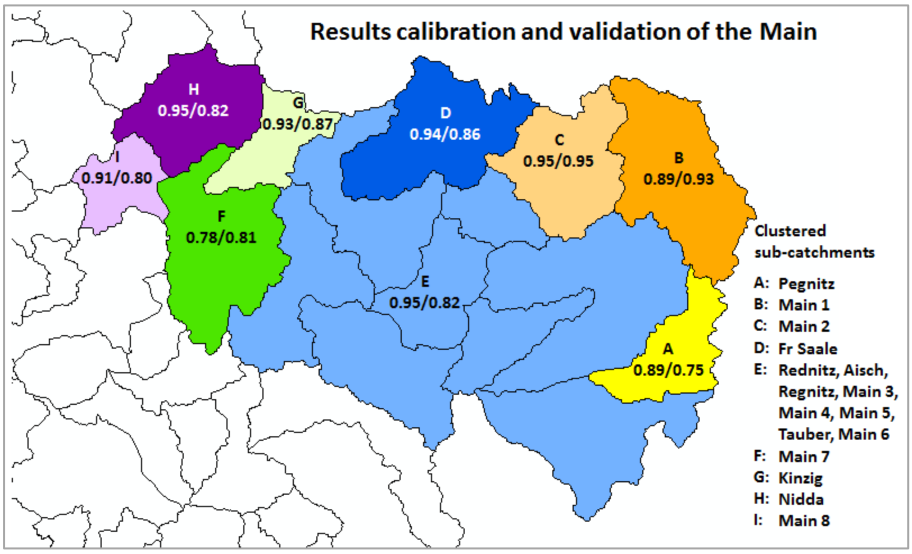

Figure 13: Results calibration and validation of the Main, first KGE value represents calibration, second validation.

Both the calibration and validation show good performances having values above 0.8. Only Pegnitz in the Main and the grouped sub-catchments Reusluze, Engebuoc and Muotinge show less performance, especially for the validation. However, the KGE still has a value above 0.74. The values of the parameters for each group of catchments are given in appendix D.

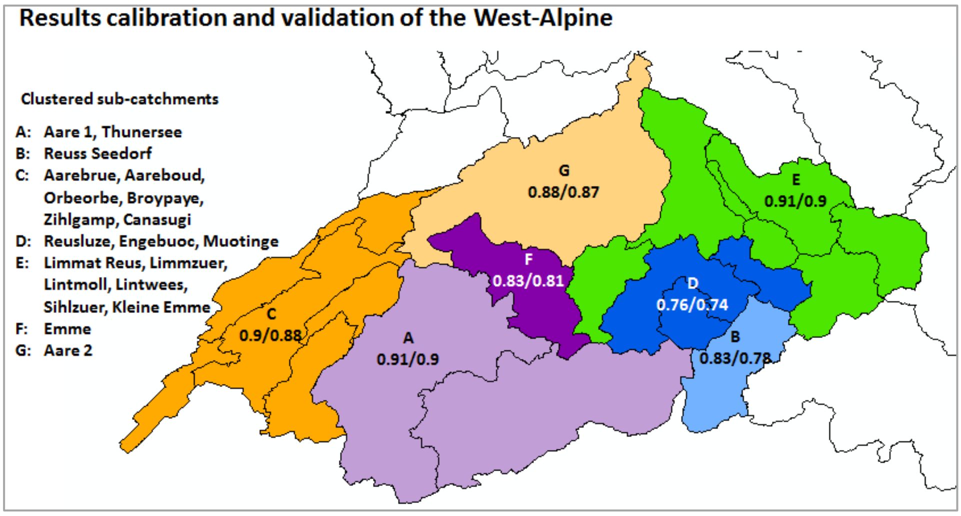

Figure 14: Results calibration and validation of the West Alpine, first KGE value represents calibration, second validation

4.1.2 Hydrological model performance HBV-96

Figure 15 shows the hydrological model performance of the calibrated HBV-96 model. The hydrological model performance contributes to the total model performance. Therefore, it is important to pay attention to the low hydrological model performances. If the ratio of $Q_{sim-obs\ P,T,PET}/Q_{obs}$ is equal to one, a perfect model performance for the mean or standard deviation is shown. If the ratio is between 0.8 and 1.2 a good model performance is reflected (black lines in Figure 15). The black circles reflect the model performance which are less good, namely below 0.8 or above 1.2 for the calibrated HBV model. In total, there are eight situations where the hydrological model performance is less good for the calibrated HBV model. However, in general the performance is good having a value between 0.8 and 1.2, especially for the annual discharges.

In depth analysis of low hydrological model performances of the calibrated HBV-96 model

The hydrological model performance is influenced by both the model structure performance and parameter performance (section 3.5.3). In other words, when analysing the model structure performance and parameter performance, the low hydrological model performances can be clarified. Since no other model structure is analysed in this research, only insight in the parameter performance is obtained. This is done by comparing the hydrological model performance of the semi-calibrated and un-calibrated HBV-96 model to the calibrated HBV-96 model. The model performances of the other two versions of HBV-96 are represented in Figure 15 as well.

If the hydrological model performance of the semi- or un-calibrated HBV model shows a value closer to 1 than the calibrated model does, the assumption can be made that when adjusting the parameter values of the calibrated model, the performance of the calibrated model still can improve. However, it is important to realise that this assumption depends on the chosen method to analyse the model performance and the type of discharge (low, high, annual) to analyse the performance. Further, since the model structure is equal for the three versions of HBV-96, the difference in performance between the three versions of HBV-96, can only be caused by differences in parameter values. Of course the hydrological model performance is influenced by a combination of the model structure and parameter performance and therefore the exact contribution of both cannot be quantified.

In the eight situations where the hydrological model performance of the calibrated HBV-96 model is below 0.8 or above 1.2, there are four situations where the semi-calibrated HBV model or un-calibrated HBV model shows a better performance. First, for the standard deviation of the high discharge for Reuss-Seedorf the un-calibrated model shows a ratio closer to 1 than the calibrated model. For the mean of the low discharge of the Main, the semi-calibrated model shows a large underestimation and the un-calibrated model an overestimation. Because of this over- and underestimation, there is a possibility that a certain parameter value combination from the semi- and un-calibrated model leads to a better hydrological model performance. Further, for the standard deviation of the low discharge for Main the un-calibrated model shows a ratio closer to 1 than the calibrated model. At last, for the mean of the low discharge for Kinzig, again the semi- and un-calibrated model together might lead to a model performance closer to 1.

The difference in hydrological model performance between the three versions of HBV-96 is caused by parameters having different values. It is interesting to first analyse which parameters cause the low hydrological model performance of the calibrated model for the 8 situations as shown in the black circles. Second, it is interesting to compare the parameter values for the three HBV-96 versions when the semi- or/and un-calibrated models show better performances. This insight can help to improve the HBV model in further research. The results of this analysis are found in appendix E.

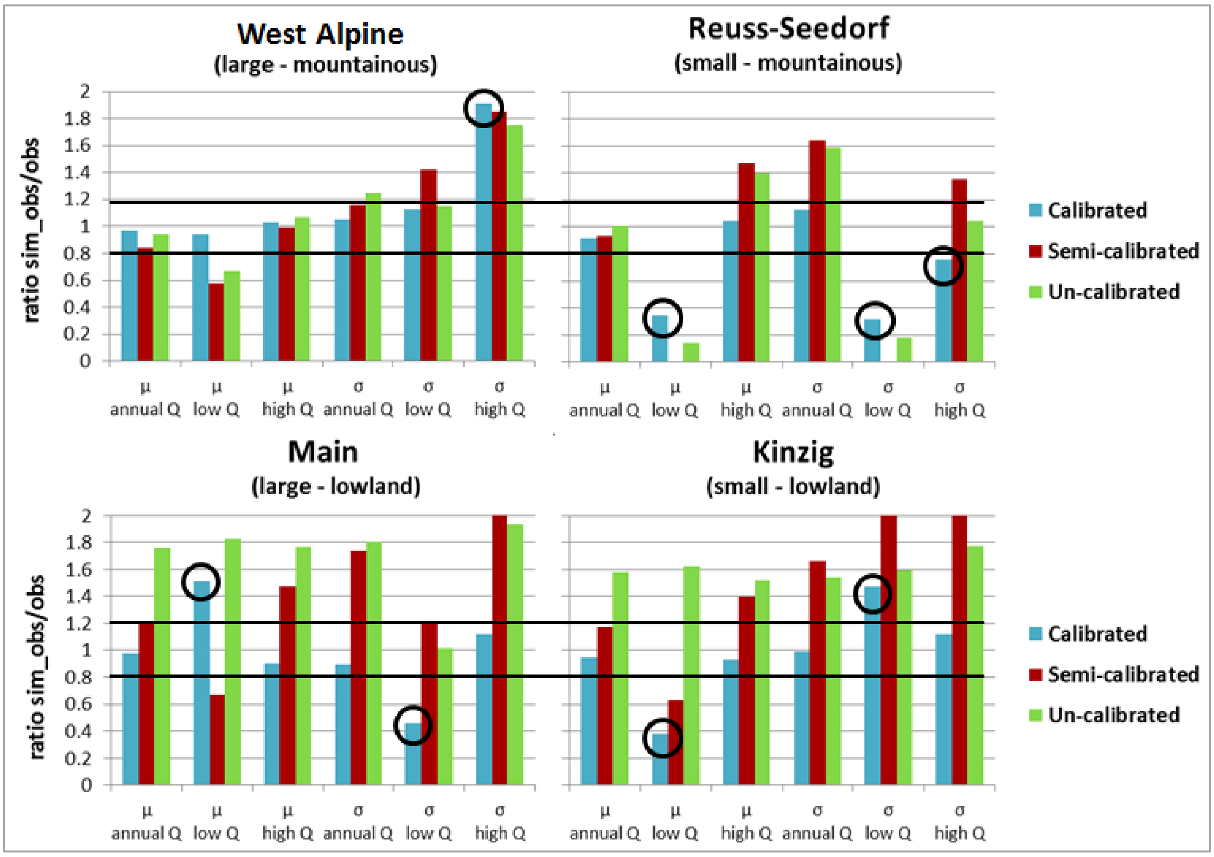

Figure 15: hydrological model performance for the calibrated, semi-calibrated and un-calibrated HBV-96 presented by the ratio of simulated discharge forced with observed meteorological data and the observed discharge. If the ratio is 1 a perfect model performance is presented and between 0.8 and 1.2 a good model performance is presented (black lines). The black circles show the performances for the calibrated model below 0.8 or above 1.2. Some performances are very low and out of the presented range. Main: semi-calibrated model, standard deviation of high discharge (2.3), Kinzig: semi-calibrated model, standard deviation low discharge (2.3), standard deviation of high discharge (2.6). The μ represents the mean and the σ the standard deviation of the annual, low or high discharge.

4.2 Contribution of the RCM RACMO performance

In this section the RCM RACMO performance is analyzed by determining the ratio $Q_{sim-RCM}/Q_{sim-obs\ P,T,PET}$ as shown in Figure 16. The RCM RACMO performance contributes to the total model performance. The lowest RCM spatial resolution is referred to as R50, the middle resolution as R25 and the highest resolution as R12. In general, only for West Alpine, Reuss-Seedorf and Main the mean of the low discharge shows a good performance (between 0.8 and 1.2). Further, the discharge is in general overestimated by the RCM RACMO since most ratios show a value above 1. However, there are some exceptions. First, for the West Alpine the mean of the low discharge underestimates the simulated discharge forced with observed meteorological data. Reuss-Seedorf overestimates the discharges, except for the standard deviation of the low discharge. Kinzig shows an underestimation or good performance for the R50. Figure 16 shows that Reuss-Seedorf in general shows the best RCM RACMO performance.

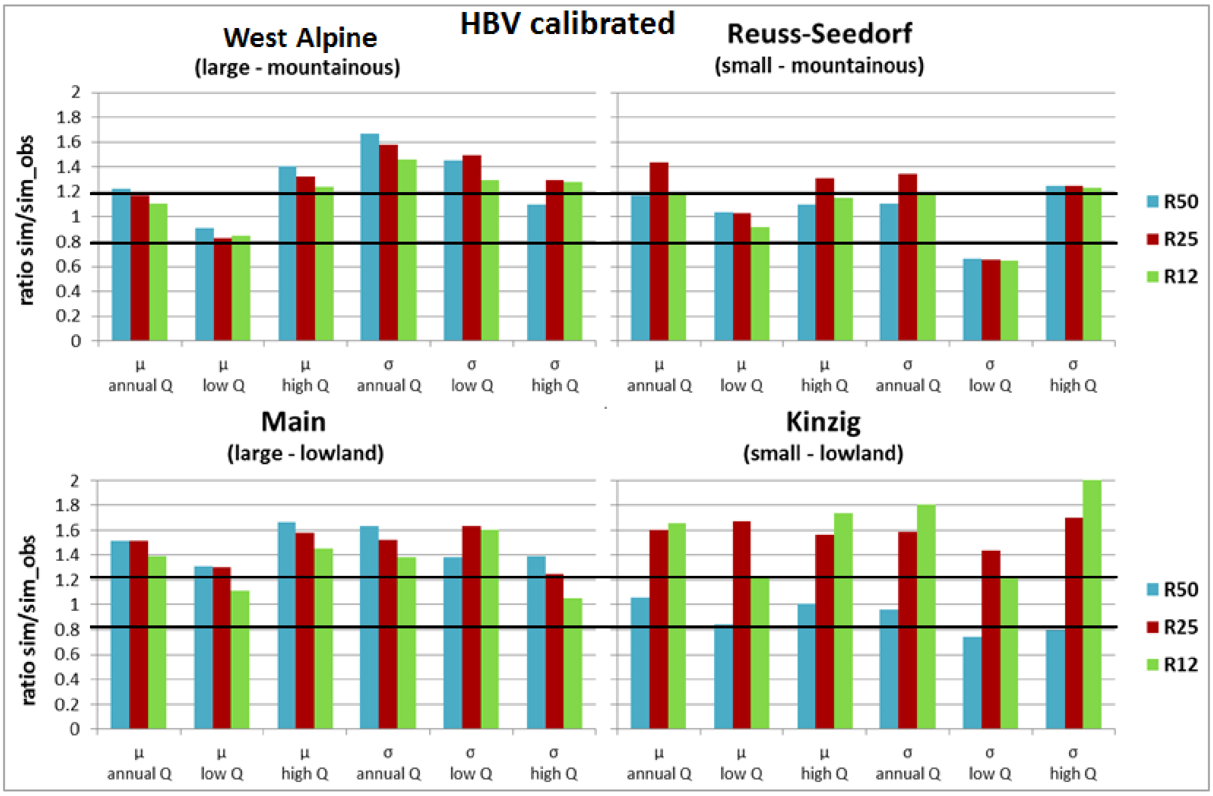

Figure 16: RCM RACMO performance for the four different catchments. The μ represents the mean and the σ the standard deviation of the annual, low or high discharge. R50 is the lowest RCM spatial resolution, R25 the middle and R12 the highest. If the ratio is 1, a perfect RCM RACMO model performance is presented and above 0.8 and below 1.2 a good model performance is presented (black lines). Some performances are very low and out of the presented range. Kinzig: standard deviation of the high discharge (R25:2.06). The ratio is calculated for a period of 16 years (1990-2006).

In depth analysis of RCM RACMO performance

The results of the RCM RACMO performance are further analysed by comparing the RACMO mean of the low, high and annual precipitation, temperature and potential evapotranspiration to the mean of the observed precipitation (P), temperature (T) and potential evapotranspiration (PET). Low is defined as the 10% lowest amounts of P, T and PET and high as the 10% highest amounts of P, T and PET. This analysis gives insight in possible relations between performance of the meteorological data and the RCM RACMO performance. The P and PET are represented by the ratio of the simulated P or PET and the observed P or PET. However, the temperature is analysed by representing the absolute difference between the mean of the observed and simulated temperature in degrees Celsius. Only the mean of the data is analysed since it is difficult to link the standard deviation of meteorological data to the standard deviation of the discharge in a sub-catchment. Further, the number of simulated dry days is analysed as well. The analysis is first performed for West Alpine and Reuss Seedorf located in the West Alpine (mountainous) and second for Main and Kinzig in Germany (lowlands) because the hydrological characteristics differ between mountainous and lowland areas. It is important to notice that the P, T and PET together contribute to the RCM RACMO performance and it is therefore not possible to quantify the influence of the three datasets separately.

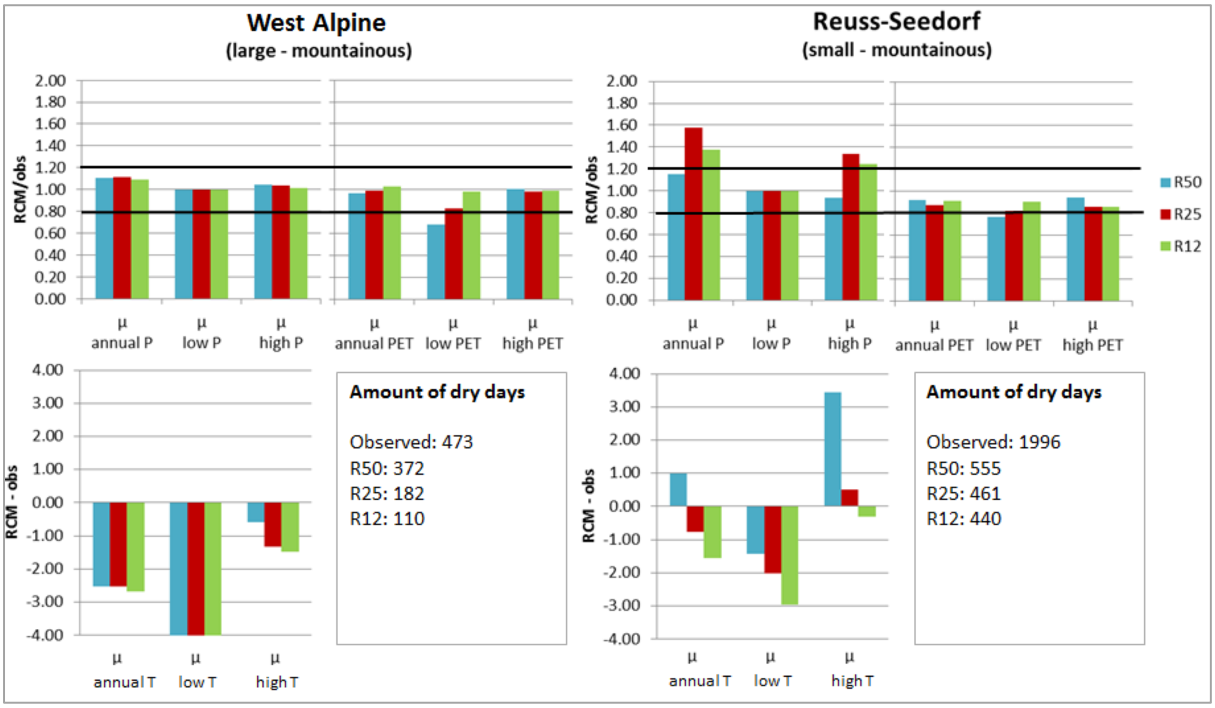

Figure 17: RCM RACMO meteorological data (P, PET (Makkink), T) compared to the observed data (P, PET (Makkink), T) for both the West Alpine and Reuss Seedorf. The P and PET are presented as ratio of the RCM data and the observed data. The temperature is presented as difference between RCM data and observed data. Further, the number of dry days over the period 1990-2006 is presented. R50 is the lowest RCM spatial resolution, then R25 and then R12

<u>West Alpine and Reuss Seedorf</u>

Figure 16 shows that for West Alpine and for Reuss Seedorf the mean of the annual and high discharge is overestimated. For West Alpine the mean for the low discharge is underestimated. For Reuss-Seedorf the mean of the low discharge shows a very good performance for R50 and R25 and an underestimation for R12.

Both West Alpine and Reuss Seedorf are located in the mountainous West Alpine. In this area there is a lot of snowfall resulting in snow melt during summer time. Therefore, the high discharge occurs in summer time and the low discharge in winter time. During winter time, the temperatures can drop below the temperature value where precipitation is defined as snowfall. For the West Alpine this threshold temperature is -3.5 ^{o}C and for Reuss Seedorf -3.9 ^{o}C. The mean of the observed 10% lowest temperatures for the West Alpine is below the -4 ^{o}C and for Reuss Seedorf below -13 ^{o}C showing that the mean of the observed low temperature has reached the threshold where precipitation is defined as snow. Figure 17 shows that both Reuss Seedorf and West Alpine show an underestimation of the temperature during winter time (mean of the low temperature). This means that the precipitation is more often defined as snowfall instead of rainfall leading to a lower discharge in wintertime. Figure 16 shows indeed an underestimation of the mean of the low discharge during winter time. The mean of the low temperature is more underestimated for West Alpine than for Reuss Seedorf which can explain why the low discharge is more underestimated for West Alpine than for Reuss Seedorf.

The overestimation of the mean annual discharge and high discharge for West Alpine and Reuss Seedorf is more difficult to clarify. When observing the amount of dry days as presented in Figure 17, it can be observed that there are too many wet days simulated by the RCM RACMO for both West Alpine and Reuss Seedorf. This means that the RCM in shows a ‘drizzling effect’. This leads to a larger amount of precipitation which is evaporated leading to a decrease in discharge. This aspect can therefore not clarify the overestimated discharges for West Alpine and Reuss Seedorf. Further, an overestimation of the discharge could be clarified by an overestimation of the mean precipitation. For Reuss Seedorf the precipitation is indeed overestimated by the R25 and R12 RCM RACMO, leading to an overestimation of the discharge of especially the R25 and R12. For West Alpine there is a small overestimation of the mean precipitation which could explain the overestimated discharge.

In general, the amount of potential evapotranspiration (PET) is lower during wintertime and higher during summer time. For West Alpine the mean of the 10% lowest PET (winter time) is underestimated which could lead to an overestimation of discharge in wintertime. However, the low discharge is underestimated for West Alpine. The mean of the PET for the annual and high amounts is simulated very well (between 0.95 and 1.05) which cannot clarify the overestimation of the annual and high discharge. For Reuss Seedorf on the other hand, the mean of the annual and high PET is slightly underestimated leading to an overestimation of discharge which can be seen in Figure 16.

At last, it is interesting to clarify the difference between the three RCM spatial resolutions in simulated discharges for both West Alpine and Reuss Seedorf. For West Alpine, the performance of the simulated mean of the annual and high discharge increases with increasing RCM spatial resolution. This increase is shown for the precipitation and PET as well. Only for the temperature the lowest RCM spatial resolution seems to show the best performances. For Reuss Seedorf, the lowest RCM spatial resolution (R50) shows the best performance in simulating the mean of the discharge, followed by the R12. The difference in performance between the three RCMs is shown in the mean of the precipitation as well. The temperature and potential evapotranspiration do not show this fluctuation.

Main and Kinzig

Figure 16 shows that the mean of the discharge is overestimated by the RCM RACMO for Main. For Kinzig the R25 and R12 in general highly overestimate the mean of the simulated discharge, while the R50 simulates the mean of the discharge very well or underestimate it.

Both Main and Kinzig are located in the lowlands (still quite hilly). This means that the high discharges occur in wintertime and the low discharges in summertime because the contribution of snowmelt to the discharge is much lower than for the sub-catchments located in the West Alpines. For this reason the amount of precipitation will have a higher influence on the simulated discharge compared to the other two sub-catchments in the West Alpines. When observing the amount of dry days as shown in Figure 18, this amount of dry days is highly underestimated by the RCM RACMO for Kinzig. This means that the RCM in general keeps ‘dripping’. This leads to a larger amount of precipitation which is evaporated leading to a lower discharge. However, since the discharge for Kinzig is overestimated, this cannot be clarified by the amount of simulated dry days. For Main the amount of simulated dry days shows that the lowest RCM resolution R50 overestimates the amount of dry days, the R25 overestimates the amount of dry days slightly and the highest RCM resolution underestimates the amount of dry days. This would suggest that for the R50 and R25 the amount of discharge is overestimated (less water that evaporates) and for R12 is underestimated. The discharge indeed shows that the discharge is overestimated for R50 and R25. The discharge for R12 is as well overestimated, but less than for the R25 and R50. This can be caused by the PET. Further, Figure 18 shows that the mean of the precipitation of Main is overestimated for the annual and high discharge. This can as well clarify the overestimation of the discharge. For Kinzig, Figure 18 shows that the mean of the precipitation is overestimated for the R25 and R12 and is underestimated for the R50. This could clarify the overestimation (R25 and R12) and underestimation (R50) of the simulated discharge.

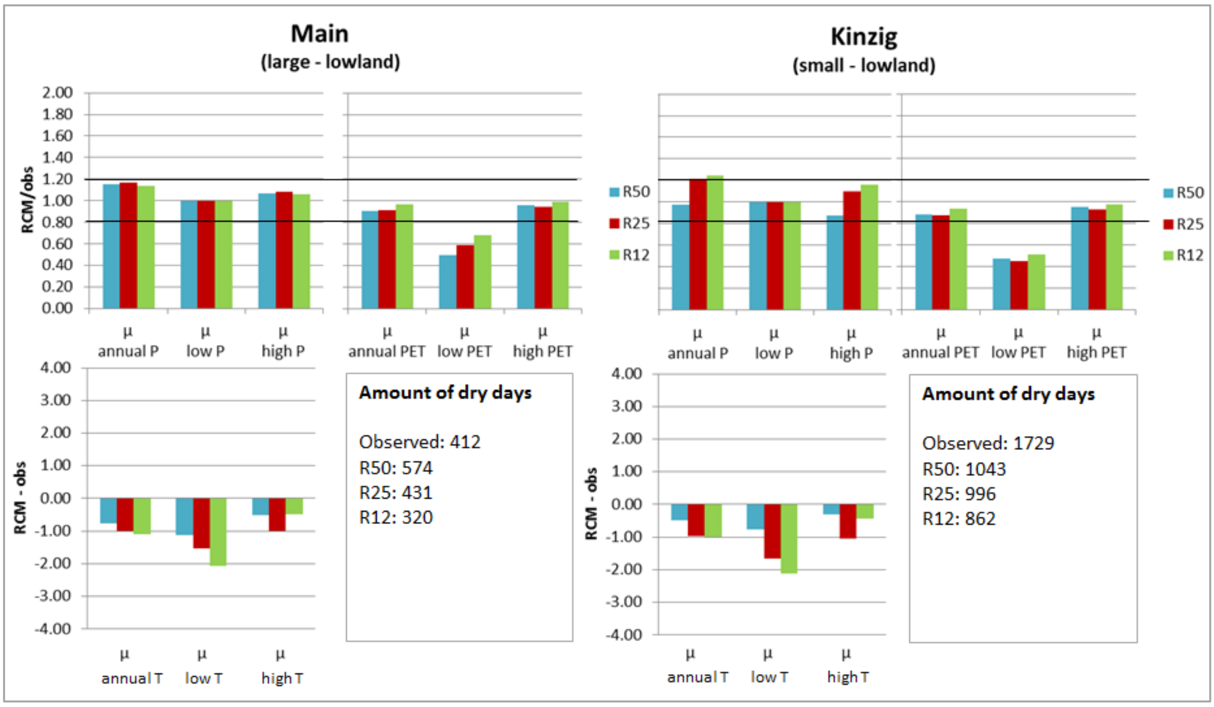

Figure 18: RCM RACMO meteorological data (P, PET (Makkink), T) compared to the observed meteorological data (P, PET (Makkink), T) for both the Main and Kinzig. The P and PET are presented as ratio of the RCM data and the observed data. The temperature is presented as difference between RCM data and observed data. Further, the amount of dry days over the period 1990-2006 is presented. R50 is the lowest RCM spatial resolution, then R25 and then R12

The temperature will mainly influences the discharge in wintertime since the value of the temperature then can drop below the temperature value where precipitation is defined as snowfall. Therefore, especially the influence of the 10% of the lowest temperature on the winter discharge (high discharge) is interesting. For both Main and Kinzig, the temperature is underestimated, mainly the 10% of the lowest temperature. An underestimation leads to an underestimation of the discharge. Since the mean of the high discharge (winter) for both Main and Kinzig is overestimated, this underestimation of the temperature does not clarify the overestimation of the discharge.

An underestimation of the PET leads to more discharge. The low PET occurs during wintertime and therefore affects the high discharge (high discharges occur in wintertime) and the high PET occurs during the summertime affecting the low discharge. For Main the mean of the low PET is underestimated which could clarify the overestimation of the mean of the high discharge. For Kinzig the mean of the annual and high PET is underestimated and for the lowest 10% PET the mean is highly underestimated. This could explain why the mean of the discharges for Kinzig (R25 and R12) are overestimated.

When analyzing the differences between the three RCM versions, for Main, the R12 shows the best performance of the mean of the simulated discharges, followed by the R25 and then the R50. These differences between the three RCM resolutions are also observed for the precipitation and potential evaporation. However, for the temperature the R50 shows the best performance. For Kinzig it can be seen that in general the R50 shows the best performance for the precipitation, PET and temperature. This could suggest why the R50 shows the best performance of the mean of the simulated discharge as well. However, the sudden increase in overestimation of the mean of the low discharge (summer time) for R25 is not reflected by the P and the PET, but only by the underestimation of the high temperature (summer time) for R25. However, it is unclear how this underestimation relates to the low discharge in summer time since the temperature especially influences the snowfall in wintertime.

4.3 (Sensitivity of) total model performance

First in section 4.3.1, the results of the total model performance are analyzed. The total model performance is represented by the ratio $Q_{sim-RCM}$ / Q_{obs} , representing the ratio of the simulated discharge (HBV forced with RCM RACMO data) and the observed discharge. Second, the results of the three sub-questions are given (4.3.2). In other words, the sensitivity of discharge characteristics to RCM spatial resolution for the size of the catchment, the topography of the catchment and the parameter estimation are shown.

4.3.1 Total model performance

Table 10, Table 11, Table 12 and Table 13 show the total model performances (1) for the four sub-catchments. The total model performance is coloured red if the ratio showing the performance is below 0.8 or above 1.2. These tables show that there are only a few situations showing a good total model performance having a ratio between the borders of 0.8 and 1.2. In general, the discharge is overestimated by HBV-96 for the three resolutions for the annual and high discharge and underestimated for the low discharges. Further, especially the mean and standard deviation of the low discharge show very bad performances.

Both the hydrological model performance $Q_{sim-obs\ P,T,PET}/Q_{obs}$ and RCM RACMO performance $Q_{sim-RCM}/Q_{sim-obs\ P,T,PET}$ contribute to the total model performance $Q_{sim-RCM}$ / Q_{obs}. As explained in section 3.5.3, when multiplying both ratios which represent the hydrological model performance and RCM RACMO performance, the ratio of the total model performance is shown. Therefore, if both the hydrological model performance and RCM RACMO performance show an over- or underestimation of the discharge, both performances are strengthening each other. On the other hand, if one performance shows an overestimation and the other an underestimation, both performances are compensating for each other's under- or overestimation. The contribution of the hydrological model performance (1.1) and RCM RACMO performance (1.2) to the total model performance (1) are analysed per sub-catchment.

West Alpine

Table 10 shows the total model performance (1), the hydrological model performance (1.1) and the RCM RACMO performance (1.2) for West Alpine. In general, the total model performance (1) shows that the discharge is overestimated for both the mean and standard deviation. Only the mean of the low discharge is underestimated. Further, the total model performance is good showing ratios between 0.8 and 1.2 for the mean of the annual and low discharge.

Table 10: West Alpine: Total model performance (1), hydrological model performance (1.1) (the same for each RCM spatial resolution) and RCM RACMO performance (1.2)

		(1)	**(1.1)**	**(1.2)**			**(1)**	**(1.1)**	**(1.2)**
Mean annual Q	R50	1.19	0.97	1.23	**STD annual Q**	**R50**	1.76	1.05	1.67
	R25	1.14	0.97	1.17		**R25**	1.66	1.05	1.58
	R12	1.07	0.97	1.10		**R12**	1.54	1.05	1.46
Mean low Q	R50	0.85	0.94	0.91	**Std low Q**	**R50**	1.64	1.13	1.45
	R25	0.78	0.94	0.83		**R25**	1.69	1.13	1.50
	R12	0.80	0.94	0.85		**R12**	1.46	1.13	1.29
Mean high Q	R50	1.45	1.03	1.41	**Std high Q**	**R50**	2.10	1.91	1.10
	R25	1.37	1.03	1.32		**R25**	2.46	1.91	1.29
	R12	1.28	1.03	1.24		**R12**	2.44	1.91	1.28

The hydrological model performance (1.1) shows an underestimation and the RCM RACMO performance shows an overestimation of the mean of the annual discharge (Table 10). Therefore, both performances compensate for each other when contributing to the total model performance. For the other type of discharges, both hydrological model performance and RCM RACMO performance are strengthening each other. The low total model performance is mainly caused by the contribution of the low performance of the RCM RACMO since the hydrological model performance is in general very good. Only for the standard deviation of the high discharge the low total model performance is mainly caused by the contribution of the low hydrological model performance.

Reuss Seedorf

Table 11 shows the total model performance (1), hydrological model performance (1.1) and RCM RACMO performance (1.2) of Reuss Seedorf. In terms of total model performance, the mean of the annual and high discharge and the standard deviation of the annual discharge are overestimated. The other types of discharges are underestimated. The total model performance is in general very low, showing ratios fluctuating between 0.2 and 1.5.

Table 11: Reuss Seedorf: Total model performance (1), hydrological model (1.1) (the same for each RCM spatial resolution) and RCM RACMO performance (1.2)

		(1)	(1.1)	(1.2)			(1)	(1.1)	(1.2)
Mean annual Q	R50	1.08	0.92	1.18	**STD annual Q**	**R50**	1.25	1.13	1.11
	R25	1.32	0.92	1.43		**R25**	1.52	1.13	1.34
	R12	1.09	0.92	1.19		**R12**	1.35	1.13	1.19
Mean low Q	R50	0.36	0.34	1.04	**Std low Q**	**R50**	0.21	0.32	0.66
	R25	0.35	0.34	1.03		**R25**	0.21	0.32	0.65
	R12	0.32	0.34	0.92		**R12**	0.21	0.32	0.65
Mean high Q	R50	1.14	1.04	1.10	**Std high Q**	**R50**	0.94	0.76	1.25
	R25	1.36	1.04	1.31		**R25**	0.94	0.76	1.25
	R12	1.20	1.04	1.15		**R12**	0.93	0.76	1.23

For the mean annual discharge, the mean of the low discharge and the standard deviation of the high discharge, the hydrological model performance (1.1) shows an underestimation of the discharge and the RCM RACMO performance (1.2) shows an overestimation. This means that these performances are compensating each other. It is interesting to notice that the hydrological model performance for the standard deviation of the high discharge shows a ratio of 0.76 and for the RCM RACMO performance a ratio of 1.25. Since both performances are compensating each other, this combination results in a good total model performance of 0.94. For the other three types of discharge, both performances are strengthening each other. Further, in three situations the total model performance is mainly caused by the low hydrological model performance and not the RCM RACMO performance, namely for the mean and standard deviation of the low discharge and the standard deviation of the high discharge.

Main

Table 12 shows the total model performance (1), the hydrological model performance (1.1) and the RCM RACMO (1.2) performance for the Main. For Main the total model performance shows that the discharges are overestimated. Only the standard deviation of the low discharge is underestimated.

Table 12: Main: Total model performance (1), hydrological model performance (1.1) (the same for each RCM spatial resolution)and RCM RACMO performance (1.2)

		(1)	(1.1)	(1.2)			(1)	(1.1)	(1.2)
Mean annual Q	R50	1.48	0.98	1.51	**STD annual Q**	**R50**	1.45	0.89	1.63
	R25	1.48	0.98	1.52		**R25**	1.35	0.89	1.52
	R12	1.36	0.98	1.39		**R12**	1.23	0.89	1.38
Mean low Q	R50	1.98	1.51	1.31	**Std low Q**	**R50**	0.63	0.45	1.38
	R25	1.97	1.51	1.30		**R25**	0.74	0.45	1.63
	R12	1.69	1.51	1.12		**R12**	0.73	0.45	1.60
Mean high Q	R50	1.49	0.90	1.66	**Std high Q**	**R50**	1.56	1.12	1.39
	R25	1.42	0.90	1.58		**R25**	1.40	1.12	1.25
	R12	1.31	0.90	1.45		**R12**	1.18	1.12	1.06

Table 12 shows that both hydrological model performance and RCM RACMO performance show an overestimation of the mean of the low discharge and the standard deviation of the high discharge. In other words, both performances are strengthening each other. For the other type of discharges, both performances are compensating for each other's performance. Further, the total model performance is mainly influenced by the low RCM RACMO performance. Only the hydrological model performance of the mean and standard deviation of the low discharge is not good and therefore influencing the total model performance more than the RCM RACMO performance.

Kinzig
Table 13 shows the total model performance (1), the hydrological model performance (1.1) and the RCM RACMO performance (1.2) for Kinzig. The total model performance shows an overestimation of the discharges for the spatial RCM resolution R25 and R12 and an underestimation for the lowest resolution R50. Only the mean of the low discharge is underestimated for the three spatial resolutions.

In general, the RCM RACMO performance and hydrological model performance are compensating each other performances. The performances are only strengthening each other for the mean of the low discharge and the mean and standard deviation of the annual and low discharge when considering the lowest RCM spatial resolution R50. In general, the RCM RACMO performance influences the contribution to the total model performance the most because the hydrological model performance shows a good performance. Only for the mean of the low discharge and standard deviation of the low discharge, the hydrological model performance is very low leading to a larger influence on the total model performance.

Table 13:Kinzig: Total model performance (1), hydrological model performance (1.1) and RCM RACMO performance (1.2)

		(1)	(1.1)	(1.2)			(1)	(1.1)	(1.2)
Mean annual Q	R50	1.00	0.95	1.06	**STD annual Q**	**R50**	0.95	0.99	0.96
	R25	1.52	0.95	1.60		**R25**	1.58	0.99	1.59
	R12	1.57	0.95	1.66		**R12**	1.79	0.99	1.80
Mean low Q	R50	0.32	0.38	0.84	**Std low Q**	**R50**	1.09	1.47	0.74
	R25	0.64	0.38	1.67		**R25**	2.12	1.47	1.44
	R12	0.47	0.38	1.22		**R12**	1.78	1.47	1.21
Mean high Q	R50	0.93	0.93	1.00	**Std high Q**	**R50**	0.89	1.12	0.79
	R25	1.45	0.93	1.57		**R25**	1.90	1.12	1.70
	R12	1.62	0.93	1.74		**R12**	2.31	1.12	2.07

4.3.2 Sensitivity of discharge characteristics to RCM spatial resolution

In this section the results of the total model performance are given representing the sensitivity of discharge characteristics to RCM spatial resolution in terms of catchment size (1), topography (2) and parameter estimation (3). To classify the results leading to more structured analysis, two types of indicators are formulated with accompanying assumptions.

1. The sensitivity: The sensitivity shows the change in total model performance when increasing or decreasing the RCM spatial resolution. The total model performance is categorized as very sensitive if the changes in ratios are above 0.2. The discharge is categorized as sensitive if the changes in ratios are between the 0.1 and 0.2 and as insensitive if the ratios are below 0.1.
2. The direction: In general it is expected that a higher RCM spatial resolution leads to a better total model performance. This sequence of the three RCM spatial resolutions in terms of total model performance is called the direction.

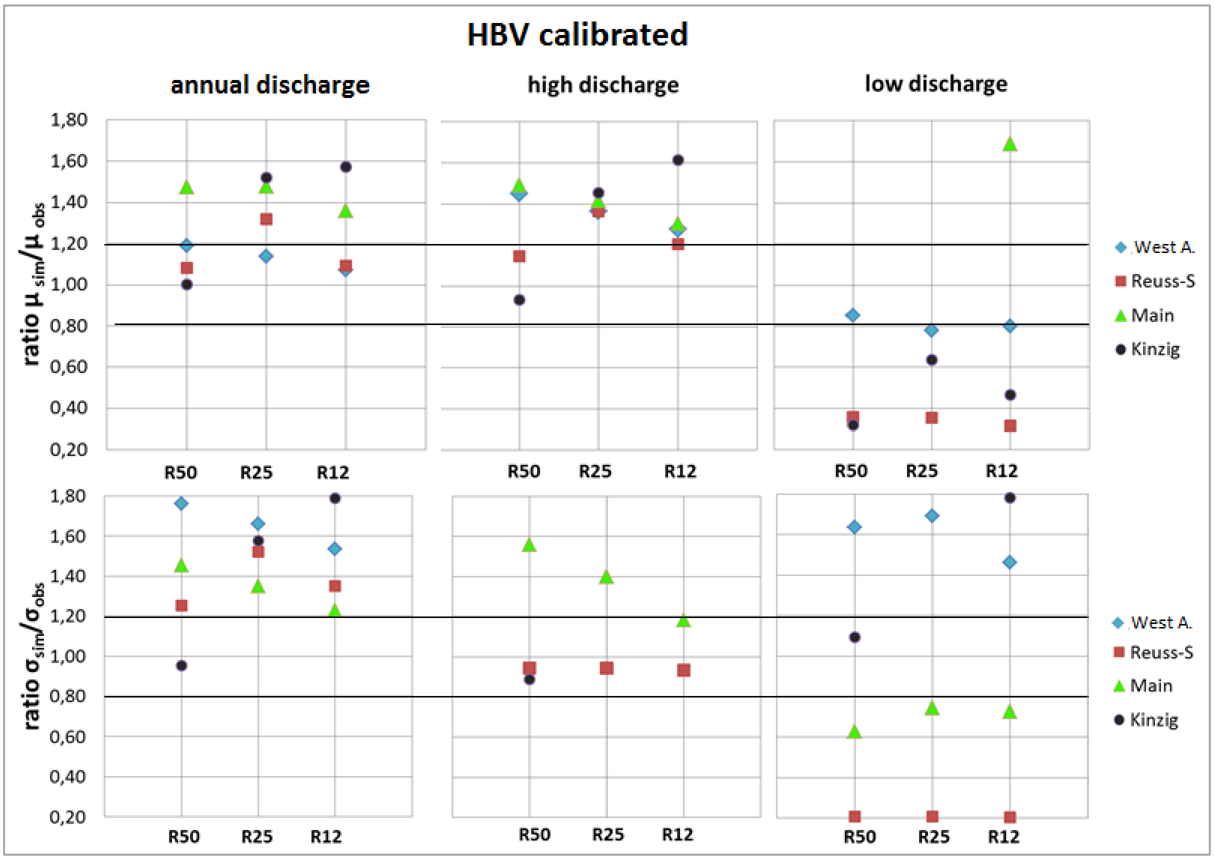

Figure 19: The total model performance in terms of ratio of the mean μ (above) and standard deviation σ (below) of the annual, low or high discharge for West Alpine (large and mountainous), Reuss Seedorf (small and mountainous), Main (large and lowland), Kinzig (small and lowland). R50 is the lowest RCM spatial resolution, R25 the middle and R12 the highest. If the ratio is 1, a perfect model performance is presented and above 0.8 and below 1.2 a good model performance is presented (black lines). Some types of discharges do not show all results because of a very low performance. Standard deviation of the high discharge: (Kinzig R25 1.9, R12: 2.31) (West Alpine: R50: 2.1, R25: 2.46, R12: 2.44). Mean low discharge: (Main: R50 1.98, R25: 1.97). Standard deviation of low discharge (Kinzig: R25: 2.12).

Sensitivity in terms of size and topography of the sub-catchment

Figure 19 shows that the total model performance of Kinzig is very sensitive to changes in RCM spatial resolution, since the ratios are varying a lot. Reuss-Seedorf is only very sensitive for the mean and standard deviation of the high discharge and for the standard deviation of the annual discharge. For the other type of discharges, Reuss-Seedorf is not sensitive at all. Further, West Alpine and Main are both showing the same sensitivity patterns. Only for the mean of the low discharge Main is much more sensitive than West Alpine and for the standard deviation of the low discharge the West Alpine is more sensitive. Both catchments are quite sensitive having values between 0.1 and 0.4. In general, no clear sensitivity patterns are observed in terms of catchment size or topography of the catchment. However, the two larger catchments Main and West Alpine show the same sensitivity patterns.

When looking at the direction of the total model performance for the four selected sub-catchments in Figure 19, it can be seen that in general for the two larger catchments West Alpine and Main the performances increases with increasing RCM spatial resolution. However, the smaller catchments Kinzig and Reuss Seedorf show in general that the lowest RCM spatial resolution R50 shows the best total model performance. For Kinzig the second best performance is in general for the middle RCM spatial resolution (R25) and the worst performance for the R12. For Reuss Seedorf on the other hand, the highest RCM spatial resolution (R12) shows the second best performance and the R25 shows the worst total model performance.

However, there are a few exceptions. For West Alpine the R50 performs best for the ratio of the standard deviation for high discharges and the mean of the low discharges, followed by R12 and then R25. At last the standard deviation of the low discharge shows that the R12 performs best, followed by the R50 and at last the R25. For Reuss-Seedorf the exceptions are as follows: In terms of the ratio of the standard deviation for high and low discharge, the performance of R50, R25 and R12 are among the same. Further, for the mean of the low discharge the R50 shows the best results, but then followed by the R25 instead of the R12. For Kinzig, there are two exceptions. The ratio of the standard deviation of the low discharge shows that the R12 shows the second-best results followed by the R25. Further, for the ratio of the mean of the low discharges the middle resolution R25 performs best and the lowest resolution R50 worst. For Main there are no exceptions.

Sensitivity in terms of parameter estimation of HBV-96

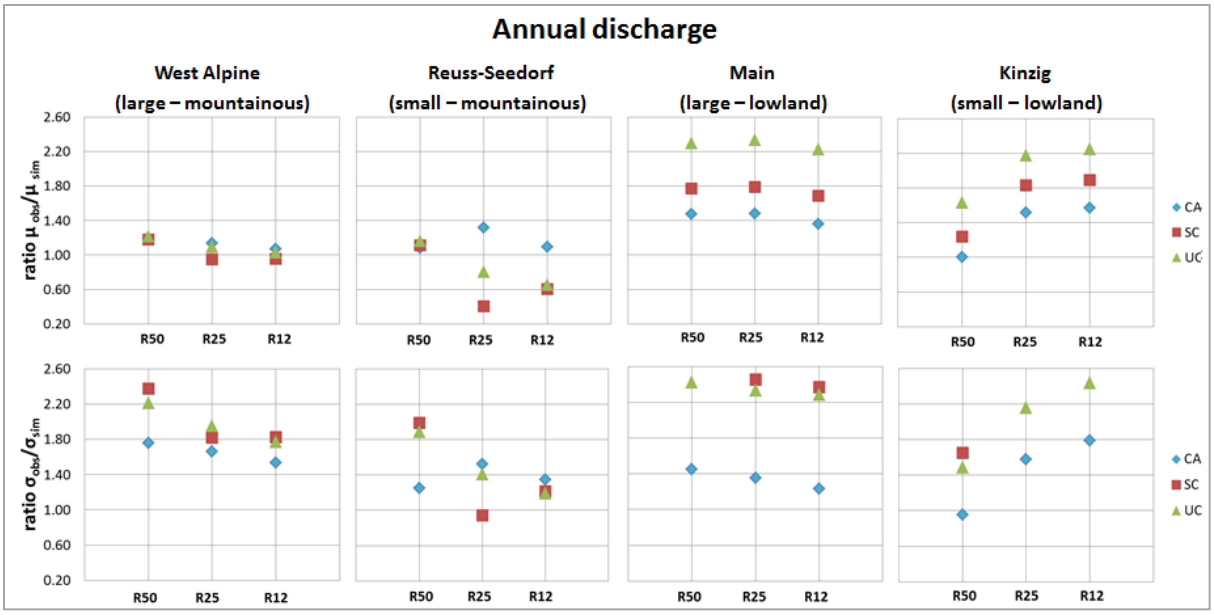

Figure 20: Total model performance of the annual discharge for the four selected sub-catchments. CA: calibrated HBV model. SC: semi-calibrated HBV model. UC: un-calibrated HBV model. For the standard deviation of the semi-calibrated HBV model for Main, the value of the ratio of R50 is 2.62. For the standard deviation of the semi-calibrated HBV model for Kinzig, the value of the ratio of R25 is 2.6 and R12 is 2.92.

When analysing the sensitivity of total model performance to RCM spatial resolution for the three versions of HBV as shown in Figure 20, it can be seen that for West Alpine and Reuss Seedorf the semi-calibrated HBV-96 model is most sensitive for changes in RCM spatial resolution, followed by the un-calibrated version and then the calibrated HBV model. For Main and Kinzig it can be analysed that there is little difference between the sensitivity of model performance to RCM spatial resolution for the three different versions of HBV.

When analysing the direction of the total model performance, Figure 20 shows for West Alpine and Main that in general the total model performance increases with increasing RCM spatial resolution for the three versions of HBV. Only the semi-calibrated HBV model for West Alpine shows that the total model performance decreases slightly from spatial resolution R25 to R12. For Main the ratio of the mean shows a slightly decrease in total model performance from R50 to R25. For Kinzig it can be observed that an increase of the RCM spatial resolution leads to a decrease of the total model performance for the three HBV models. For Reuss Seedorf Figure 20 does not show a clear trend for the change of total model performance when increasing the RCM spatial resolution at all for the three different HBV models.

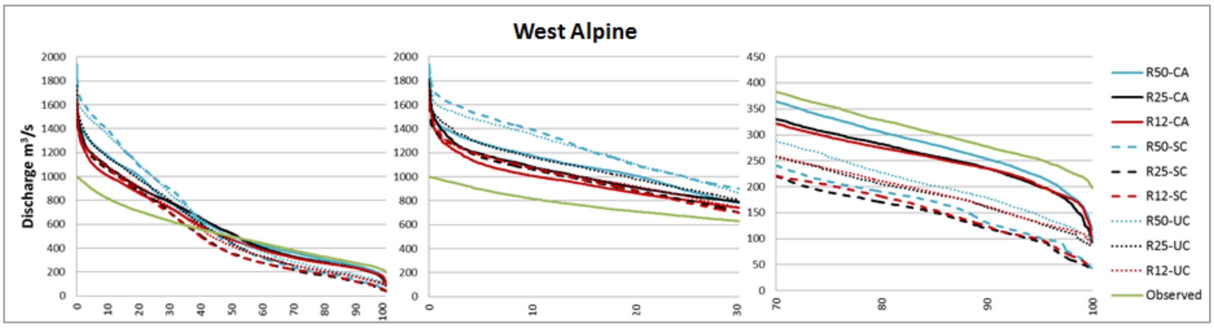

Figure 21: Flow Duration Curve for West Alpine. The left figure represents the FDC for the whole discharge time series, the middle for the 30% lowest discharge and the right for the 30% highest discharge. CA means calibrated HBV model. SC means semi-calibrated HBV model and UC means un-calibrated HBV model. The green line represents the observed discharge series

Figure 21 shows the flow duration curve (FDC) for West Alpine for the three HBV versions and the three RCM spatial resolutions. These FDC can be compared to the FDC of the observed discharge. For the 30% of the highest discharge the same observations are made as based on Figure 20: It can be seen that increasing the RCM spatial resolution leads to a simulated discharges closer to the observed discharges for the three HBV versions. However, for the 30% of the lowest discharges, the lowest RCM spatial resolution R50 (blue line) shows a better FDC followed by the R25.

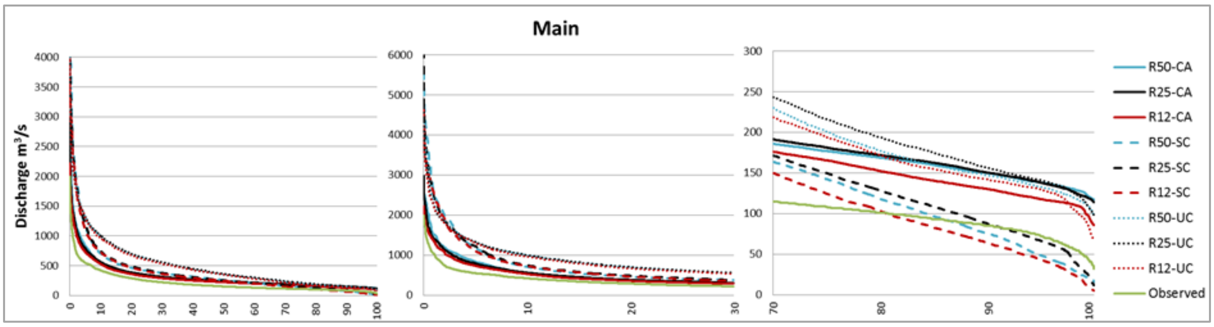

Figure 22: Flow Duration Curve for Main. The left figure represents the FDC for the whole discharge time series, the middle for the 30% lowest discharge and the right for the 30% highest discharge. CA means calibrated HBV model. SC means semi-calibrated HBV model and UC means un-calibrated HBV model. The green line represents the observed discharge series

Figure 22 shows the FDC of the Main and shows the same conclusions as presented by Figure 20. Namely, the FDC of the simulated discharge is closer to the FDC of the observed discharge for the highest RCM spatial resolution, followed by the R25 and then the R50 for all three HBV-96 versions.

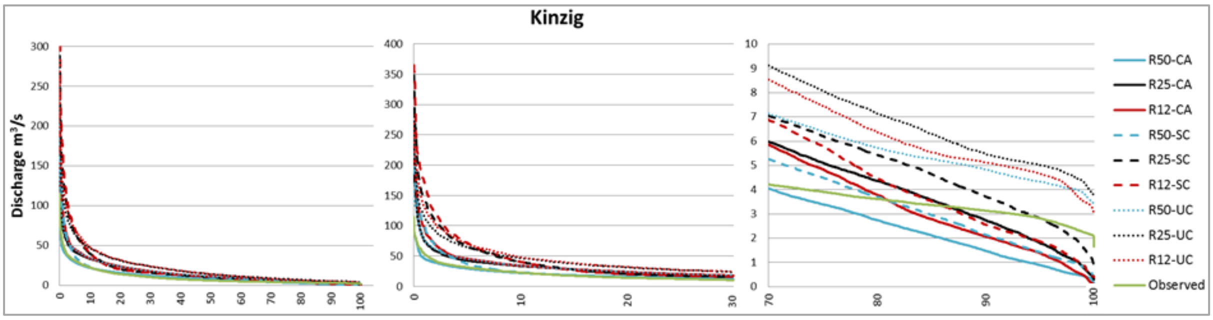

Figure 23: Flow Duration Curve for Kinzig. The left figure represents the FDC for the whole discharge time series, the middle for the 30% lowest discharge and the right for the 30% highest discharge. CA means calibrated HBV model. SC means semi-calibrated HBV model and UC means un-calibrated HBV model. The green line represents the observed discharge series

Figure 23 shows the FDC of Kinzig and shows the same conclusions as presented by Figure 20. The lowest RCM spatial resolution R50 (blue lines) shows the best performance for all the three versions of the HBV model. This is followed by the R25 (black lines) and at last the R12 shows the best performance (red line). This is the situation for the low and high discharges.

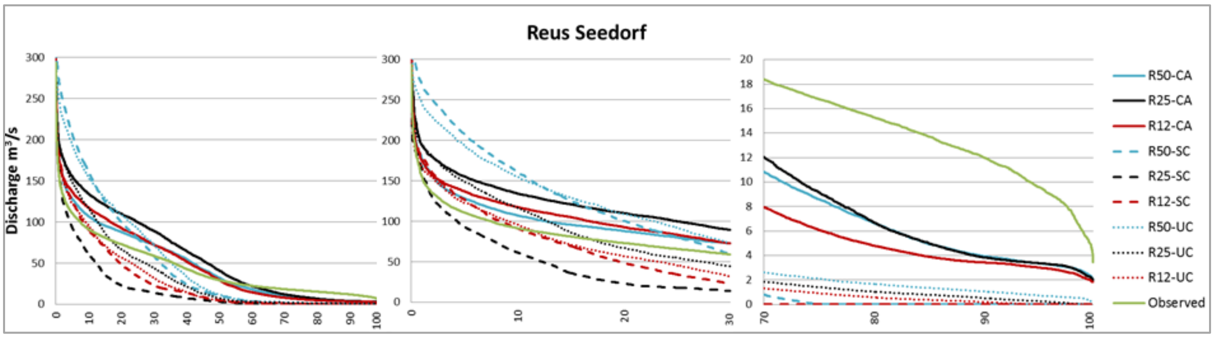

Figure 24: Flow Duration Curve for Reuss Seedorf. The left figure represents the FDC for the whole discharge time series, the middle for the 30% lowest discharge and the right for the 30% highest discharge. CA means calibrated HBV model. SC means semi-calibrated HBV model and UC means un-calibrated HBV model. The green line represents the observed discharge series

Figure 24 shows the FDC of Reuss Seedorf for the three versions of HBV and the three RCM spatial resolutions. For the low discharge it can be seen that the calibrated HBV model shows FDC which are much better than the semi-calibrated and un-calibrated HBV model. However, for the high discharge again no clear trend can be observed which is shown in Figure 20 as well.

Above figures give not only insight in the sensitivity of total model performance to RCM spatial resolution for the three HBV models. The effectiveness of increasing RCM spatial resolution can as well be compared to the effectiveness of calibrating the HBV model. For the West Alpine it is observed that increasing the RCM spatial resolution shows a clear improvement of total model performance, while calibrating the HBV model only shows an improvement for the standard deviation and when not taking into account the semi-calibrated model. For Reuss Seedorf nothing can be said about the effect of calibrating in comparison to the effect of increasing the RCM spatial resolution since no clear trends are obtained. For Main it can be seen that both increasing the RCM spatial resolution and calibrating the HBV model lead to an increase of total model performance. In general, Main is more sensitive to the calibration which means that calibrating is more effective for Main than increasing the RCM spatial resolution. For Kinzig it is analysed that calibrating the HBV model leads to an increase in model performance except for the standard deviation of the semi-calibrated HBV model. Increasing the RCM spatial resolution leads to a decrease of total model performance. This suggests that calibrating is more effective than increasing the RCM spatial resolution for Kinzig.

5 Discussion

In section 5.1 the results of the sensitivity of discharge characteristics to RCM spatial resolution are compared to previous research. In section 5.2 the RCM RACMO performance is compared to previous research and in section 5.3 the hydrological model performance is analysed. In section 5.4 the observed discharge and meteorological data are discussed. In section 5.5 the general potential of this research is described partly based on the discussion given in the sections before. In section 5.6 the limitations of this research are given, partly based on the discussion given in the sections before.

5.1 Sensitivity of discharge characteristics to RCM spatial resolution

Section 4.3 shows the results of the sensitivity of discharge characteristics to RCM spatial resolution in terms of catchment size, catchment topography and parameter estimation. These results are compared to literature.

Catchment size

Kleinn et al. (2005) analyzed four different sub-catchments of the river Rhine having sizes similar to the larger selected sub-catchments in this research (Main and West Alpine). Kleinn et al. (2005) concluded that the simulated discharges driven by the higher RCM spatial resolution (14 km) correlate better to the observations than the lower RCM spatial resolution (56 km). However, the impact of RCM spatial resolution for runoff is not as remarkable as for precipitation (Kleinn, et al., 2005). This study shows as well an increase in total model performance when increasing the RCM spatial resolution for the larger catchments (Main and West Alpine). Dankers et al. (2007) studied as well catchments having sizes comparable to the West Alpine and the Main and concluded that for the annual discharge the performance of the hydrological model is more or less the same for the different RCM spatial resolutions. Since the study area is different for Dankers et al. (2007) this could explain why the results are slightly different. However, all three studies agree that the influence of increasing the resolution on model performance is much smaller than beforehand expected.

While Kleinn et al. (2005) did not study the effect of RCM spatial resolution on simulated discharges for smaller sub-catchments, Kleinn et al. (2005) expected that smaller sub-catchments would benefit more from an increase in RCM spatial resolution than larger sub-catchments. The reason for this is that an increase in RCM spatial resolution leads to a better representation of small scale precipitation patterns. For larger catchment of several thousand square-kilometres and for the runoff evolution of a daily timescale, the fine-scale distribution of precipitation within the catchment is less important than for smaller sub-catchments (Kleinn, et al., 2005). However, for the two smaller sub-catchment Reuss Seedorf (836 km^2) and Kinzig (928 km^2), this study does not support this expectation by Kleinn et al. (2005). One of the reasons could be that Kleinn et al. (2005) performed a bias correction method for both precipitation and temperature, while this study did not. Graham et al. (2005) concluded that a finer RCM spatial resolution resulted in biases of temperature and precipitation that were more systematic and less spatially variable. Olsson et al. (2014) supported this by concluding that the bias was steadily reduced or remained unchanged when increasing the resolution. This shows that catchments might profit more from an increase in RCM spatial resolution when a bias correction is applied.

Both Dankers et al. (2007) and this study analysed the influence of increasing RCM spatial resolution on high discharges events. Dankers et al. (2007) conclude that the different sub-catchments profit from the increase of RCM resolution when analysing high discharge events. The results in this study show for the Main and West Alpine as well that the high discharge shows a larger profit from increasing RCM spatial resolution than the annual discharge. However, this is not supported by the smaller sub-catchments Reuss Seedorf (836 km^2) and Kinzig (928 km^2). These two smaller sub-catchments are five times smaller than the smallest sub-catchments (4500 km^2) as analysed by Dankers et al. (2007) which might explain the differences in results.

Topography of the catchment
Kleinn et al. (2005) conclude that even the high-altitude Alpine catchments do no significantly improve the discharge performance when increasing RCM spatial resolution. In general, in the Alpines the biases are larger of precipitation and temperature and there are errors in the altitudinal distribution of the precipitation. Therefore, it would be expected that especially in the Alpines (mountainous region) the simulated discharge would benefit from an increase in RCM spatial resolution. This study showed for the West Alpine that an increase in RCM spatial resolution led to a small increase in total model performance. However, this study did not support this for Reuss Seedorf. In summary, both studies show that mountainous regions do not profit more from an increase in RCM spatial resolution than sub-catchments located in lowlands.

Hydrological model - parameter estimation
Mendoza et al. (2016) compared (among others) the effect of RCM spatial resolution on simulated discharges for four different hydrological models. Mendoza et al. (2016) did not apply a bias correction method but calibrated the four selected hydrological models for the meteorological data simulated by the highest RCM spatial resolution. Mendoza et al. (2016) concluded that increasing the RCM spatial resolution has large effects on the portrayal of hydrologic change at an annual basis, regardless which hydrologic model structure was selected. Moreover, the effect of RCM horizontal resolution on hydrologic change may overwhelm the uncertainty from hydrological model choice (Mendoza, et al., 2016). However, it can be questioned if it can indeed be concluded that increasing the RCM spatial resolution leads to a better simulation of the discharge if the hydrological models are calibrated for the highest RCM spatial resolution. On the other hand, the conclusion about the hydrological model choice is supported by this study. The three versions of HBV are showing the same sensitivity to RCM spatial resolution for the three selected sub-catchments. It is important to realise that in this study the parameter estimation is analysed and not the model structure.

5.2 RCM performance
In terms of precipitation, Olsson et al. (2014) concluded that a higher RCM spatial resolution led to an increase in overestimation of the amount of wet days. This analysis is supported by this study for all four selected sub-catchments. The reason for this is that the grids are aggregated to the sub-catchments. A higher RCM spatial resolution leads to more grid cells which are aggregated for one sub-catchment leading to a bigger chance that there will be at least one grid cell showing more than 0 mm of precipitation. This leads to less simulated dry days.

Olsson et al. (2014) further concluded that in general no positive impact was analysed on monthly total precipitation amounts when increasing the spatial resolution. Only for short-term variability and extreme rainfall events, the agreement with observations increased with increasing resolution. Further, Dankers et al. (2007) concluded as well that the extreme rainfall events were better represented by the high RCM spatial resolution (12 km) than the low spatial RCM resolution (56 km). Kleinn et al. (2005) did apply a bias correction for precipitation and concluded that the coarser RCM resolution captures the main precipitation features, where the higher resolution captures the smaller scale patterns as well. An increase in RCM resolution introduces considerable spatial variations in the precipitation fields. In summary, a higher RCM spatial resolution leads to a better representation of the extreme precipitation events and a better representation of the smaller scale patterns. In this research the small scale patterns were not analysed since the amounts of precipitation were aggregated to one sub-catchment and therefore no comparison is possible. The extreme rainfall events are partly analysed depending on the definition of extreme. In this research the 10% of the highest amount of precipitation are analysed. For West Alpine and Main the increase in resolution led to a very small increase in precipitation performance. For Kinzig this increase was much larger. However, for Reuss Seedorf no increase was analysed in precipitation performance when increasing RCM spatial resolution. One of the reasons could be that in this research the amount of precipitation was aggregated to one sub-catchment therefore leading to other results.

Only Graham et al. (2005) explicitly analysed the increase of RCM spatial resolution and the influence on simulated temperature. Especially in the mountainous regions, the simulated temperature profit from the increased resolution. In this study this is result is not supported. However, this could be explained by the fact that Graham et al. (2005) applied a bias correction method, while this study did not. As explained by Kleinn et al. (2005) in the altitudinal regions a larger bias of precipitation and temperature was observed. Further, as explained by Graham et al. (2005), an increase in resolution leads to more systematic and less spatially variable biases. This suggests that especially in the Alpines, the temperature could benefit from a bias correction leading to an increase in temperature performance when applying the bias correction.

5.3 Hydrological model performance

The hydrological model performance consists mainly of the parameter performance and model structure performance. Other contributions to the hydrological model performance are the input data and the temporal resolution. Unfortunately, it was not possible to analyze the model structure performance since no other hydrological model is used in this research. However, even if another model was used, it is very difficult to quantify the contribution of the different aspects in the structure to the hydrological model performance.

Further, insight in the parameter performance is obtained by comparing the three versions of the HBV model. By comparing the different parameter values, it can be determined which parameter influences the parameter performance. However, often different parameters are dependent on each other and therefore the combination of parameters instead of individual parameter values lead to a clarification of the parameter performance. The analysis of the parameter values in this research are only based on individual parameter values. The dependency is not analyzed and therefore it is not quantified which parameter value contribute to what extent to the parameter performance. Insight in the influence of the parameters can be obtained by performing a sensitivity analysis. However, that is out of the scope of this research.

5.4 Quality of the observed data

Quality of the observed discharge data

The observed discharge data is in this research assumed to perfectly match the reality. However, most of the discharge data as used in this thesis is derived from measured water levels and calculated using a Q-H relation (Winsemius, Verseveld, Weerts, & Hegnauer, 2013). The Q-h relations are often outdated or do not take into account some processes such as high water events (Tillaart S. v., 2010). This leads to an error in the observed discharges.

Further, for the discharge station Aare-Untersighenthal, there are many missing values. In general, these missing values are representing the higher peak discharges. During the analysis, the days having missing values are skipped for both the observed discharge time series and the simulated time series. However, since most of the missing values are peak values, the mean and standard deviation of the 10% highest discharge in the analysis might be in reality belonging to the 20 or 30% highest discharge.

At last, the operational water management and the reservoirs and locks are not taken into account in the HBV model (Kleinn, et al., 2005). However, these measures are influencing the observed discharge data. Therefore, the simulated discharge might over- or underestimates the amount of real discharge. When the HBV model for a certain sub-catchment always overestimates the discharge, this can be caused by the fact that the 'anthropogenic influences' are not taken into account in the HBV model.

Quality of the observed meteorological data

The discharges are both simulated by using RACMO RCM data as input data and observed precipitation and temperature data. The observed precipitation data is the dataset known as HYRAS data. This dataset is a gridded dataset having a spatial resolution of 1 km^2. This gridded dataset is based on 6200 precipitation stations within the spatial domain covering the river basins in Germany and neighboring countries (Rauthe, et al., 2013). In this research the HYRAS data is assumed to reflect the reality. It is good to keep in mind that there are uncertainties within this dataset. The calibration in this study is based on the HYRAS dataset. This means that the calibration might have corrected the uncertainties in the HYRAS dataset by adjusting certain parameters. Further, this means that these uncertainties are as well corrected for the RACMO RCM data while these uncertainties might not exist in the RACMO dataset. One of the reasons for the uncertainties within the HYRAS dataset is as follows: The precipitation stations are all located on a certain height. However, when aggregating the locations to a gridded dataset, it is important that this difference in height is taken into account since the wind speed influences the precipitation and wind is different for different altitudes (Zhihua & Mingqin, 2007). For the HYRAS dataset a multiple linear regression tool is used to correct for the elevation (Rauthe, et al., 2013). I think it is better to use the tool as described by (Davids, et al., 2015) where first the stations are brought down to a reference level and then increased again to the used topography.

5.5 General potential of this research

As explained in section 1.1.2, many decisions need to be made within the modeling chain, such as the choice of RCM spatial resolution and bias correction method. Each choice leads to another result and therefore another model performance. So far, previous researchers on this topic show contradictory results. This research used the philosophy to keep the methods as simple as possible to make sure that observed differences in model performance are for sure caused by differences in RCM spatial resolution and are not influenced by for example a bias correction method. Further, since the influence of some components (hydrological model performance) cannot be neglected, the total model performance was decomposed to analyze the different performances as well. Therefore, it can be referred where the values of the total model performance comes from. This makes it much easier to compare the results to other researches and to draw conclusions about the influence of RCM spatial resolution on discharge characteristics.

5.6 General limitations of research

In this study one hydrological model (HBV) and three different resolutions (RCM RACMO) are studied for sub catchments in the Rhine having different characteristics. Due to the limitation of time (the master thesis takes 20 weeks, 30 European Credits) and available RCM resolutions forced with reanalysis data, it is impossible to compare more resolutions and hydrological models for more than one study area. Therefore, it can be questioned if the sensitivity of discharge characteristics to RCM spatial resolution is quantified well enough when only using 3 RCM spatial resolutions. Further, the results about the hydrological model use are only based on the parameter estimation of the hydrological model. Therefore, nothing is said about the hydrological model structure. Further, since no bias correction method is applied, other studies where the bias correction is applied could have other results. Moreover, it is important to keep in mind that studies using other hydrological models and another RCM can show other results.

6 Conclusions and recommendations

The conclusion of this thesis consists of two parts. The first part consists of answering the three sub-questions about the sensitivity of discharge characteristics to RCM spatial resolution when looking at the size of the sub-catchment (question 1), the topography of the sub-catchment (question 2) and hydrological model (question 3). The second part provides some general conclusions.

6.1 Conclusion research questions

Research question 1: Size of the sub-catchment

The two larger catchments West Alpine and Main show an increase in total model performance for annual, high and low discharges when increasing the RCM spatial resolution. For the two smaller catchments Kinzig and Reuss Seedorf, the lowest RCM spatial resolution shows the best performance for all discharge characteristics. For Kinzig the R25 (middle resolution) shows the second best total model performance for all discharge characteristics and for Reuss Seedorf the R12 (highest resolution) shows the second best total model performance. In conclusion, the two larger sub-catchments show an increase in total model performance when increasing the RCM spatial resolution, while the two smaller sub-catchments do not.

Further, when analysing the sensitivity of discharge characteristics to RCM spatial resolution, the two larger sub-catchments West Alpine and Main are sensitive to changes in RCM spatial resolution and are showing the same change in total model performance when increasing the resolution. For the two smaller catchments, no relation is found. In general, Kinzig is much more sensitive to changes in RCM spatial resolution than Reuss Seedorf. At last, for the Main, West Alpine and Kinzig the high discharges are more sensitive to changes in RCM spatial resolution than the annual discharges and low discharges. For Reuss Seedorf the annual discharge is most sensitive. In conclusion, the two larger sub-catchments are showing the same sensitivity patterns and for the two smaller sub-catchments no relation has been observed.

Both the RCM RACMO performance and hydrological model performance contribute to the total model performance. When only analysing the RCM RACMO performance, the RCM RACMO performance as well increases with increasing RCM spatial resolution. This shows that the conclusions are not influenced by the hydrological model performance. When analysing the output of the RCM RACMO model, the precipitation, temperature and potential evapotranspiration can clarify the results as shown by the simulated discharges of the RCM RACMO.

Research question 2: Topography of the sub-catchment

When analysing the sensitivity of discharge characteristics to RCM spatial resolution in terms of topography, no relations are found. It was expected based on the study by Kleinn et al. (2005) that the sub-catchments located in the Alpines would benefit more from an increase in RCM spatial resolution than the sub-catchments located in the lowlands. The West Alpine shows indeed an increase in total model performance. However, the same increase is observed for the Main. Reuss Seed does not show an increase in total model performance at all. It is concluded that the increase in RCM spatial resolution has more to do with the catchment size than the fact that it is located in the mountainous region. In conclusion, the influence of RCM spatial resolution on discharge characteristics is independent of the topography of the catchment. Both the RCM RACMO performance and hydrological model performance contribute to the total model performance. When only analysing the RCM RACMO performance, the same conclusions are drawn. When observing the absolute total model performance, the performance is very low for the four sub-catchments. Kleinn et al. (2005) concluded that the performance of the sub-catchments located in the Alpine are in general much lower than the performances for the lowlands. Kleinn et al. (2005) applied a bias correction while this study did not. For this study the performances of all sub-catchments is low.

Research question 3: Hydrological model – parameter estimation
The hydrological model performance contributes to the total model performance and therefore influences the results. When the hydrological model performance is low for a certain discharge characteristics, the influence of the RCM spatial resolution on the total model performance is bigger since both performances are strengthening each other. However, in this research it is observed that the hydrological model performance does not influence the sensitivity of discharge characteristics to RCM spatial resolution, but only the absolute value of the total model performance.

When analysing the sensitivity of discharge characteristics to RCM spatial resolution for the three versions of HBV, it is concluded that for the Main, West Alpine and Kinzig the sensitivity is the same for the three different versions. For the Main and West Alpine the total model performance increases when increasing the RCM spatial resolution for all three versions of HBV. For Kinzig the total model performance decreases when increasing the RCM spatial resolution for the three versions of HBV. Only for Reuss Seedorf the sensitivity is different for the three hydrological model versions. The lowest RCM spatial resolution shows the best performance, followed by the R12 for the semi-calibrated and calibrated model and followed by the R25 for the un-calibrated model. In general, the change in total model performance when increasing the spatial resolution does not depend on the hydrological model – parameter estimation.

Further, the results of the sensitivity of discharge characteristics to RCM spatial resolution in terms of hydrological model – parameter estimation give as well insight in the effectiveness of increasing the RCM spatial resolution compared to the effectiveness of calibrating the HBV model. For the West Alpine for all three versions of HBV, an increase RCM spatial resolution leads to an increase in total model performance. If calibrating HBV leads to an increase in total model performance, depends on the RCM spatial resolution. For the Main both calibrating and increasing the RCM spatial resolution lead to an increase of total model performance. For Kinzig the calibration leads to an increase in total model performance, while the increase of RCM spatial resolution leads to a decrease in total model performance. For Reuss Seedorf there is no clear trend at all. These observations are as well supported when only analysing the RCM RACMO performance. It is concluded that for the lowlands the calibration of the hydrological model is more effective than increasing the RCM spatial resolution. For the mountainous sub-catchments no clear conclusion is drawn. This could be partly because the hydrological model structure of HBV in general is less good for mountainous sub-catchments.

6.2 Conclusion research objective

The research objective of this study thesis is as follows:

To assess the sensitivity of discharge characteristics to RCM spatial resolution (12.5, 25 and 50 km) simulated by different versions of HBV having different parameterizations for catchments with different characteristics (sizes and topography) in the Rhine basin.

In this research it is concluded that there is no clear relation between the total model performance and the RCM horizontal resolution. The topography of the sub-catchment does not influence the sensitivity of discharge characteristics (annual, high and low discharges) to RCM spatial resolution. The discharge characteristics are not sensitive to RCM spatial resolution in terms of hydrological model – parameter estimation. Only the size of the sub-catchments influences the sensitivity of discharge characteristics to RCM spatial resolution. In general, an increase in RCM spatial resolution leads to an increase in total model performance for the two larger sub-catchments West Alpine and Main. This increase is larger for high discharges instead of the annual discharge and lower for the low discharges. Further, these two catchments are both showing the same changes in total model performance when increasing the RCM spatial resolution and are therefore called both sensitive. Additionally, it depends on the catchment if calibrating or increasing the RCM spatial resolution is more effective in terms of simulating discharge characteristics. The two catchments in the lowlands

(Main and Kinzig) are in general more sensitive to calibration than for the increase in RCM spatial resolution. The two catchments in the Alpines are less sensitive for calibration than the two catchments in the lowlands, however, for these two catchments no clear conclusions can be drawn. Moreover, when analyzing the absolute total model performance it can be concluded that the performance is low (presented by a ratio above 1.2 and below 0.8), especially for the low and high discharges.

Apart from a conclusion about the sensitivity of discharge characteristics to RCM spatial resolution, another conclusion is drawn as well. The results of the hydrological model performance and RCM RACMO performance showed that they are strengthening and compensating each other performances and together contribute to the total model performance. This means that in general no conclusion can be drawn on the total model performance only. A very good example is the total model performance of the standard deviation of the low discharge for Kinzig where the hydrological model performance shows a ratio of 1.47 and the RCM RACMO performance a ratio of 0.74. Both performances are compensating each other leading to a total model performance of 1.09 which is very good. This example shows very clearly that when not decomposing the total model performance, it cannot be concluded that the total model performance showing certain changes in discharge characteristics when changing the RCM spatial resolution, are mainly caused by the changes in spatial RCM resolutions. These results can as well be influenced by for example a very bad performance of the hydrological model or bias correction method. This explains why different researches may come up with different conclusions.

When comparing above conclusion to the presented discussion in chapter 0, an observation can be added to the general discussion about the sensitivity of discharge characteristics to RCM spatial resolution. In terms of sensitivity of discharge characteristics to RCM spatial resolution, it is analysed that only for the two larger sub-catchments an increase in RCM spatial resolution leads to an increase in total model performance (although this performance is still very low). However, as explained by Kleinn et al. (2005), it would be expected that especially smaller sub-catchments can benefit from an increase in RCM spatial resolution. The reason for this is that Kleinn et al. (2005) concluded that an increase in RCM spatial resolution leads to a better representation of small scale precipitation patterns. For larger catchment of several thousand square-kilometres and for the runoff evolution of a daily timescale, the fine-scale distribution of precipitation within the catchment is less important than for smaller sub-catchments (Kleinn, et al., 2005). However, this study did not support this expectation. Graham et al. (2005) concluded that a finer RCM spatial resolution resulted in biases of temperature and precipitation that were more systematic and less spatially variable. Olsson et al. (2014) supported this by concluding that the bias was steadily reduced or remained unchanged when increasing the resolution. Kleinn et al. (2005) did apply a bias correction while this study did not. When combining these aspects, it is expected that, especially smaller sub-catchments, only profit from an increase in RCM spatial resolution when a bias correction is applied. The larger sub-catchment already profit from an increase in RCM spatial resolution although the performance only slightly increases. This suggests that as well the larger sub-catchments could benefit from a bias correction.

6.3 Recommendations

Based on above conclusions and the discussion, several recommendations are formulated. First, the hypothesis is formulated that, especially smaller sub-catchments, seems to only benefit from an increase in RCM spatial resolution when applying a bias correction. Previous researches indeed concluded that an increase in RCM spatial resolution leads to less spatially variable biases. However, there is no research that analyzed the effect of a bias correction method in combination or independent of increasing the RCM spatial resolution for smaller sub-catchments. It is interesting to focus further research on this topic. What is the effect of bias correction on total model performance for smaller and larger sub- catchments and is this bias correction necessary to simulate more realistic discharges? What is the effect of the combination of the bias correction and increase of RCM spatial resolution on total model performance for smaller and larger sub-catchments? In other words, is the application of a bias correction necessary when profit from an increase in RCM spatial resolution?

Second, in this research four sub-catchments are analyzed all having a different combination of size and topography. It would be interesting in further research to analyze different catchments having the same characteristics and size. This analysis gives insight if the RCM RACMO performance and hydrological model performance are showing the same values for different type of discharges for the same type of sub-catchments. This would give a better insight in the effect of changing RCM spatial resolution on simulated discharges.

Third, as explained in section 4.1.2 and appendix E, the difference between the three versions of HBV-96 are the parameter values. To be able to improve HBV-96 for future research, it is interesting to analyze if the different parameters are dependent of each other and therefore contribute together to the hydrological model performance. Moreover, which of the parameters are most interesting? This could be analyzed by performing a large sensitivity analysis.

Fourth, it is recommended to analyze the hydrological model structure as well. In this research only the parameter performance is analyzed since no second hydrological model is taken into account. It is concluded that the parameter estimation does not influence the increase of total model performance when increasing RCM spatial resolution. However, to be able to say something about the hydrological model performance in total, the exact same circumstances need to be analyzed for another hydrological model. Only then a good insight is obtained about the sensitivity of discharge characteristics to RCM spatial resolution in terms of hydrological models.

Fifth, it would be interesting as well to analyze the effect on discharge simulation when first aggregating the highest RCM spatial resolution R12 to R50 and then compare this aggregation to the original R50. Does the R50 than includes more detail and what is the influence on simulating the discharge?

Sixth, as shown in appendix E, the actual evaporation influences the simulated discharge. Normally, another method to calculate the potential evapotranspiration is used in HBV. It is interesting to compare the method of calculating the PET and to analyze the effect on the model performance.

At last, it is highly recommended to have a critical attitude against the contribution of the different type of performances to the total model performance. This means that for example a high total model performance can be caused by a RCM performance which shows an overestimation of the discharge and a hydrological model performance which shows an underestimation of the discharge leading to a compensation of each other's over- and underestimation. This means that conclusions based on the total model performance are in fact caused by other aspects than assumed.

7 Bibliography

BAFU. (2012). *Thema Wasser*. Retrieved from Bundesamt für Umwelt BAFU: https://www.bafu.admin.ch/bafu/de/home/themen/wasser.html

Berglöv, G., German, J., Gustavsson, H., Harbman, U., & Johansson, B. (2009). *Improvement HBV model Rhine in FEWS - Final report.* SMHI. Hydrology.

Bergström, S. (1976). *Development and application of a conceptual runoff model for scandinavian catchments.* Norrköping: Swedish Meterological and Hydrological Institute.

BfG. (2017). *The german Federal Institute of Hydrology (BfG)*. Retrieved from Bundesanstatt für Gewässerkunde: http://www.bafg.de/EN/03_The_%20BfG/the_bfg.html

Booij, M. (2005). Impact of climate change on river flooding assessed with different spatial model resolutions. *Journal of Hydrology, 303*, 176-198. doi:10.1016/j.jhydrol.2004.07.013

Christensen, J. H., Kjellstrom, E., Giorgi, F., Lenderink, G., & Rummukainen, M. (2010, December). Weight assignment in regional climate models. *Cliamte research, 44*, 179-194. doi:10.3354/cr00916

Clark, M. P., Wilby, R. L., Gutmann, E. D., Gangopadhyay, J. A., Wood, A. W., Fowler, H. J., . . . Brekke, L. D. (2016, april 06). Characterizing Uncertainty of the Hydrologic Impacts of Climate Change. *Curr Clim Change Rep, 2*, 55-64.

Dankers, R., Christensen, O. B., Feyen, L., Kalas, M., & de Roo, A. (2007). Evaluation of very high-resolution climate model data for simulating flood hazards in the Upper Danube Basin. *Journal of Hydrology, 347*, 319-331. doi:10.1016/j.jhydrol.2007.09.055

Davids, F., Velden, C. t., Eilander, D., & Verseveld, W. v. (2015). *Kalibratie en aanpassingen HBV model voor de Rijn voor laagwater.* Delft: Deltares.

Dee, Dick, Fasullo, John, Shea, Dennis, . . . John. (2016, 12 12). *Atmospheric reanalysis: Overview & Comparison tables*. (National Center for Atmospheric Research) Retrieved from The climate data guide:: https://climatedataguide.ucar.edu/climate-data/atmospheric-reanalysis-overview-comparison-tables

Demirel, M., Booij, M., & Hoekstra, A. (2014). Impacts of climate change on the seasonality of low flows in 134 catchments in the River Rhine basin using an ensemble of bias-corrected regional climate simulations. *Hydrology and Earth System Sciences, 17*, 4241-4257. doi:10.5194/hess-17-4241-2013

Diermanse, F. (2001). *Physically based modelling of rainfall-runoff processes.* Delft: Delft University Press Science.

Duan, Q., Sorooshian, S., & Gupta, V. K. (1994). Optimal use of the SCE-UA global optimization method for calibrating watershed models. *Journal of Hydrology, 158*, 265-284. doi:SSDI 0022-1694(94)02467-P

ESGF. (2016). *CORDEX*. Retrieved February 2016, from Welcome to the DKRZ ESGF-CoG Node: https://esgf-data.dkrz.de/search/cordex-dkrz/

Goovaerts, P. (2000). Geostatistical approaches for incorporating elevation into the spatial interpolation of rainfall. *Journal of Hydrology, 228*, 113-129. doi:PII: S0022-1694(00)00144-X

Görgen, K., Beersma, J., Brahmer, G., Buiteveld, H., Carambia, M., Keizer, O. d., . . . Volken, D. (2010). *Assessment of Climate Change Impacts on Discharge in the Rhine River Basin: Results of the RheinBlick2050 Project.* International Commission for the Hydrology of the Rhine Basin.

Graham, L., Andréasson, J., & Carlsson, B. (2007, March 17). Assessing climate change impacts on hydrology from an ensemble of regional climate models, model scales and linking methods - A case study on the Lule River basin. *Climatic Change, 81*, 293-307. doi:10.1007/s10584-006-9215-2

Gupta, & Sorooshian. (1995). *Chapter 2: Model calibration.* Littleton: Computer models of watershed hydrology.

Gupta, H. V., Kling, H., Yilmaz, K. K., & Martinez, G. F. (2009). Decomposition of the mean squared error and NSE performance critera: Implications for improving hydrological modelling. *Journal of Hydrology, 377*, 80-91. doi:10.1016/j.jhydrol.2009.08.003

Haylock, M., Hofstra, N., Tank, A. K., Klok, E., Jones, P., & New, M. (2008). A European daily high-resolution gridded data set of surface temperature and precipitation for 1950-2006. *Journal of geophysical research, 113*, 12. doi:10.1029/2008JD010201

Hegnauer, M., Beersma, J., Boogaard, H. v., Buishand, T., & Passchier, R. (2014). *Generator of Rainfall and Discharge Extremes (GRADE) for the Rhine and Meuse basins; Final report of GRADE 2.0.* Delft: Deltares.

Hegnauer, M., Verseveld, W. v., Weerts, A., & Blom, G. (2013). *Generalised Likelihood Uncertainty Estimation for the daily HBV model in the Rhine Basin - Part B: Zwitserland.* Delft: Deltares.

Houska, T., Kraft, P., Chamorro-Chavez, A., & Breuer, L. (2015). *SPOTting Model Parameters Using a Ready-Made Python Package.* PLoS ONE. doi:10.1371/journal.pone.0145180

IPCC. (2014). *Climate change 2014: Synthesis Report. Contribution of Working Groups I, II and III to the Fifth Assessment Report of the Intergovernmental Panel on Climate Change.* Geneva, Switzerland: Core Writing Team, R.K. Pachauri and L.A. Meyer (eds).

Jeon, J.-H., Park, C.-G., & Engel, B. A. (2014). Comparison of Performance between Genetic Algorithm and SCE-UA for calibration of SCS-CN Surface Runoff Simulation. *Water, 6*, 3433-3456. doi:10.3390/w6113433

Kersbergen, A. (2016). *Skill of a discharge generator in simulating low flow characteristics in the Rhine basin.* Enschede: University of Twente.

Kleinn, J., Frei, C., Gurtz, J., Lüthi, D., Vidale, P., & Schär, C. (2005, February 18). Hydrologic simulations in the Rhine basin driven by a regional climate model. *Journal of geophysical research, 110*, 18. doi:10.1029/2004JD005143

Klemes, V. (1986). Operational testing of hydrological simulation models. *Hydrological Sciences Journal, 31*(1), 13-24. doi:10.1080/02626668609491024

Kysely, J., Rulfova, Z., Farda, A., & Hanel, M. (2016). Convective and stratiform precipitation characteristics in an ensemble of regional climate model simulations. *Climate Dynamics, 46*, 227-243. doi:https://doi.org/10.1007/s00382-015-2580-7

Lenderink, G., van den Hurk, B., van Meijgaard, E., van Ulden, A., & Cuijpers, H. (2003). *Simulation of present-day climate in RACMO2: first results and model developments.* de Bilt: KNMI.

Lindström, G., Johansson, B., Persson, M., Gardelin, M., & Bergström, S. (1997). Development and test of the distributed HBV-96 hydrological model. *Journal of Hydrology, 201*, 272-288. doi:S0022- 1694(97)00041-3

Meijgaard, E. v. (2017, 06). RCMs spatial resolution. (I. v. Brink, Interviewer)

Mendoza, P. A., Mizukami, N., Ikeda, K., Clark, M. P., Gutmann, E. D., Arnold, J. R., . . . Rajagopalan, B. (2016, April 17). Effects of different regional climate model resolution and forcing scales on projected hydrologic changes. *Journal of Hydrology, 541*, 1003-1019. Retrieved from http://dx.doi.org/10.1016/j.jhydrol.2016.08.010

Monteith, J. (1965). Water in the plant. *Evaporation and environment*, 205-234.

Muleta, M. K. (2012, June). Model Performance Sensitivity to Objective Function during Automated Calibrations. *Journal of Hydrologic Engineering, 17*(6), 756-767. Retrieved from https://doi.org/10.1061/(ASCE)HE.1943-5584.0000497

Olsson, J., Berg, P., & Kawamura, A. (2014, November 4). Impact of RCM spatial resolution on the reproduction of local, subdaily precipitation. *Journal of hydrometeorology, 16*, 534-547. doi:10.1175/JHM-D-14-0007.1

Prein, A. F., Holland, G. J., Rasmussen, R. M., Done, J., Ikeda, K., Clark, M. P., & Liu, C. H. (2013, 07 01). Importance of Regional Climate Model Grid Spacing for the Simulation of Heavy Precipitation in the Colorado Headwaters. *Journal of climate, 26*, 4848-4857. doi:10.1175/JCLI-D-12-00727.1

Rauthe, M., Steiner, H., Riediger, U., Mazurkiewicz, A., & Gratzki, A. (2013). A Central European precipitation climatology - Part I: Generation and validation of a high-resolution gridded daily data set (HYRAS). *Meteorologische Zeitschrift, 22*(3), 235-256.

Rijtema, P. (1959). *Calculation methods of potential evapotranspiration.* Wageningen: Insitituut voor Cultuurtechniek en Waterhuishouding.

Rwasoka, T., Madamombe, C., Gumindoga, W., & Kabobah, A. (2013). Calibration, validation, parameter identifiability and uncertainty analysis of a 2-parameter parsimonious monthly rainfall-runoff model in two catchments in Zimbabwe. *Physics and Chemistry of Earth, 67-69*, 36-46. doi:10.1016/j.pce.2013.09.015.

SMHI. (2006). *Integrated Hydrological Modelling System - Manual - Version 5.10.* Swedish Meteorological and Hydrological Institute (SMHI).

Tallaksen, L., & Lanen, H. V. (2004). Hydrological Drought: Processes and Estimation Methods for Streamflow and Groundwater. *Developments in Water Science, 48*.

te Linde, A., Aerts, J., Bakker, A., & Kwadijk, J. (2010). Simulating low-probability peak discharges for the Rhine basin using resampled climate modeling data. *Water resources research, 46*, 19. doi:10.1029/2009WR007707

te Linde, A., Aerts, J., Hurkmans, R., & Eberle, M. (2008). Comparing model performance of two rainfall-runoff models in the Rhine basin using different atmospheric forcing data sets. *Hydrology and Earth System Sciences, 12*, 943-957. Retrieved from www.hydrol-earth-syst-sci.net/12/943/2008/

Thornthwaite, C. (1948). An approach toward a rational classification of climate. *Geographical Review, 38*(1), 55-94.

Tillaart, S. P., Booij, M. J., & Krol, M. S. (2013). Impact of uncertainties in discharge determination on the parameter estimation and performance of a hydrological model. *Hydrology Research, 44.3*, 454-466. doi:10.2166/nh.2012.147

Tillaart, S. v. (2010). *Influence of uncertainties in discharge determination on the parameter estimation and performance of a HBV model in Meuse sub basins.* Enschede: University of Twente.

Uehlinger, U., Wantzen, K. M., Leuven, R. S., & Arndt, H. (2009, December). The rhine river basin. *Rivers of Europe*, 199-245. doi:10.1016/B978-0-12-369449-2.00006-0

van der Linden, P., & Mitchell, J. (2009). *ENSEMBLES: Climate Change and its Impacts: Summary of research and results from the ENSEMBLES project.* FitzRoy Road, Exeter EX1 3PB, UK: Met Office Hardley Centre.

van Meijgaard, E., van Ulft, L., Lenderink, G., de Roode, S., Wipfler, L., Boers, R., & Timmermans, R. (2012). *Refinement and application of a regional atmospheric model for climate scenario calculations of Western Europe.* De Bilt; Wageningen; Utrecht: KNMI; Soil Physics, Ecohydrology and Groundwater Management GroupR; TNO.

van Meijgaard, E., van Ulft, L., van de Berg, W., Bosveld, F., van den Hurk, B., Lenderink, G., & Siebesma, A. (2008). *The KNMI regional atmospheric climate model RACMO, version 2.1.* De Bilt: KNMI.

Wagener, T., McIntyre, N., Lees, M., Wheater, H., & Gupta, H. (2003). Towards reduced uncertainty in conceptual rainfall-runoff modelling: Dynamic identifiability analysis. *Hydrological processes, 17*, 455-476. doi:10.1002/hyp.1135

Winsemius, H., Verseveld, W. v., Weerts, A., & Hegnauer, M. (2013). *Generalised Likelihood Uncertainty Estimation for the daily HBV model in the Rhine Basin - Part A: Germany.* Delft: Deltares.

Zhihua, R., & Mingqin, L. (2007). Errors and Correction of Precipitation Measurements in China. *Advances in atmospheric sciences, 24*(3), 449-458. doi:10.1007/s00376-007-0449-3

Appendix

A: Makkink calculation

To calculate the Potential evapotranspiration, Makkink has been selected. The Potential evapotranspiration (kg m^{-2} s^{-1}) is calculated using the following equations.

$$PET = \frac{s}{s+\gamma} * \frac{6{,}5*10^{6} R_s}{\rho * \lambda} \quad \text{(Equation 1)}$$

In this equation the following variables are represented as shown in Table 14

Table 14: The different variables as shown in the equation to calculate Makkink (Rijtema, 1959)

Variable	Definition	Unit	Value	Source
$\boldsymbol{R_s}$	Surface downward shortwave radiation	(W m^{-2})		RCM RACMO
$\boldsymbol{\rho}$	density of water	(kg m^{-3})	1000	
$\boldsymbol{\lambda}$	heat of vaporization	(J kg^{-1})		Equation 2
$\boldsymbol{\gamma}$	psychometric constant	(hPa $°C^{-1}$)		Equation 3
$\boldsymbol{s}$	slope of function of vapour pressure versus air temperature	(hPa $°C^{-1}$)		Equation 4

The latent heat of vaporization λ is calculated using T which is the observed daily temperature in °C.

$$\lambda = 1000 * (2501 - 2.38)\, T \quad \text{(Equation 2)}$$

The psychometric constant γ has been calculated using equation 3 where T is the observed daily temperature in °C.

$$\gamma = 0.646 + 0.0006 * T \quad \text{(Equation 3)}$$

The slope of the function of vapour pressure versus air temperature s is calculated using equation 4, where e_s is the saturation vapour pressure (equation 5) and T is the observed daily temperature in °C.

$$s = \frac{7.5*237.3}{(T+237.3)^2} * \ln(10) * e_s \quad \text{(Equation 4)}$$

The saturation vapour pressure e_s has been calculated using equation 5, where T is the observed daily temperature in °C.

$$e_s = 6.107 * \exp\left(\frac{7.5*T}{T+237.3}\right) \quad \text{(Equation 5)}$$

B: HBV layers with three RCM versions

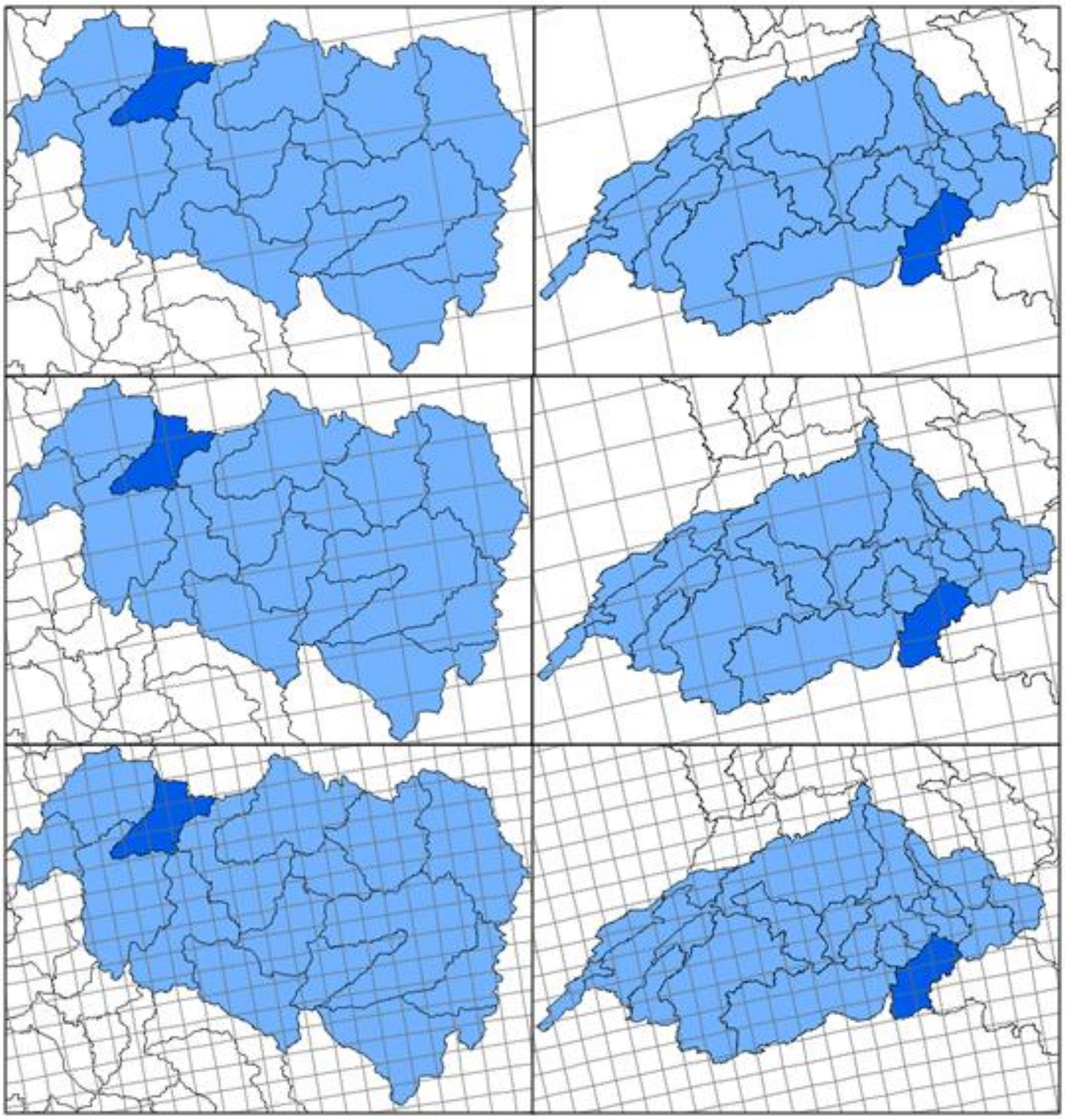

Figure 25: Main (left) and West Alpine (right), from top to down RCM spatial resolution R50 - R25 - R12

C: Parameter values of the three HBV versions

Table 15 shows values of the parameters for the different HBV models, the calibrated (CA), the semi-calibrated (SC) and the un-calibrated (UC) HBV model. Only the parameter values are shown having a different value for the three HBV-96 versions. Further, it is important to keep in mind that some parameters for the calibrated HBV model have different values for each sub-catchment.

Table 15: Parameter values of the three HBV versions. The value with underscore is not given and therefore assumed

		CA	SC	UC	
Parameter	**Source**	1	2	3	1: (Winsemius, Verseveld, Weerts, & Hegnauer, 2013) 2: (Berglöv, German, Gustavsson, Harbman, & Johansson, 2009) 3: (SMHI, 2006)
					1: Precipitation and snow routine
pcalt	Mm/°C	0	0.1	0.1	Lapse rate parameter for precipitation is applied to adjust to the current altitude
sfcf	-	1	1.1	1	Snowfall correction factor
tti	°C	2	2	0.5	Temperature interval for rain/snow mixing
fosfcf	-	0.8	1	0.8	Factor that will be multiplied by SFCF for zones of type forest
cfmax	mm/°C /day	3.5	3.5	3	The melting factor per day
dttm	°C	0	0	-0.5	Dttm + tt = Threshold temperature for snow melt
ecalt	-	0	0	0.1	Elevation adjustment to allow for a decrease in potential evaporation with elevation
ered	-	1	0	<u>0</u>	Used to reduce actual evaporation when interception is included in the computation in order to avoid values of total actual evaporation (sum of soil and interception evaporation) which are too large.
icfo		4	1.5	<u>0</u>	Introduces an interception storage. From this storage, evaporation equal to potential evaporation will occur as long as water is available
					2: Soil routine
lp	-	0.7	0.9	1	Soil moisture value above which evapotranspiration reaches its potential value
beta	-	2	2.5	1	Control for the increase in soil moisture for every mm of precipitation
cevpfo	-	1.2	1	1.15	Correction factor for potential evaporation in forest zones
					3: Response routine
perc	mm/day	0.5	2	0.5	Percolation capacity from upper to lower response box → slow responding reservoir
k4	day^{-1}	0.01	0.05	0.01	Recession coefficient lower reservoir → slow responding reservoir
khq	day^{-1}	0.09	0.2	0.09	Recession coefficient from the upper box water discharge equals hq → fast responding reservoir = upper box
alfa	-	1	1	0.9	Measure of the non-linearity, typically in the order of 1 → fast responding reservoir = upper box
cflux	Mm/day	0	0	0.5	Maximum capillary flow from upper response box to soil moisture zone
epf	-	0	0.02	<u>0</u>	Potential evaporation may be reduced during rainfall events by: Epot * e^(-epf*P)
					4: routing
maxbas	-	0.042	0.5	1	The time base of the triangular distribution

D: Results calibrated parameters

In appendix D the results for the calibration are shown. Each table shows the calibrated sub-catchment groups in the first column, the criteria for the KGE and NSE where the selection of the calibration parameters is based on in the second and third column and the results of the calibrated parameters in the other columns.

Table 16: Values for different parameter values obtained from calibration Main

	KGE	NSE	Alfa	Beta	Fc	K4	Khq	Lp	perc
Unit			-	-	mm	-	1/day	-	mm/day
Main1	8%	15%			134.331		0.127	0.898	2.713
Main2	3%	1%		2.471	182.218	0.028	0.083		0.602
Rednitz, Aisch, Regnitz, Main3, Main4, Main5, Tauber, Main6	10%	15%			189.467	0.002	0.052		1.173
Pegnitz	18%	15%	0.293	0.627	419.260	0.003	0.084		2.002
FrSaale	12%	15%			231.006	0.047	0.144		1.999
Kinzig	10%	15%			219.312	0.083	0.112		5.498
Main7	1%	1%		3.991	499.399			0.300	
Nidda	10%	15%		1.073	309.501		0.117	0.302	0.505
Main8	0.5%	0.5%			100.060	0.100			

Table 17: Values of different parameter values obtained from calibration West Alpine

	KGE	NSE	tt	Cfmax	Alfa	Beta	Fc	K4	Khq	Lp	perc
Unit			°C	mm	-	-	mm	-	1/day	-	mm/day
Thunersee, Aare1	10%	15%				0.001		0.752	0.036	0.874	0.734
Emme	5%	10%		5.997	0.533				0.206		1.713
KleineEmme, Limmat_reus, Sihlzuer, Lintmoll, Lintwees, Limmzuer	2.5%	5%				0.002			0.068	0.747	2.360
Aare2	0.5%	0.5%						0.023	0.116		4.170
Orbeorbe, Areuboud, Broypaye, Canasugi, Zihlgamp, Aarebrue	1%	1%		5.968			18.199				
Reuss-seedorf	5%	10%	-2.993	5.296					0.152		0.505
Muotinge, Engebuoc, Reusluze	2.5%	5%		1.017				0.095	0.207		0.502

E: Analysis HBV model structure and HBV parameter values

In section 4.1.2 the hydrological model performance $Q_{sim-obs\,P,T,PET}/Q_{obs}$ is analysed for the four selected sub-catchments and the three versions of HBV-96 (Figure 26). There are eight situations as presented by the black circles where the hydrological model performance of the calibrated HBV-96 model is low (ratio below 0.8 or above 1.2). The hydrological model performance is influenced by both the model structure performance and parameter performance (section 3.5.3). Since no other model structure is analysed in this research, only insight in the parameter performance is obtained. This is done by comparing the hydrological model performance of the semi-calibrated and un-calibrated HBV-96 model to the calibrated HBV-96 model as shown in section 4.1.2. The differences in hydrological model performance between the three versions of HBV-96 are caused by parameters having different values. In this appendix the parameter values of the three versions of HBV are compared for the eight situations where the calibrated HBV model shows a low performance. This comparison can give insight in which parameters are causing this low performance and which parameters are explaining the difference in hydrological model performance between the three HBV versions. It is important to keep in mind that the parameters could be dependent of each other and therefore, it could be an interaction between different parameters which lead to the observed differences.

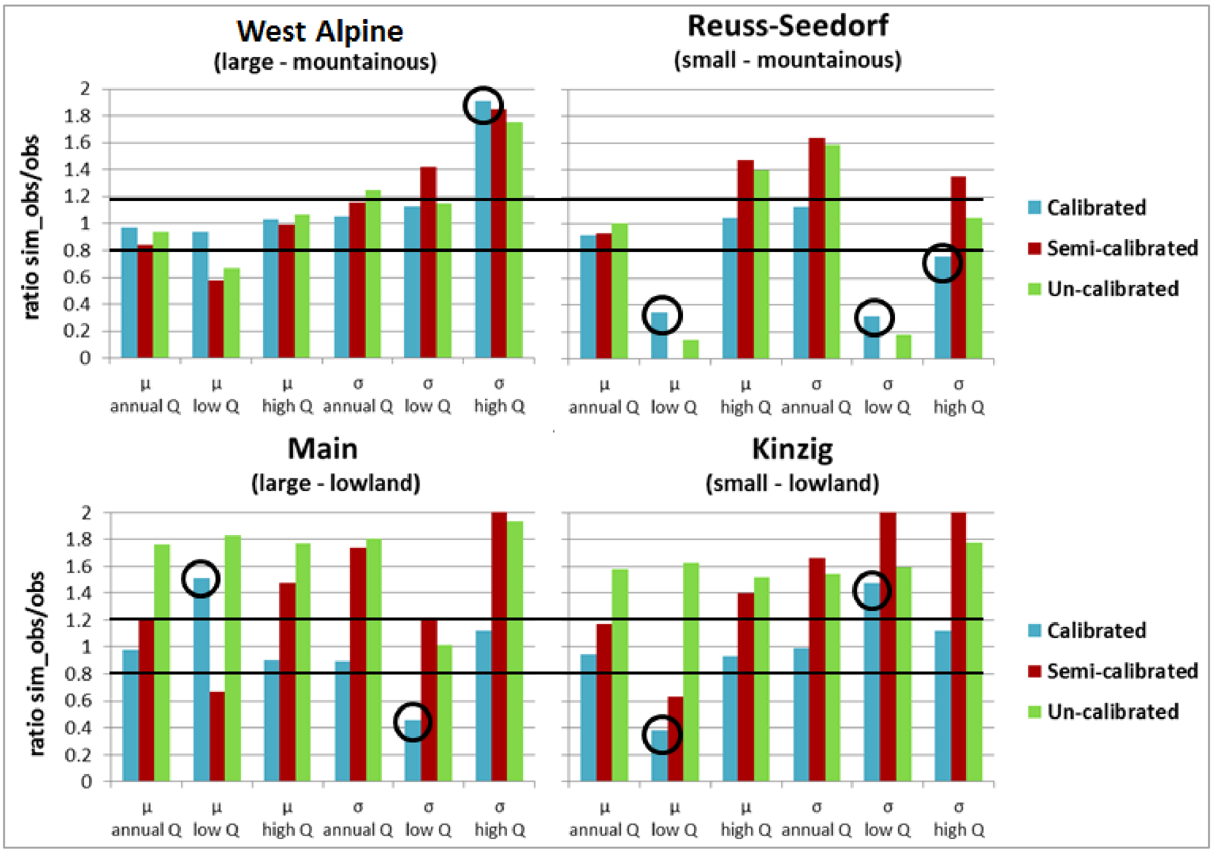

Figure 26: hydrological model performance for the calibrated, semi-calibrated and un-calibrated HBV-96 presented by the ratio of simulated discharge forced with observed meteorological data and the observed discharge. If the ratio is 1 a perfect model performance is presented and between 0.8 and 1.2 a good model performance is presented (black lines). The black circles show the performances for the calibrated model below 0.8 or above 1.2. Some performances are very low and out of the presented range. Main: semi-calibrated model, standard deviation of high discharge (2.3), Kinzig: semi-calibrated model, standard deviation low discharge (2.3), standard deviation of high discharge (2.6). The µ represents the mean and the σ the standard deviation of the annual, low or high discharge.

West Alpine

The West Alpine is located in the mountainous Alpines. In this area there is a lot of snowfall resulting in snow melt during summer time. Therefore, the high discharge occurs in summer time and the low discharge in winter time (Figure 27). For the West Alpine the hydrological model performance of the standard deviation of the high discharge is analysed (Figure 26).

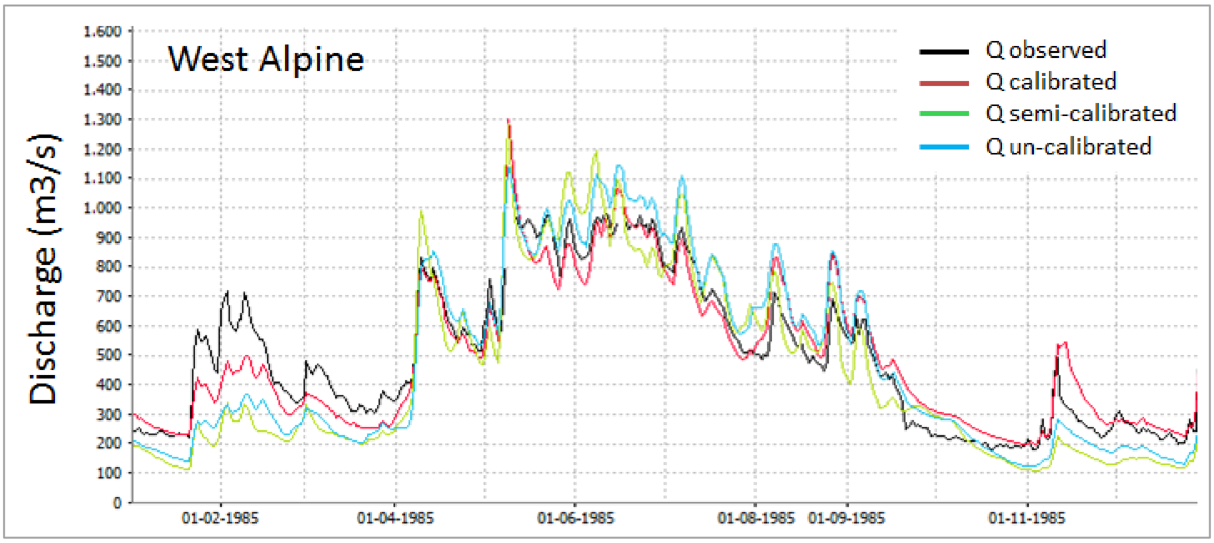

Figure 27: The observed and simulated discharge of West Alpine for 1985. The missing values of the observed discharge and the corresponding days for the simulated discharges are not used in the analsysis.

1: Precipitation and snow routine

When looking at the actual evaporation as shown in Figure 28, the calibrated model shows more outliers leading to a higher standard deviation. This might be the explanation for the higher standard deviation of the high discharges.

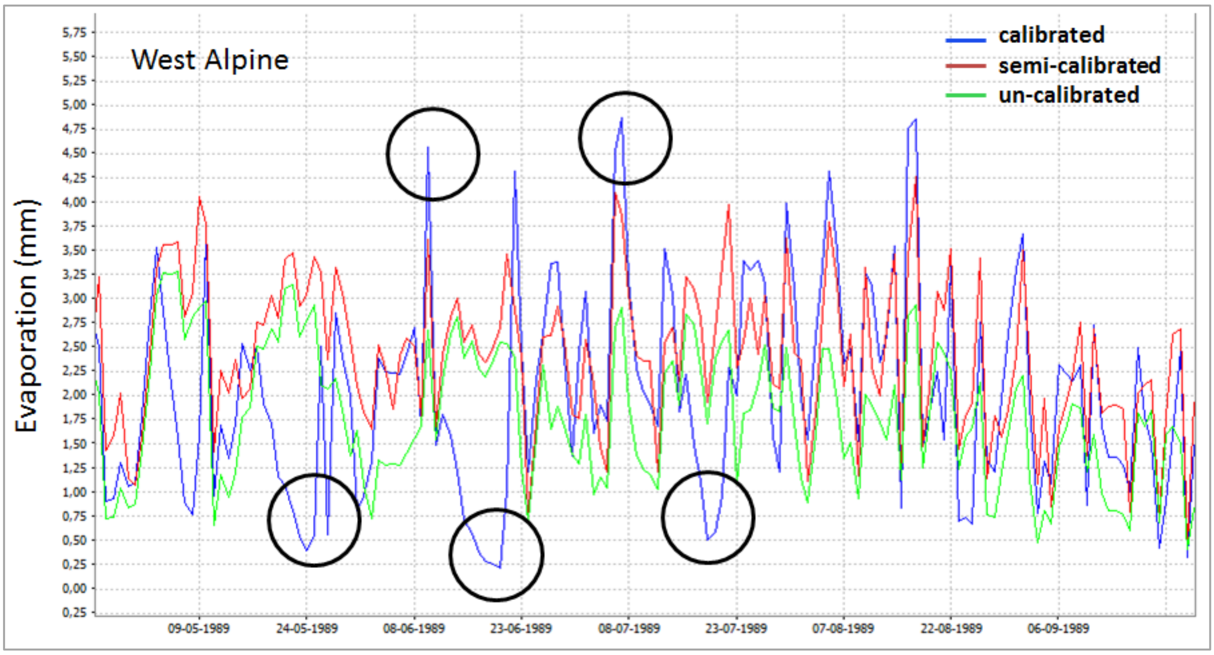

Figure 28: Actual evaporation West Alpine for three model versions in summer time in 1989

The outliers for the calibrated model might be caused by the parameter values as shown in Table 18. The lower (lp) value for the calibrated model means that the actual evaporation has sooner reached the value of the potential evaporation leading to more actual evaporation compared to the other models. Further, the (fc) is much lower for the calibrated HBV model. The ratio of actual evaporation and potential evaporation is based on the actual soil moisture divided by the (fc). A lower (fc) means that the decrease or increase of the actual soil moisture has a higher influence on the ratio of the actual evaporation and the potential evaporation. This leads to a faster increase or decrease in actual evaporation.

Table 18: Parameter values evaporation routine West Alpine

West Alpine	Calibrated	Semi-calibrated	Un-calibrated
Fc (mm)	21.209	200	200
Lp (-)	0.7	0.9	1.0

Reuss-Seedorf

For Reuss-Seedorf the mean of the low discharge and the standard deviation of the low and high discharge are analyzed. Figure 29 shows that in general the calibrated HBV model simulates discharges more equal to the observed discharges than the semi- and un-calibrated HBV model. Further, since Reuss-Seedorf is located in the Alpines, it is mainly a snow-fed sub-catchment having high discharges during summer.

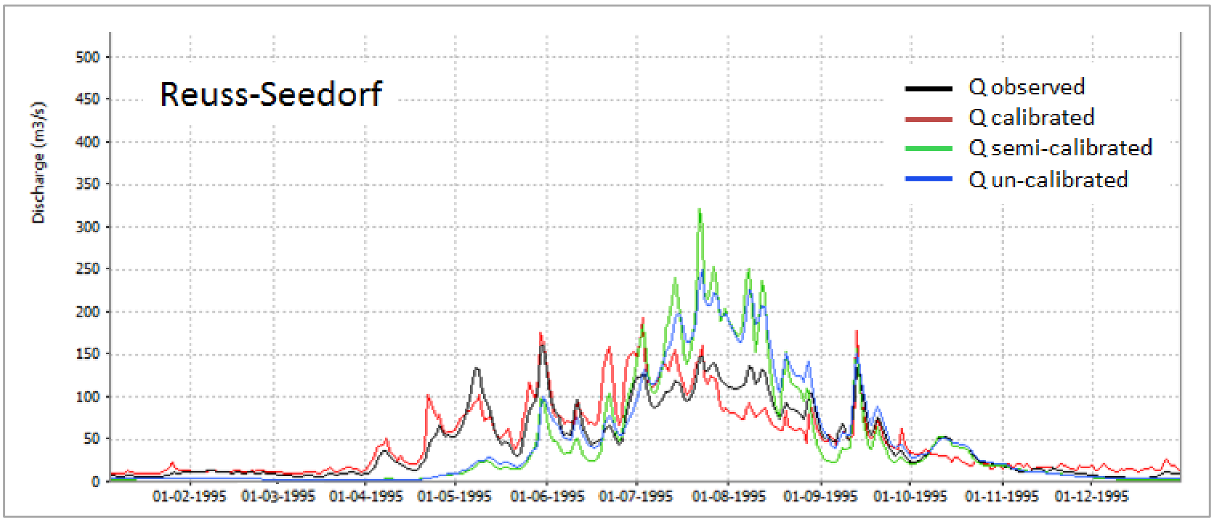

Figure 29: observed discharge (black line) and simulated discharges by 3 HBV versions for Reuss-Seedorf.

1: precipitation and snow routine

Table 19: Differences in parameter values for the three versions of HBV for the precipitation and snow routine

Reuss-Seedorf	Calibrated	Semi-calibrated	Un-calibrated
tt	-2.993	0	0
tti	2	2	0.5
dttm	0	0	-0.5
Pcalt	0	0.1	0.1

The parameters (tt) and (tti) together determine from which threshold precipitation falls as snow, rain or a mix according to the following equation:

$$Rainfall\ if\ T > tt + tti/2$$
$$Snowfall\ if < tt - tti/2$$
$$Snow\ melt\ starts\ T > tt + dttm$$

These equations and parameters (Table 19) show that below T = -3.993 ^{o}C the precipitation falls as snowfall for the calibrated model, for the semi-calibrated model below T = -1 ^{o}C and for the un-calibrated model below T = -0.25 ^{o}C meaning that there is much more snowfall for the semi- and un-calibrated model resulting in a thicker snowpack than for the calibrated HBV model (Figure 30).

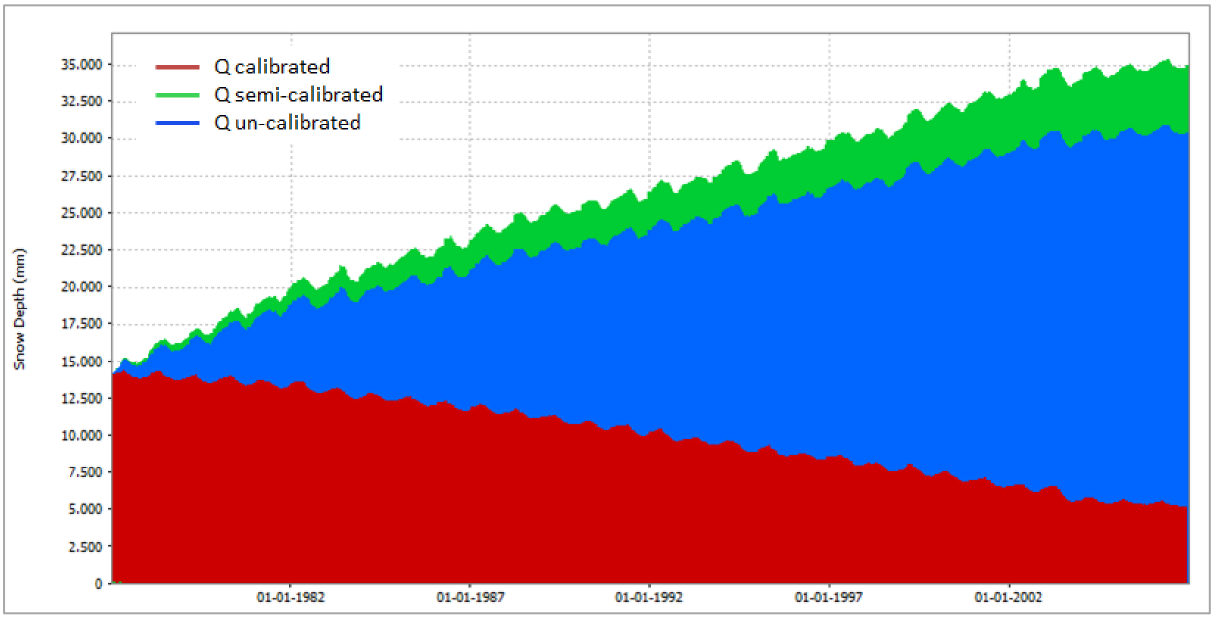

Figure 30: snowpack Reuss-Seedorf

The snow melt starts for the calibrated HBV model much sooner in the year (T > -2.993 ^oC) than for the un-calibrated (T > -0.5 ^oC) and semi-calibrated (T > 0 ^oC) HBV model resulting in the high discharge in April as shown in Figure 29. However, in winter time (low discharges) the temperature does not exceed the 0 ^oC for Reuss-Seedorf which explains that for the semi-calibrated HBV model no snow melt occurs during the winter period and for the un-calibrated HBV model only a bit snow melt occurs during the winter period leading to less discharge than for the calibrated HBV model. Especially when this is as well linked to the fact that most of the precipitation during the winter period falls as snow for the semi- and un-calibrated HBV model accumulating the snowpack but not resulting in discharge. This explains that the underestimation of both the mean and standard deviation of the low discharge is much higher for the semi-calibrated HBV model followed by the un-calibrated HBV model than for the calibrated HBV model. However, the calibrated HBV underestimates the low discharge as well. These parameters (tt), (tti) and (dttm) could be improved to decrease the underestimation.

In summer time the discharge consists of melt water and precipitation. The standard deviation of the high discharges is underestimated by the calibrated HBV model, overestimated for the semi-calibrated HBV model and simulated as good for the un-calibrated model. This is explained by looking at the precipitation (Figure 31). The calibrated HBV model has a standard deviation of 3.95 while the standard deviation of the semi-calibrated model is 7.27 and of the un-calibrated HBV model 6.72 over a period of 19 years. Further, the total amount of rainfall is 21701 mm for the calibrated model, 39966 for the semi-calibrated model and 36963 for the un-calibrated model. The reason that the amount of rainfall is much lower for the calibrated HBV model is because of the parameter (pcalt). The (pcalt) is the lapse rate which corrects precipitation with 0.1 for each 100 meter increase in height. As explained in section 2.3, each sub-catchment is divided into elevation zones instead of having one height. Therefore, for each elevation zone this (pcalt) is applied for the amount of precipitation. For the Main the differences in precipitation are much smaller since these sub-catchments are much flatter having a lower difference in elevation. The reason that the total amount of precipitation and the standard deviation of precipitation is higher for the semi-calibrated model in comparison to the un-calibrated HBV model could be because of the temperature range defining when precipitation consists of a mix of snow and rain (-1 to 1 for semi-calibrated and -0.25 and 0.25 for un-calibrated).

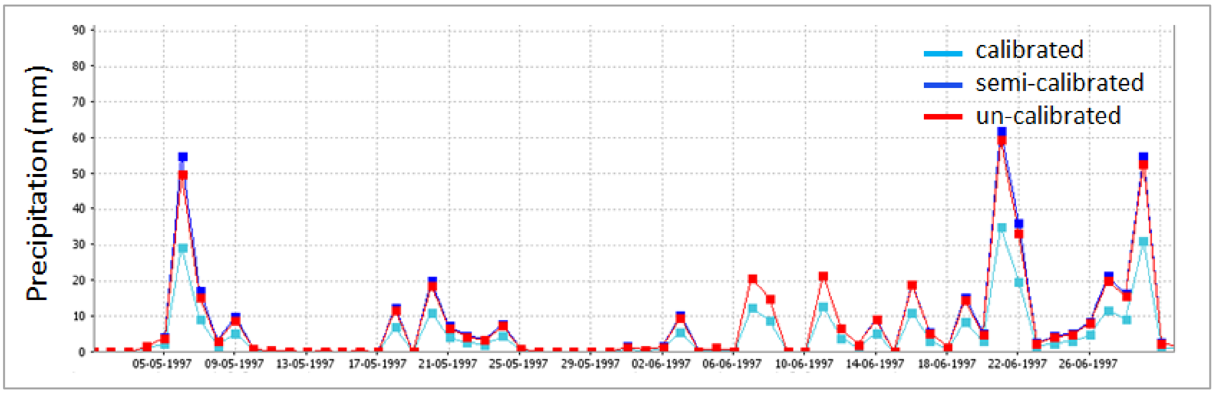

Figure 31: Precipitation Reuss-Seedorf for the three HBV models

2: evaporation routine

Table 20: Differences in parameter values for the three versions of HBV for the evaporation routine

Reuss-Seedorf	Calibrated	Semi-calibrated	Un-calibrated
Fc (mm)	12.459	200	200
Lp (-)	0.7	0.9	1.0
Icfo (-)	4	1.5	0
Ered (-)	1	0	0

In the summer period there is two times more actual evaporation for the calibrated HBV model then for the semi-calibrated HBV model and four times more actual evaporation then for the un-calibrated model as shown in Figure 32. This explains that during the summer period there is more runoff for the semi-calibrated and un-calibrated HBV model as shown in Figure 29. This as well explains why in general the high discharges are overestimated more by the semi- and un-calibrated HBV model.

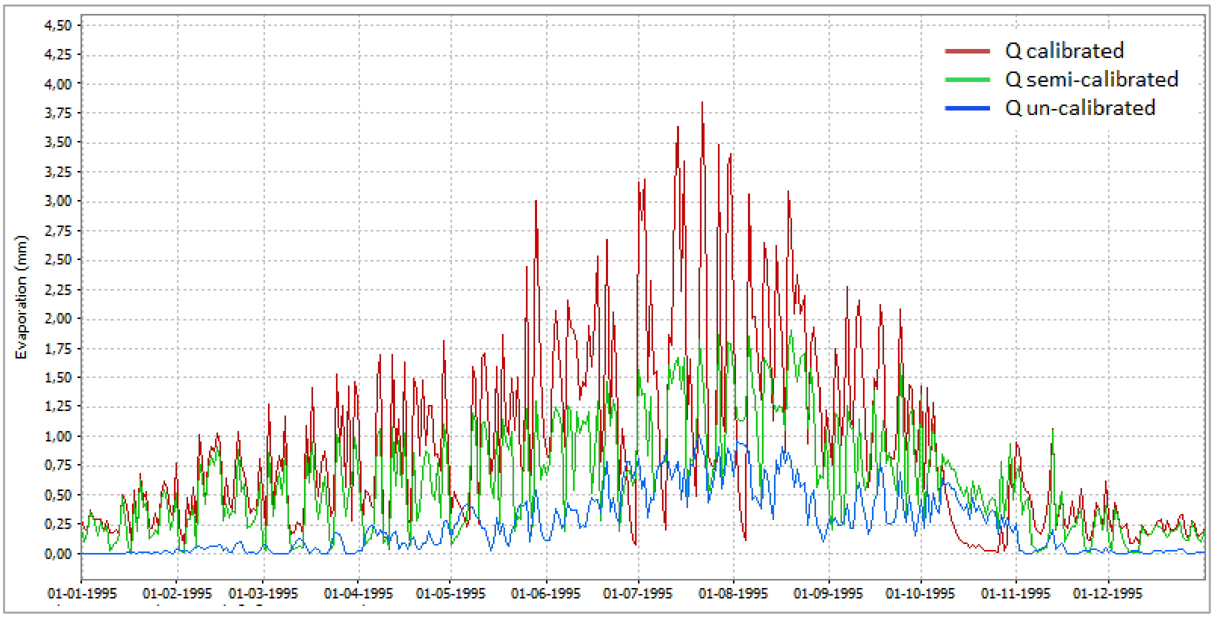

Figure 32: Actual evaporation for Reuss-Seedorf in the year 1995

The reason there is more actual evaporation in the calibrated model, is because of the parameter (fc) and (lp). The parameter (fc) (maximum soil moisture storage) is much lower than for the semi- and un-calibrated HBV model. This means that the actual soil moisture divided by the fc (-) sooner reaches the value of lp (-). When the value of lp is reached, the actual evaporation is equal to the potential evaporation. The value of lp is lowest for the calibrated model and highest for the un-calibrated model.

However, another explanation for the actual evaporation difference is that the parameter (icfo) introduces an interception storage. From this storage, evaporation equal to potential evaporation will occur as long as water is available. This value is zero for the un-calibrated model, 1.5 for the semi-calibrated model and 4 for the calibrated model. The parameter (ered) is used to reduce the actual evaporation when interception is included which is 1 for the calibrated model and 0 for the semi-calibrated model which shows that the actual evaporation of the calibrated model is reduced. It is unclear how this reduction of evaporation is calculated. However, the combination of these parameters could explain the differences in actual evaporation.

Main

For the Main two different types of discharges are observed, the mean and standard deviation of the low discharge. For the Main the high discharges occur in winter time and the low discharges in summer time. This is because Main is more rain-fed than snow-fed.

1: Precipitation and snow routine

The rainfall data is the same for the three different models. This means that it is not the rainfall occurring in Main which is causing the difference in low discharge. Further, for the Main the low discharge occurs in summer time which means that the snow routine cannot have influenced the low discharge. In summer time, the amount of actual evaporation is for semi-calibrated HBV model slightly higher than for the calibrated model. This could be part of the reason why the mean low discharge is underestimated by the semi-calibrated HBV model. However, the difference between the over- and underestimation is that big that it is assumed this is not the only cause. Further, the standard deviation of the calibrated model is 0.45, for the semi-calibrated model 1.22 and for the un-calibrated model 1.02. This cannot clarify the difference in standard deviation of the low discharge simulated by the different models.

3: Response routine

Within the response routine, the low discharge mainly consists of slow runoff. The equation to calculate the slow runoff is as follows where k4 is the recession coefficient and LZ the water content of the lower store:

$$Q = k4 * LZ$$

Table 21 shows that the recession coefficient is highest for the calibrated model, followed by the semi-calibrated model and then the un-calibrated model. This parameter would suggest that the low discharge is highest for the calibrated model, followed by the semi-calibrated model and then the un-calibrated model. However, that is not what the model performance suggests. The parameter (perc) shows the amount of water percolating from the upper soil to the lower storage. This value would as well suggest that there is more water in the lower storage leading to low discharges for the calibrated model.

Table 21: Main: parameters of the response routine for the three HBV versions

Main	Calibrated	Semi-calibrated	Un-calibrated
K4 (day^{-1})	0.1	0.05	0.01
Perc (mm/day)	3.349	2	0.5
Beta	1.168	2.5	1.0

For the Main it is difficult to determine the cause of the low hydrological model performance. This suggests that the difference is mainly caused by the low discharges upstream of Main.

Kinzig

For Kinzig the mean low discharge is analysed because it is highly underestimated by the calibrated HBV model, slightly underestimated by the semi-calibrated model and overestimated by the un-calibrated model.

1: Precipitation and snow routine

Figure 33 shows that in general the evaporation of the calibrated model (mean of 1.5 mm and total of 9407 mm) is higher than the actual evaporation of the semi-calibrated model (mean of 1.47 mm and total of 9204 mm) and even higher from the un-calibrated model (mean of 1.0 mm and total of 6459 mm). This could explain why the low discharges in summertime are highly underestimated by the calibrated model, followed by the semi-calibrated model and overestimated by the un-calibrated model.

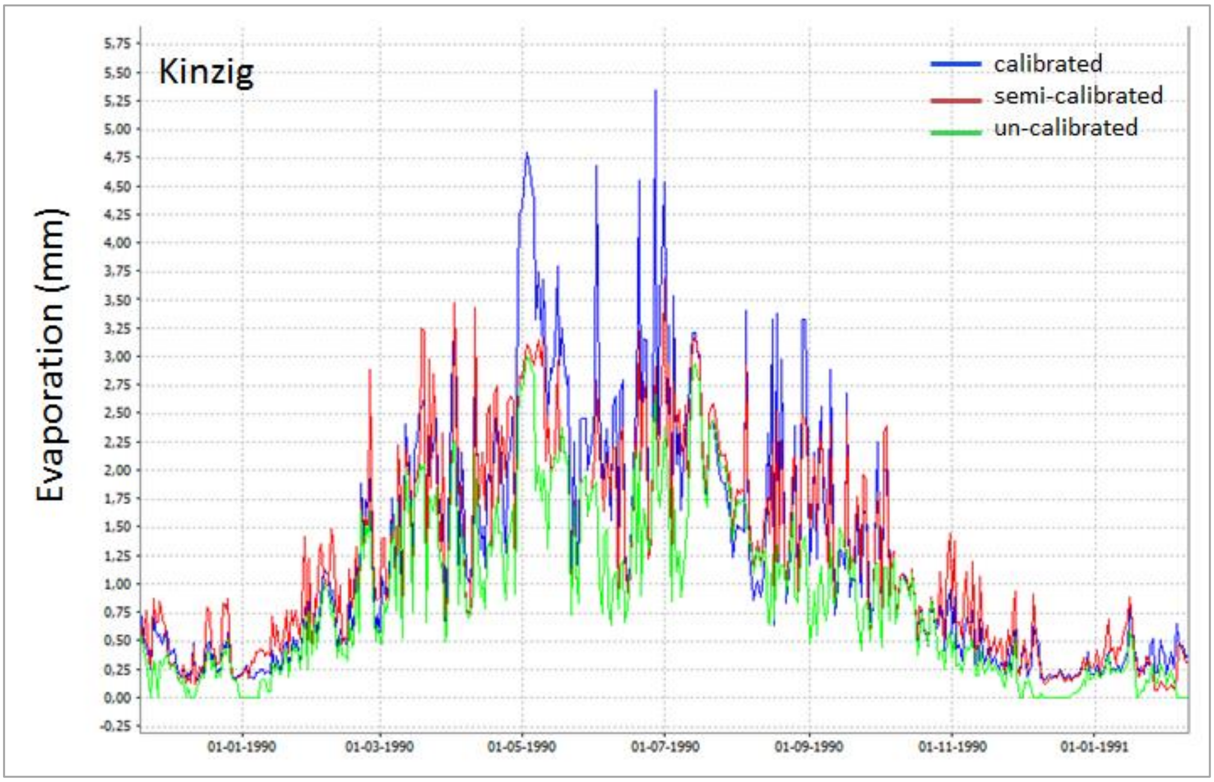

Figure 33:Actual evaporation Kinzig for the three versions of HBV for the summertime in 1990

These differences in evaporation are explained by the parameters (fc) and (lp) as shown in Table 22. The lower (lp) value means that the actual evaporation has sooner reached the value of the potential evaporation leading to more evaporation. Further, it means that the slope of the line as shown in Figure 33 is steeper as well, meaning that, if the (fc) is around the same, the amount of evaporation is higher for the same amount of actual soil moisture.

Table 22: Parameters Kinzig which determine the evaporation

Kinzig	Calibrated	Semi-calibrated	Un-calibrated
Fc (mm)	219.312	200	200
Lp (-)	0.632	0.9	1.0